BERICHTE
aus dem Fachbereich Geowissenschaften
der Universität Bremen

No. 166

Adler, M.

MODELING OF ONE-DIMENSIONAL TRANSPORT IN POROUS MEDIA WITH RESPECT TO SIMULTANEOUS GEOCHEMICAL REACTIONS IN CoTReM

Berichte, Fachbereich Geowissenschaften, Universität Bremen, No. 166,
147 pages, Bremen 2000

ISSN 0931-0800

The "Berichte aus dem Fachbereich Geowissenschaften" are produced at irregular intervals by the Department of Geosciences, Bremen University.

They serve for the publication of experimental works, Ph.D.-theses and scientific contributions made by members of the department.

Reports can be ordered from:

Gisela Boelen

Sonderforschungsbereich 261

Universität Bremen

Postfach 330 440

D 28334 BREMEN

Phone: (49) 421 218-4124

Fax: (49) 421 218-3116

e-mail: boelen@uni-bremen.de

Citation:

Adler, M.

Modeling of one-dimensional transport in porous media with respect to simultaneous geochemical reactions in CoTReM.

Berichte, Fachbereich Geowissenschaften, Universität Bremen, No. 166, 147 pages, Bremen, 2000.

ISSN 0931-0800

Modeling of one-dimensional transport in porous media with respect to simultaneous geochemical reactions in CoTReM

Dissertation
zur Erlangung des Doktorgrades
der Naturwissenschaften

im Fachbereich 5
der Universität Bremen

vorgelegt von
Matthias Adler

Bremen
2000

Tag des Kolloquiums: 6. November 2000

Gutachter:

Prof. Dr. Horst D. Schulz

Dr. habil. Tilo von Dobeneck

Prüfer:

Prof. Dr. Klaus Herterich

Prof. Dr. Reinhard X. Fischer

Preface

This work consists mainly of three publications. The CoTReM User Guide is published in its latest version 2.3 in the internet, the first study (Computer simulation of deep sulfate reduction in sediments of the Amazon Fan) is already published and the second study (Modeling of calcite dissolution by oxic respiration in supralysoclinal deep-sea sediments) is in press in an international journal. For all three publications my contribution consists in the main authorship, responsible with the final say in conclusions, formulations and editing.

The CoTReM User Guide documents possibilities and usage of the simulation model and reflects in addition some acquired knowledge about modeling necessities, techniques and concepts in the field of research covered by the model. This knowledge has been extended during the application of the program and due to discussions within the research group "Geochemie und Hydrogeologie" at the University of Bremen. Especially the Co-authors Dr. C. Hensen and Prof. Dr. H. D. Schulz contributed intensively to this process, which is manifested likewise in the studies. My function as the current simulation model developer qualified me to add further important aspects and to summarize this complete knowledge in the User Guide.

Consequently, the studies concentrate on modeling. The realization of the necessary simulations as well as summarization of considerations about simulation results and the final conclusions were my part in these studies. Support on this work on an "every day" basis was given by my room-mate Dr. C. Hensen. Dr. S. Kasten contributed general considerations to the complex of questions around sulfide and iron in the first paper and K. Pfeifer contributed discussions and preliminary modeling results of site GeoB 4906 in the second study, which I completed to the form presented in the study.

I would like to point out, that I was in no way involved in data sampling, sample analyzation and the necessary first steps of raw data conversion to significant data of physical and chemical measures like concentrations. Generally, this is the contribution of Co-authors or Prof. Dr. H. D. Schulz as coordinator of the research group. Especially Dr. F. Wenzhöfer has contributed his unique calcium *in situ* data as well as other critical *in situ* data for the success of the second study.

Table of contents

Introduction

1 Main objectives

Summarized, the main objective for this dissertation was the further development of the modeling tool of the **Co**lumn **T**ransport and **Re**action **M**odel (CoTReM; LANDENBERGER, 1998) as well as its application. Geochemical simulations in marine sediments and groundwater environments are important to certain geoscientist's examinations. These examinations determine the scientific questions CoTReM is developed for. Basically, this and comparable simulation programs (CANDI, STEADYSED1 and other {e.g. BOUDREAU, 1996A; VAN CAPPELLEN AND WANG, 1996; SOETAERT ET AL., 1996}) are made to master an important task. They have to achieve the quantitative, simulated verification of qualitatively assumed and/or known processes like chemical reactions and physical transport occurring in natural environments of porous media due to comparisons between simulated and measured data. The determining parameter of these processes cannot be derived directly from the measured porewater profiles. Instead the profiles determine directly the state of the geochemical system while the process parameters have to be calculated by models. Generally, it is one main purpose of modeling to yield results for parameters in examined systems, which are not or cannot be measured directly.

1.1 Modeling in CoTReM

CoTReM is a numerical, finite-difference model and was developed for the simulation of one-dimensional transport processes and bio-geochemical reactions of solute and mineral phases and has a precursor in the model CoTAM (SIEGER, 1993; HAMER AND SIEGER, 1994). It is based on the calculation concept of operator-splitting (YANENKO, 1971), which allows the simplification to calculate for each simulated chemical species the contributions of transport and reaction processes separately. Therefore exists the possibility to model even geochemical questions with high complexity without CoTReM being especially designed for only one concrete family of problems. This wide applicability is a great advantage of CoTReM.

Numerically are non-steady state conditions and inhomogeneous discretizations of the model area possible, while geochemically the simulation of one-dimensional problems, including transport phenomena like sedimentation, advection, dispersion, diffusion, bioturbation, bioirrigation as well as reactions of reoxidation, dissociation, complex-formation, sorption, dissolution and precipitation, is covered by CoTReM. The reactions are coupled to the

transport algorithm due to a modification to the algorithm for sorption, the use of CoTReM's own redox reaction module (REDOX) and the incorporation of the equilibrium reaction model PHREEQC (PARKHURST, 1995).

The main objective regarding CoTReM was its further development according to the questions and needs, which arose from the considered specific applications. Consequently, more and more options to simulate additional classes of processes and necessary redesigns for earlier included processes were added. This programming evolved mainly from problems and questions recognized in applications, when simulated results differed from qualitative considerations or when qualitatively considered processes were not yet available in CoTReM for a simulation.

The main points in the development of CoTReM since LANDENBERGER (1998) are:

- Bioirrigation is included
- Extensive inclusion of the solid phases, which means regarding

  Transport:

  a) The solid phase species transport is generally calculated by the same algorithm as it is used for the aqueous species, only parameter values and boundary conditions differ.
  b) Bioturbation of solid phases is completely and directly covered by the molecular diffusion algorithm of aqueous species.
  c) Advective transport is distinguished by the parameters "flow velocity" for the real advection (covering only aqueous species) and "sedimentation rate" for the artificial advection relative to the coordination system (covering all species).
  d) An optional useable modification in the advection calculation (Backward-Taylor-Series approximation), especially important for solid phase mass balances.
  e) A correction in the upper boundary calculation terms. This was formerly not necessary but in case of (pure) advection, which incredibly breaks the Peclet criterium, the correction is definitely needed.

Redox reactions:

f) The solid phase species concentration changes according to the full reaction equations and rates in the REDOX module are fully implemented as like as aqueous species.

Equilibrium reactions:

g) The changes of the solid phase species concentrations due to the PHREEQC equilibration calculations are completely ensured. The algorithm differs from the aqueous species algorithm and distinguishes between the cases of instant equilibration and the methods of kinetically modified equilibration.

- Changes in the calculation algorithm for the maximum reaction rates in REDOX due to problems, when two or more reactions compete for the same species
- Redesign of the units used in CoTReM
- Redesign of the simulation column within the program (organizing the order of the cells in the transport algorithm in relation to REDOX and the connection to the boundaries)
- Major redesign of the coupling between CoTReM and PHREEQC (especially miscalculation of pH repaired)
- pH and pOH calculation and the return of their values from PHREEQC
- Kinetic rate laws for dissolution and precipitation of solid phases
- Various small changes in output data formats and graphic design according to the developments above

An up to date description, how to handle CoTReM and how the included processes are mathematically based, is covered by the CoTReM User Guide (ADLER ET AL., 2000B; see below or in the WWW under http://www.geochemie.uni-bremen.de/cotrem.html).

1.2 Applications

The usefulness of CoTReM as a transport and geochemical reaction model is demonstrated here by two studies, where measurements from sites of the South Atlantic are used to simulate interesting ongoing processes specific to these places of marine early diagenesis.

The first study is based on gravity core data sets (simulated sediment depth = 7.30 m) and the examination concentrates on processes in the deeper, anoxic environment. The examined processes include the diffusion of downward moving sulfate and upward moving methane into a small redox reaction zone of these species. Main question in this application is the

whereabout of the reduced sulfur, the produced sulfide in the reaction, because the sulfide itself is much too marginally visible in the porewater measurements. The precipitation to ironsulfides, especially mackinawite, was examined by simulations and demanded a steady source of available iron. The source of iron was implemented within the simulation due to permanent equilibration of a solid phase of ironhydroxides. However, the results demonstrated in comparison to the measured iron porewater profile, that the ironhydroxide phase cannot be uniform in all simulated layers. A depth-dependent distribution of solubility constants was sought after and found to characterize the available ironhydroxides, while the sulfide and iron porewater measurements are also simulated. It was important from the numerical point of view, that the CoTReM ability to set up depth-dependent the conditions for the solid phase equilibration was demonstrated.

The second study is mainly based on microelectrode data sets (the simulated sediment depth is about a few centimeters) in the oxic and suboxic environment. The examined main processes include diffusion of oxygen into the simulated sediment column from the model boundary according to bottom water concentrations, oxic respiration fitted to the measured *in situ* oxygen profile and kinetically restricted calcite dissolution to simulate the measured profiles of inorganic carbon, calcium and especially the pH. Main point in this application is the examination of the calcite dissolution, which results in simulated kinetic parameters for calcite dissolution rate laws comparable to former studies. However, the setup of boundary conditions (e.g. depth distribution of oxic respiration rates, solubility constants of calcite, inorganic carbon concentrations at upper and lower boundary of the simulated column) to examine the dissolution – and these conditions define the important theoretical case of equilibrium (equaling instant kinetics) – is at least as difficult and important (kinetic results are based on the set up of the equilibrium case) as the fit of the "best" kinetic parameters of a particular form of a dissolution rate law. From the numerical point of view the highlight of this study is certainly the application of CoTReM's kinetic options due to the calcite dissolution and the successful simulation of the most sensitive species H^+, expressed as pH, which is heavily influenced by all applied processes (equilibration of the solution composition, equilibration to calcite including the kinetics, conversion of organic matter by oxic respiration, diffusion) .

2 Special considerations regarding this field of research

When geochemical simulations are applied during the examinations of questions arising from natural environments in porous media, there are some points to consider, which are specific for simulations in this field of research (or at least specific while working with CoTReM).

2.1 One-dimensional transport

The Column Transport and Reaction Model, like several other combined transport and geochemical models (e.g. CANDI, STEADYSED1), covers only geochemical questions in environments, which are reducible to one dimension regarding space discretization. The question, why three dimensions are not regarded will automatically arise. For the present another question has to be faced first. Why regarding a space dimension at all? There are several geochemical zero-dimensional simulation models available (e.g. WATEQ / WATEQF / WATEQ4F {TRUESDELL AND JONES, 1974; PLUMMER ET AL., 1976; BALL AND NORDSTROM, 1991}, EQ3/6 {WOLERY, 1979; WOLERY, 1993}, PHREEQE / PHREEQC {includes also a small transport option; PARKHURST ET AL., 1980; PARKHURST, 1995}, SOLMINEQ {KHARAKA ET AL., 1988}), which consider the equilibria within a given aqueous solution composition of dissolved species.

Furthermore, the (dis-) equilibria to gaseous and solid phases in reactive contact to the solution composition are concerned. CoTReM incorporates even one of these models (PHREEQC). This is possible, because the limitation of these zero-dimensional models – no exchange of the aquatic system contents per transport processes – is a requirement within each cell for a transport model. This requirement exists, because the cells are per definition the discretisized units in simulated space between them, and not within them, transport is calculated.

While the concept of zero-dimensional models fits the necessary requirements for any cell in any kind of transport models very well, a calculation without transport processes (within each cell to chemical equilibrium, instantly or kinetically restricted {the restrictive option is for CoTReM added to the PHREEQC program routines by active inclusion of the time dimension to include mineral dissolution and precipitation kinetics}), is very often not sufficient for geochemical questions. Especially non-artificial geological systems are commonly open systems. Therefore, changes in the space discretisized solution compositions of the system by

transport are often the main driving force of "never-ending" system dynamics or at least transport is not disregardable.

Inclusion of a space dimension in geochemical models, meaning coupling of transport and biogeochemical reactions, therefore extends essentially in a qualitative way the field of geochemical questions, which could be solved by a simulation program. The extension to higher dimensions regarding space discretization certainly even more extends the number of possible and imaginable applications, but the enormous qualitative difference is already taken into account during the step from zero- to one-dimensional models. Regarding modeling, additional dimensions could simply add, according to the superposition and operator splitting principles, their independently calculated contributions to a cell's sum of concentration changes by transport in a time step. Therefore, all necessary qualitative considerations about transport processes, algorithms to solve them, special cases at the boundaries and so on are already included in an one-dimensional model like CoTReM. Nevertheless, in an possible extension of CoTReM to more dimensions one has to consider separately for each point, despite the superposition principle, if the existing program structure can simply be expanded to more dimensions or a fully redesigned algorithm is demanded.

One-dimensional transport models are often sufficient in porous, geochemical environments, because either the effective species fluxes by transport mechanisms are known to be dominated by one dimension, qualitatively disregarding the orthogonal dimensions, or/and the available set of measured data is limited to one dimension, disallowing to simulate more dimensions seriously. CoTReM covers only one-dimensional transport, because so far it was applied in such appropriate cases. This means mainly marine sediments with one-dimensional measured data into depth – diffusive gradients orthogonal to the interface of bottom water and sediment determine usually in this case the dominating transport process due to the "reservoir ocean" – and groundwater questions, where geochemical reactions along a known predominant flow path are the main focus of interest. Regarding porous media, the parameter porosity is standardly used to take transport differences in porous media compared to pure aqueous environments into consideration.

2.2 Chemical reactions in porous media

The modeling of aqueous solution compositions in porous media is of special interest due to the more complex (and more difficult to simulate) possibilities of the aqueous phase to

interact, because automatically solid phases have to be regarded at least as imaginable reaction partners for dissolved species. Even more, the place of reactive interaction between species of these phases is not limited to the system boundary interfaces in porous media. These reactions may occur quasi everywhere within the concerned system. However, the problems arising by this fact for simulations are usually detectable from the porewater profiles, because profiles are differently characterized by these source/sink type of concentration changes due to reaction processes (creating porewater gradients for the few species involved in the reaction) than by transport processes (diffusion equalizes porewater gradients; bioirrigation may create gradients, but should act on all species equally). This is especially perceptible in case of so-called redox reaction zones, where a species within a small range of depth is converted at least in an important fraction into another species with a characteristic element of these species changing its redox state.

However, the effect of simulated chemical reactions clearly seen within each cell due to the located sinks and sources of species – not causing concentration exchanges along a space dimension – may be somewhat hidden and the importance of the reaction underestimated, if contrary working reactions, which balance their main effects mostly, are at work in the same layer of depth (e.g. calcite dissolution caused by and balancing effects of oxic respiration {buffering the pH}; cf. ADLER ET. AL., in press). Additionally, non-steady state problems are not reliable regarding what the concentration distribution should look like after a long time span due to transport, because that assumes steady state conditions (or at least dynamic equilibrium of processes; cf. ADLER ET. AL., in press).

The covered reaction processes are chemical in nature and exclude nuclear physic reactions like the fission process. This is the usual approach for numerical models simulating aqueous solution filled porous media, because conversion between atoms or of matter to energy or vice versa is no point of interest in this environment. This remark leads in consequence to the fact, that the mass conservation law is totally valid separately for each element in CoTReM simulations, barring deviations due to restrictions of the numerical precision.

2.3 Geochemical environments

"Geo"-chemical refers to the scientific field, where the questions to answer with CoTReM come from. An important note regarding modeling in geosciences is, that the examined questions and applications, apart from the exceptional cases of artificially prepared sample

material similar to geoenvironments (e.g. column experiments), come from the lab "Earth" (or any part thereof), an open system with often extremely difficult to define boundary conditions (uncontrollable time and space dependence of parameters; e.g. temperature) and sometimes sparse data in the modeled area.

This is quite contrary to data acquisition in other scientific fields, where examinations are based overly on data samples taken or "produced" under well defined experiments in scientific labs with mainly known and controlled parameter/boundary conditions. This is for many sciences the normal way to yield data, which their results are based on. These examinations and lab-experiments fulfill the common demand in these sciences, that the possibility to repeat an data sample under the same conditions shall exist. In contrast, data recovering by sample examination from the open lab "Earth" cannot exactly be repeated (the sample was already taken and severed from its environment). Regarding geochemical porewater modeling of one-dimensional only once taken profiles, this may lead to the question, if observed concentration changes are caused by time or space dependent processes, which may be difficult to decide.

2.4 Coupling of geochemical reactions and transport

Transport simulations regarding simultaneous reactions need a numerical method to couple their effects in a simulation. There are several designs to couple transport and reactions in geochemical (and early diagenesis) simulation models.

CoTReM uses operator splitting (OS; YANENKO, 1971; or mixing-cell approach; SCHULZ AND REARDON, 1983), which inherently approximates the problem by allowing all contributing effects of different processes to be applied sequentially. According to STEEFEL AND MACQUARRIE (1996) the operator splitting method is also known as "Sequential non-iterative approach" (SNIA). CoTReM uses the SNIA with the exception of the sorption reaction. These reactions are coupled to diffusive and advective transport by iterating (Newton-Raphson) back and forth the changes of these processes until an implicitly achieved solution composition of the new time step fulfills all demands to a chosen precision. This feature is best described as "Global implicit approach", but this term is commonly applied to simulation programs, which use this approach to all included processes and reactions. This leads usually to the disadvantage, that in the source code separate modifications to the general program

algorithms have to be included for each species used in the program[1], because the species are affected differently by the reactions (e.g. CANDI). The "Sequential iterative approach" (SIA) is something in between and difficult to describe. The main property is an iteration between the results according to a SNIA (STEEFEL AND MACQUARRIE, 1996), but the iteration alternates between applying transport changes first and reaction changes first. LANDENBERGER (1998) has given an overview of such geochemical models coupled to transport in use for the scientific field of marine sediments.

3 Philosophical aspects of modeling

This work really is made about the main concept "modeling" from the title, however, what does this concept mean? An artist carving a sculpture out of granite surely faces other facets of "modeling" and perceives it differently than a scientist examining scientific questions by simulation methods. Even scientists may face different aspects regarding modeling with respect to the scientific field, they are interested in. So, has the term "modeling" to be used and understood sometimes completely different according to the taken points of view or is it only a perceptive difference?

The common property in the concept of modeling will always be a connection to mathematics. Mathematics create, describe and explain virtual worlds of their own, which can be treated in case of similar properties as equivalent to a fraction from the real world (even a sculptor's imagination about the next piece of work uses inherently mathematical concepts like qualitative relations and measures regarding the length and angles between different details of the sculpture to "define" its properties or proportions. The real sculpture can even be "measured" using these concepts). Identity between this virtual world and an examined scientific system, within the limits of knowledge about the system in question, allows to use the mathematical, virtual representation as an explanation of the real system. While the real examined system is fixed and (partly) given by measurements, the used virtual world may be formed, modified or "modeled" to match the properties of the real system (artist's may call their modeling or creation process of a second real system forging, if it matches the properties of the "real examined system"/original). Indeed, this process of identity-forming or comparison between simulated virtual and measured real representation is basically the concept sought after: Modeling.

[1] This leads normally to a fixed species limit in the program design and limits the field of simulatable problems.

While this connection to mathematics suggests to be the essential (and somewhat trivial) property of modeling, it nevertheless seems to neglect the differences modeling is perceived. But implicitly, these differences are regarded, they are hidden within the word "identity" and in which kind of matter mathematics are connected to the concerned term "modeling". A closer view suggests, that varying points of view and perceptions depend on the question, how exact is the term identity used and by what means is it tested. The mathematical, virtual concept of "identity" is clear, it allows no deviations, but science deals with real systems and this necessarily leads to deviations during comparisons. These non-suppressible deviations between simulated and measured representation of the system can be caused by several reasons. These include uncertainties of measurements, limited knowledge of data and system boundaries, not included (neglected or unknown) processes in the simulation, the modeling of processes (e.g. diffusion), which are scientifically described by measures used as simulation system-constituents (e.g. concentration of chemical species) due to the validity of a statistical law (Fick's laws) for a totality of one step more "true" system-constituents (e.g. atoms and molecules), and obviously the non-scientific question, if reality is at all treatable as equivalent to any virtual representations[2]. Therefore, at least some (small) deviations are tolerated in comparisons of measured and simulated data, because such non-exact mathematical use of "identity" can and must nevertheless be accepted for the idea of scientific evidence.

The different concepts of modeling might be described by their basic properties into only two main classes. The first class of modeling concepts may be understood as every conceptual, qualitative and potentially possible explanation made up in someone's mind for a given (scientific) question. Regarding the realm of mathematics, this class describes each process per qualitative relation, if a (possibly located) system-constituent will in- or decrease (e.g. the concentration of oxygen decreases due to oxic respiration near the surface of sediments). An important, notable method within this concept is often used, if two (or more) processes with conflicting effects (or even, if the have qualitatively the same effects) are regarded. Instead of applying a process with "smaller effect" regarding a specific property, the process may be disregarded as a whole (e.g. disregarding molecular diffusion, if dispersion effects are dominating like often in groundwater environments). Thus, it is a property of this qualitative conception, that decides, if a process or system-constituent is included at all.

[2] Science is founded on an agreement to posit this possibility.

The second class of modeling concepts is the one of quantitative description, either by means of analytical or numerical calculation methods. Each interesting system-constituent is simulated by a set of numbers, e.g. concentration in dependence on time, location and chemical species, and every process is described in mathematical equations including material dependent parameter (e.g. diffusion coefficients). Qualitative statements about system properties can be deduced in this case from resulting quantities.

How are these main classes connected? The hypothetical ideas derived from observations simply lead first to qualitative explanations, which processes and system-constituents have to be regarded. Next, the corresponding description of a quantitative approach is at least important and often even necessary for the final foundation of scientific evidence. Very inappropriate quantitative results will lead to the reexamination of the qualitative considerations, followed by new calculation. This scheme of iterating these approaches will go on until the sought after (or maybe the so far best possible) level of optimization regarding the results is reached, because calculated results and qualitative considerations contain no more (important) contradictions.

Increasing complexity in examined systems is usually characterized by an increasing number of system-constituents and processes. Correspondingly, the connection increases, because the qualitative option to decide about totally disregarding a process or system-constituent in a quantitative modeling approach has to be made separately for each of those components. The results can be better validated due to the higher level of connection between both approaches, because each contradiction due to an included process or system-constituent has to be dealt with for the optimization of the results. In addition, increased complexity usually decides the question which calculation method to use for the quantitative approach in favor of the numerical method, because analytical solutions are only suitable for a relative small amount of scientific questions. In these cases of high nonlinear problems one has to rely on numerical modeling approaches to simulate the system.

Analytical "paper & pencil" solutions, usually subject to stringent idealizations, were the preferred quantitative method until the rise of computers, because numerical schemes profited enormously from this alternative to "paper & pencil" and are more widely applicable. The introduced approximations for numerical (and computer-based) algorithms, inherent due to

the formulation and discretizations of the examined system, can usually be constrained to a known order of negligible deviations compared to a hypothetical exact result.

Pure analytical results may still contribute significantly to a complex question, because they provide usually the exact terms, which would solve an isolated, particular problem within the system of partial differential equations (PDE's), which describes the whole question (e.g. diffusion and advection terms in the PDE's, which CoTReM is able to simulate; see Appendix A of the User Guide). Apart from the approximation due to the necessary transfer from PDE's to partial difference equations to be able to compute at all, the used method of operator-splitting in CoTReM is especially useful to include particular analytical results, or basically is the concept of their sequential inclusion, into the whole concept to solve the question. The disadvantage is the needed small time step to justify the sequential approach, the advantage is the reduction of the non-linear problem to several linear PDE systems. Global approaches to solve the PDE system do not need a time step as small as the operator-splitting method (STEEFEL AND MACQUARRIE, 1996). On the other hand, they need to solve numerically the highly non-linear PDE systems by coupling directly the effects of the processes. None of these coupled processes will contribute simulation changes within a time step exactly the same as the comparable known, isolated and possibly analytically solved process. Therefore, the global coupling may involve other, additional approximations during the conversion from PDE to partial difference equations or elsewhere than operator-splitting.

However, the behavior of a complex (geochemical) system is not easy to understand, because of the interactions of all participating processes. Even more difficult is the decision to set up qualitatively the PDE of the geochemical system with the "correct" parameters and boundary conditions. Due to the complex geochemical solution compositions considered, modeling with CoTReM should be understood within this work as a detailed quantitative modeling approach. This includes a lot of chemical species concentrations as system-constituents[3] and the determining processes in groundwater and marine geochemical environments. Nevertheless, even the development of the modeling tool was based on and combined with a supplement of qualitative considerations to make each setup of possibly "correct" parameters and boundary conditions available.

[3] Remember, that the use of concentrations instead of atomar particles as system-constituents allows and requires inclusion of macroscopic, statistical laws to simulate processes like diffusion.

The qualitative considerations of the concrete applications have still to answer, where to include redox reactions, how to modify dissolutions and precipitations, or simply what's up exactly with the system boundary conditions. Therefore, the actual presentation of modeled examples in the papers is emphasized qualitatively, but the quantitative basis to rely on is given due to the modeling tool CoTReM.

CoTReM
Column Transport and Reaction Model
User Guide Version 2.3

M. ADLER, C. HENSEN, AND H.D. SCHULZ

University of Bremen, Department of Geosciences, P.O. Box 330 440, Germany

Corresponding author: Matthias Adler Phone: 0049-421-2183967
Fax: 0049-421-2184321
e-mail: madler@geochemie.uni-bremen.de

Introduction

The computer program CoTReM is a numerical, one-dimensional, finite-differences model to simulate the distribution of chemical species in geochemical systems affected by transport and chemical reactions. The theory of operator-splitting allows to calculate separately contributions of transport and reaction processes what makes it possible to model even problems with high complexity.

Therefore, a simulation run with CoTReM may include all of the following operations:

- Initialization operations for all concentration data.
- Time dependent processes calculated in each time step, adjusting the depth distribution of the concentrations in a simulation run of CoTReM:
  - The contribution of the bioirrigation process separately cell by cell.
  - The combined contribution of other transport processes like advection, dispersion, molecular diffusion and bioturbation in all cells through one equation system. This contribution is combined with the contribution resulting from sorption processes.
  - The contribution of the chemical processes by redox reactions in each cell (module REDOX).
  - The contribution of the chemical processes by thermodynamical equilibrium reactions (PHREEQC; PARKHURST, 1995) in each cell.
  - Modifications of the thermodynamical equilibrium calculations to minerals regarding kinetic rate laws for these solid phases within the PHREEQC-module.
  - Display of species in a direct graphic output.
- Output operations for all data.

The great advantage of CoTReM is, that its complexity allows to simulate many different biogeochemical and transport processes under non-steady-state conditions. The character and file based concept of input data in CoTReM is used to maintain a higher flexibility for any further developments of the program.

This User Guide is especially thought to allow the preparation of the input files necessary for modeling with CoTReM. The geochemical and mathematical basis of hydrochemical simulations is more deeply discussed in a book about the former model CoTAM (HAMER AND SIEGER, 1994). Additionally, general theoretical aspects can be derived from two PhD-theses (SIEGER, 1993; LANDENBERGER, 1998). These are available in the report series of the Department of Geosciences at the University of Bremen as No.40 and No.110. The usability of CoTAM/CoTReM will be further investigated in different applications, while the development process is still going on. Presently, there are several investigations of application problems in groundwater systems (HAMER ET AL., 1992; HAMER, 1993; SIEGER, 1993; HAMER ET AL, 1994; ISENBECK-SCHRÖTER AND HAMER, 1994; ISENBECK-SCHRÖTER ET AL., 1994; VON LÜHRTE ET AL., 1994; EBERT ET AL., 1995) and in marine systems (HENSEN ET AL., 1997; LANDENBERGER ET AL., 1997; LANDENBERGER, 1998; ADLER ET AL., 2000A).

Newer possibilities and concepts of CoTReM include:

- CoTReM is connected to the widely accepted program PHREEQC (PARKHURST, 1995) including the option of calculating thermodynamical equilibria to mineral phases.
- Equilibrium calculations may be modified by kinetics. Version 2.3 of CoTReM includes two general formats of kinetic rate laws for dissolution and for precipitation.
- Solid species are fully integrated in each simulated process. Solid species concentrations may be transported (sedimentation/bioturbation), changed through redox-reactions and are

part of PHREEQC equilibrium calculations with optional depth-dependent saturation indices for each phase. The depth-variation of non-zero saturation indices may emulate the change of log k values.

- The redox reactions are completely new formulated as full reaction equations. The algorithm is driven by rates of used redox reactions. The user defines these rates as maximal rates for each reaction in each cell. These rates might be used or are reduced by an algorithm to prevent negative concentrations.
- The earlier pure DOS compilation was further developed to be able to use CoTReM under Windows. The direct graphic output is written for DOS, thus the graphic version allows no multitasking. However, there is a Win32/WinNT-compilation which allows to simultaneously start different CoTReM_NT.EXE in different directories each using an own DOS-window.

The use of descriptive names, registered names, trademarks, etc. in this publication does not imply, that a violation of relevant protection laws etc. is intended, e.g. the proxy EXCEL stands within this User Guide for the registered name of the corresponding Microsoft Corporation product without any challenge to the corporation's rights about the name or product.

Disclaimer
Neither the authors nor the department of Geosciences nor the University of Bremen make any representation or give any warranty with respect to the adequacy of this User Guide or the program and methods which it describes for any particular purpose or with respect to its adequacy to produce any particular results. In no event shall the authors or the department of Geosciences or the University of Bremen be liable for any kind of damages, losses or disadvantages due to the use of this User Guide or the program and methods which it describes.

Table of Contents

1 General information about CoTReM

This part describes the hardware and compilers, how to set directory paths to files used for running the program and how to use the character mode CoTReM.EXE with a batch-file.

1.1 Computer and compiler software

The development area used (WATCOM Integrated Development Environment Version 10.5 with FORTRAN 77 and C/C++ compilers) gives the choice which kind of executable files for PC's should be made. These choices include: Executable files under DOS (16- and 32-bit) and Windows (16 -and 32-bit, NT/Win95/Win32s). Furthermore a compatibility with the Microsoft Foundation Classes is possible. Developing and testing CoTReM was done as a 32-bit DOS-application at Pentium computers with at least 16 MB RAM and 90 MHz processor frequency. Especially high processor frequency is very useful when the incorporated PHREEQC is used. Without PHREEQC even computers with 486 processors and 4MB RAM are able to handle CoTReM appropriately.

All needed CoTReM files require less than 2.0 MB of free space on the disk. Additionally, each simulation example needs a set of input/output-files with up to 0.5 MB and one special output, concentration over time, grows with the specified maximum time.

Running mode and graphic screen
CoTReM is run in the character mode, therefore, the program is used with batches. There are several character mode options to choose the form of the direct graphic output.

1.2 Setting the file paths

There are several files which have to be in the same directory as the CoTReM executable file. These are the files DOS4GW.EXE, SMALLE.FON (replaces VGAFIX.FON), COTREM.INI, COTREM.STO (for REDOX) and PHREEQC.DAT (for PHREEQC). The file path of the executable file is given through the batch file and all paths of specific files for a simulation example are given in the file COTREM.INI.

The actually needed or active input/output files are set by the batch. Their names (not paths) are changed to NONAME in COTREM.INI after a run of CoTReM, if they are inactive. Otherwise, if active, their name is specified in the batch. The DAT input file is always needed and the PRX output file is always given. As an example the COTREM.INI of a simulation called MARIN may look like this:

```
|FILES|
C:\COTREM\DATA\MARIN_1.DAT
C:\COTREM\DATA\MARIN.PAR
C:\COTREM\DATA\MARIN.UMS
C:\COTREM\DATA\MARIN.PHR
C:\COTREM\DATA\MARIN.EXP
C:\COTREM\DATA\MARIN.PRN
C:\COTREM\DATA\MARINS.PRX
C:\COTREM\DATA\MARIN.PRX
C:\COTREM\DATA\MARIN.SI

|SCREEN|
6
```

Different simulation runs of the MARIN project may therefore have their own initialization files, MARIN.INI, MARIN_2.INI and so on. Utilizing them only requires to copy the actually needed *.INI to COTREM.INI before the CoTReM run starts via batch.

The directory paths will be used to read the input files and write the output files, even overwriting (WITHOUT WARNING) similar named existing files. The directories must exist. Inactive files *.XYZ will be noted in COTREM.INI as NONAME.XYZ as explained above. Similar to the filename limitation (8 characters, dot, 3 character extension) a file path limitation exists within the COTREM.INI. It is limited to a 32-character-string (without filename characters). A longer file path will be read without warning and usually result in a misread filename (followed by stopping the simulation run).

1.3 Starting the program with COTREM.BAT

CoTReM should be started with a batch file *.BAT (or directly with the same commands as in the batch). The upper COTREM.INI could be created after a simulation run by the MARIN.BAT:

```
c:
cd \COTREM\DATA
cotrem.exe /i marin_1 /p marin /u marin /phr marin /m marin /o marin /c marins
           /s marin /gs
```

The first two rows are used to set the path to the disk and the directory. The third command is shown here in two rows. This example utilizes all possible command parameter options for input/output files and the option /gs for the marine sedimentary graphic output. In most cases less options will be chosen.
CoTReM recognizes the following (optional) command parameters:

COTREM.EXE [/<d> <Filename>] [/g] [/gg] [/gue] [/guea] [/gs] [/text]

Substitute <d> with one or more command parameters, commanding these file input/output operations:

- i Load <Filename>.DAT (simulation data file). Always needed in a simulation.
- o Write the output file <Filename>.PRN with the breakthrough curve data and the last calculated depth-depending concentrations to the output file <Filename>.PRX.
  If "o" is not set, the name of the simulation data file (*.DAT) is used to write the PRX-file.
  Therefore, the PRX output is always given.
- c Load <Filename>.PRX (background concentrations).
  The PRX fileformat is used as input data here. It is a dual purpose format and the input variant should be used with *S.PRX to have different filenames.
- m Load <Filename>.EXP (measured data).
  One set of measured data may be shown in the direct graphic output.
- p Load <Filename>.PAR (depth-dependent parameter).
- u Load <Filename>.UMS (reaction rates).
- phr Load <Filename>.PHR (PHREEQC data input).
- s Load <Filename>.SI (variable saturation indices for PHREEQC).

The other parameters define the type of direct graphic output:

- g The simulation results will be graphically shown as breakthrough curve.
- gg The simulation results will be graphically shown as breakthrough curve and then the concentration as resulting distribution over the length of the column.
- guea The simulation results will be graphically shown as concentration distribution over the length of the column, developing with time.
- gs The simulation results will be graphically shown as concentration distribution over the depth of the column, developing with time. This is a variant of guea for marine sediments.
- text The simulation results will be shown as text data.

Starting CoTReM is done via these command parameters in MARIN.BAT. The above mentioned third batch command line will load the simulation data file MARIN_1.DAT, the depth-dependent parameters in MARIN.PAR, the reaction rates in MARIN.UMS, the PHREEQC parameters in MARIN.PHR, the measured data from MARIN.EXP, the starting background concentrations in MARINS.PRX (usually with an added S-ending for starting at the input-PRX-filename) and the saturation indices in MARIN.SI.

Usually, only the PRX output is written to a file named like the *.DAT file (here MARIN_1.PRX). Here the specified "/o" command parameter gives MARIN.PRN and MARIN.PRX as output data.

Further output data of actually resulting reaction rates are written to MARIN.AUR.

Generally, the simulation in CoTReM may be finally stopped with the escape key < *esc* >. It may be temporarily stopped with the blank key. The graphic output vanishes or is interrupted in this case, when all calculations of a time step are done. More time is needed when PHREEQC is used. PHREEQC lists the actually calculated cell of a time step in addition to the simulation time.

1.4 Comments to COTREM.INI and COTREM.BAT

Some details of the file management should be mentioned before each parameter in the input/output files will be discussed in the next chapter.

Files and their names in COTREM.INI and COTREM.BAT

The names of files have to follow the MS-DOS convention, meaning 8 characters as a maximum. The 3 character addendum defines the kind of the input/output file. In the batch file the addendum does not have to be written. Instead, each of the command parameters is connected to one addendum. The paths and the names of used active files will be written to COTREM.INI when CoTReM finishes (see chapter 1.2).

Given paths and filenames in COTREM.INI and COTREM.BAT will be checked at the start of the program.

2 Working with CoTReM

The different input parameters, file formats and units are explained below.

2.1 Units in CoTReM

The units for substance [mol] and volume [l] in CoTReM are internally fixed. Therefore, all input concentrations have to be in mol/l (except CoTReM is used with a non-standard INPUT_OPTION, cf. 2.2.1.1, which allows different units for solids and pH/pOH). The other fundamental units for time and length are free. They only have to be chosen consistently.

The algorithms in CoTReM solve the problem determining partial differential equations independent from prechosen units for data. Therefore, all input data have to be (and output data will be) in the same units. These chosen units may vary in different simulations. So the user is free to choose the units for time and length, that best fit to a given problem.

Note that there are other input data which depend on the fixed unit-dimensions of substance [mol], volume [l], and the chosen dimensions for time and length. The list below summarizes these important rules for units.

Fixed units		
Substance	:	mol
Volume	:	$l = dm_{(aq)}^3$
Free units		
Length	:	cm (as example)
Time	:	yr (as example)
Dependent units		
Concentration	:	$mol / dm_{(aq)}^3$
Reaction rate	:	$mol / (dm_{(aq)}^3 * yr)$
Velocity	:	cm / yr
Diffusion coeff.	:	$(cm)^2 / yr$
Dispersivity	:	cm
Rate of sorption	:	1 / yr
Bonding affinity	:	$dm_{(aq)}^3 / mol$
Henry and Freundlich coefficient	:	1

Attention: It is important to note that for concentration the program uses the relation to a volume which consists only of aqueous porewater ($dm_{(aq)}^3 = l$ = liter). If a dm^3 is filled with solid phase ($dm_{(s)}^3$) or the sediment mixture of aqueous species and solids (dm^3), this would mean different relative volumes.

All species, even solid species (minerals), are standardly given in relation to a $dm_{(aq)}^3$ or liter of the aqueous part of the sediment (or porewater). This type of definition for concentrations is required to calculate the changes in CoTReM's concentration matrix C (species times depth-cells) consistently. In addition, note that only concentrations, but no masses and no amounts of substance are used in CoTReM. They cannot be used in a one-dimensional model. Only concentrations (substance in relation to volume) can be used. Furthermore, volume may only be used to make this concentration relation substance per volume. Therefore, the values

representing substance are always in relation to the volume of one $dm_{(aq)}^3$ in CoTReM. If values of fluxes are needed per unit of area, the user has first to define that unit of area and may then use existing data to calculate fluxes.

The comments below concern the values not used in CoTReM, some important definitions and how to convert the weight-value of a mass of a solid species, related to $dm_{(s)}^3$, into a value of substance in relation to a liter of porewater ($dm_{(aq)}^3$). Porosity is not needed for conversions within CoTReM and not standardly used in calculations, because the conversion below is supposed to be done already for CoTReM input data in the standard case of mol/l. However, input/output data may need porosity for a non-standard INPUT_OPTION (see 2.2.1.1 below).

Comments to units

Not used units

Mass	:	kg or g
Flux	:	mol / (dm^2 * yr)
Area	:	dm^2
Porosity	:	1

Conversion definitions

Porosity P [1]	:	$dm_{(aq)}^3$ / dm^3
Density ρ	:	$kg_{(s)}$ / $dm_{(s)}^3$ = $g_{(s)}$ / $cm_{(s)}^3$
GFW	:	g / mol

Conversion

C [g / $kg_{(s)}$] / GFW	= C [mol / $kg_{(s)}$]
C [mol / $kg_{(s)}$] * ρ	= C [mol / $dm_{(s)}^3$]
C [mol / $dm_{(s)}^3$] * (1 - P)	= C [mol / dm^3]
C [mol / dm^3] / P	= C [mol / $dm_{(aq)}^3$]
C [mol / $dm_{(aq)}^3$]	= C [mol / l]

2.2 Input/Output parameters and files

Please compare these descriptions with the corresponding file formats from a given example.

The file paths for a simulation run are set in COTREM.INI. Additionally, a parameter for the type of screen graphics is set in COTREM.INI. It is useful to save this file in MARIN.INI for a MARIN project, because, if other project simulations are running in the same directory, the file COTREM.INI will be overwritten.

2.2.1 General simulation data in *.DAT

The *.DAT file contains all necessary, general data input to run a CoTReM simulation. This includes column, hydrodynamical, time, numerical, sorption and control parameters. Some

are dependent of the species. The handling of the depth dependent variation of parameters is described in 2.2.2 (*.PAR).

Several *.DAT parameters are duplicated in the *.PAR file. Therefore, if the PAR file for depth dependent data is used, the values in *.PAR are the valid ones. In a homogenous simulation the *.DAT is used alone.

Annotation: Format of *.DAT

The first two rows are not used. All other rows first have some descriptive ascii characters and then the data input. The title rows three and four have 28 characters comment and a 37 long ascii character string as input (the FORTRAN format '(A27,1X,A37)' is read). The rows with species names have 28 character commentary and read a 21 long ascii character string (Format: '(A27,1X,A21)'). All data input for integer and double precision values is read after 27 character comment with a positive signed exponential format of 11 characters (Format: '(A27,1PE11.4)'). A simple ascii editor should be used for changes, because editing per EXCEL usually leads to a violated format.

All data, which use integer formats, will be converted. For example, one has to write 1.0000E+00 if a parameter value of one is wanted. All parameters have to be set in this format, even when they are generally or temporally not used, because they will be read. Values other than integer will be converted into the REAL*8 datatype (FORTRAN) and double datatype (C/C++).

2.2.1.1 Non-species-specific data in *.DAT

The first four rows are only for information, especially two title rows for the simulation.

Column parameters

- "Density": The density ρ is defined in $kg_{(s)}/dm_{(s)}^3$. It is standardly not used, except for solid phase conversions (cf. 2.1) applied per "INPUT_OPTION".

- "Porosity": The porosity ϕ of the sediment. It is standardly not used, except for solid phase conversions (cf. 2.1) applied per "INPUT_OPTION". In addition, the porosity modifies the diffusion coefficients in sediment D_S (cf. 2.2.2).

- "Column": Defines the length of the "Column" and its lower boundary only in the homogeneous case (==> No PAR-File used). The column length will be divided by the length dx_num (see below) of one representative elemental volume (REV) or cell. This results in the number of simulated cells, which has to be used correctly in other file formats (*S.PRX, *.UMS etc.).

Hydrodynamical parameters

- "Flow velocity": The "Flow velocity" (or "Abstandsgeschwindigkeit") v_a. This is the transport velocity of solutes through the model column. This parameter does not affect solid species.

- "Dispersivity": The "Dispersivity"(α_L) is the longitudinal dispersivity coefficient and only effective, if the flow velocity is greater zero.

- "Diffusion coefficient": This is the "Diffusion coefficient" in sediment (D_S). This diffusion parameter affects all active species and is only used in the homogenous case. Different coefficients for each species and/or depth depending coefficients are set with the *.PAR-file. Even to solid species a value may be applied, which reflects a bioturbation coefficient D_B.

WARNING !
The D_S is applied between upper boundary (concentration C_0) and first cell, too. In case of bioturbation this leads to the usually unsatisfactory addition or removal of solid phases across the sediment water interface (like aqueous diffusion) apart from sedimentation. Therefore, bioturbation coefficients D_B (the D_S of solid species) should always be set to zero in the first diffusion coefficient line (first cell) within *.PAR, except the user has explicitly other intentions.

The apparent diffusion coefficient D is calculated in CoTReM:

$$D = \alpha_L \, v_a + D_S.$$

CoTReM uses this parameter D to solve the transport contribution of the partial differential equation system. The parameter D makes it possible to use the same algorithm for problems in groundwater systems ($\alpha_L \, v_a >> D_S$) and marine systems ($\alpha_L \, v_a << D_S$).

Time parameters

- "t_max": The maximal simulation time is "t_max". If the actual simulation time reaches t_max, the simulation run will stop, producing all the output files.

- "dt" : The parameter "dt" describes the time-step for graphic output and the breakthrough curve file output *.PRN. It is recommended to fulfill the condition: dt equals an integer times dt_num (see below). Nevertheless, dt is free chooseable except that dt must of course be greater or equal to dt_num.

Numerical parameters

- "dt_num": "dt_num" defines the length of the time step for all time dependent calculations in CoTReM's algorithms.

- "dx_num": "dx_num" defines the length of each cell in the case of a homogeneous discretization of the column length.

Annotation: Criteria for numerical stability by PECLET and COURANT

One has to consider the criterium given by Peclet to fulfill numerical stability. The number of Peclet P_e is:

$$P_e = | \, v_a \cdot dx\_num / D \, |$$

The criterium is defined by $P_e \leq 2$. Therefore, the Peclet criterium will give a maximal value for dx_num, while v_a and D are given by the hydrodynamical parameters.

The other criterium is given by the number of Courant $C_{Courant}$:

$$C_{Courant} = | v_a \cdot dt\_num / dx\_num |$$

The criterium is defined by $C_{Courant} \leq 1$. This means that the advection is not able to transport species further than one cell in one time step. This is an obvious requirement and often dt_num has to be even lower for simulations in CoTReM, because these limits only regard the transport effects. The operator splitted interaction of transport effects with effects by chemical reactions may require even lower time steps.

When the Courant-criterium is fulfilled the criterium condition of Peclet may be formulated as:

$$dx\_num \leq 2 * D$$

If any of these stability criteria is not fulfilled numerical errors may occur and result in erroneous simulation results. These can often be recognized as oscillations of concentrations.

Note that v_a must be substituted by w (sedimentation rate) when calculating problems derived from marine systems.

- "t_analy": "t_analy" defines the time for an analytical equation to calculate starting background concentrations over depth, if the command parameter "/c" is not used. In this case the background concentrations over depth are calculated at time t = t_analy. This concentration distribution is given by an analytical expression in the case of a tracer with continuous input into the column and the result is only affected through advection, diffusion/dispersion and sorption. The analytical calculation follows KINZELBACH (1986) with an expression for the complementary error function erfc from PRESS ET AL. (1992).

Annotation: Loading background concentrations

A simulation run will always give results as concentration distribution over the length of the modeled column. This PRX-output may be taken, perhaps manually modified, and used as input background concentrations with the command parameter "/c <Filename>".

- "Iter_max": "Iter_max" defines in the transport algorithm the maximal possible number of iterations in one time step for the used NEWTON-RAPHSON-scheme.

- "Epsilon": "Epsilon" defines a value for the quality result of the NEWTON-RAPHSON-scheme. The condition must be fulfilled, that the sum of the deviation squares of two sequential calculation results is lower than "Epsilon". The value for epsilon may not be lower than the precision of the used digital numbers of the compilation. This ultimate limit to "Epsilon" is around 10E-16 for the used double precision numbers.

Control parameters

- "SET_SI_Zero": Defines the used saturation indices.
  - "SET_SI_Zero" equal 0: All used saturation indices are 0.0.
  - "SET_SI_Zero" equal 1: All used saturation indices are taken from the *.SI-file (depth-dependent and non-zero is possible).

- "Density H2O": It defines the density of water used in the conversion of concentrations from mol/l (Transport/REDOX) to mol/kgw (PHREEQC).

- "Type of advection": This defines, which of two different approximations for differential quotients is used for the advection.
  - "Type of advection" equal 1: The Central-Taylor-Series is used with the approximation $\partial C/\partial x \mid_x \cong [C_{i+1}(t) - C_{i-1}(t)] / 2 \Delta x$.
  - "Type of advection" equal 2: The Backward-Taylor-Series is used with the approximation $\partial C/\partial x \mid_x \cong [C_i(t) - C_{i-1}(t)] / \Delta x$.

  Advantages of type Central (=1) are:
  This form has clearly less numerical dispersion and it has a second order deviation in the approximation.
  Disadvantages:
  The mass-balance is not completely fulfilled. Mass will be created in small amounts inside the column. If a concentration peak is transported, it will move its relative maximum slower than expected. Examples including solid phase sedimentation should use type 2. Without bioturbation a high numerical dispersion is caused in this case, because D is zero (or very small with bioturbation) and the Peclet criterium is violated.
  Recommended only/especially for breakthrough curves.

  Advantages of type Backward (=2) are:
  Very exact mass-balance, only the simulation boundaries and the precision of digital numbers disturb as usual the balance (not removable). If a concentration peak is transported, it will move its relative maximum exactly as expected.
  Disadvantages:
  A clearly higher numerical dispersion.
  Therefore, recommended for problems which require exact mass-balances.

- "Irrigation": It defines if the option of bioirrigation is used.
  - "Irrigation" equal 0: All irrigation is zero. NOTE: Ignores all "Alpha_x" in *.PAR.
  - "Irrigation" equal 1: The irrigation coefficients will be defined depth-dependent per *.PAR with the values of "Alpha_x".

Annotation: Bioirrigation

The change $\partial_t C$ in the depth-distribution through irrigation is described by:

$$\partial_t C = \alpha_x (C_0 - C)$$

α_x is the function to describe the exchange over depth. The irrigation coefficients "Alpha_x" in the *.PAR-file are the rates of the irrigation exchange and the exchange itself is calculated as follows:

$$\Delta C = \text{Alpha\_x} (C_0 - C(x)) \text{ dt\_num}$$

Bioirrigation affects only aqueous species.

The equation would produce erroneous results for Alpha_x times dt > 1. This would mean that a concentration lower than C_0 at certain depth, C(x), could become higher than C_0 by mixing. Since this is impossible, CoTReM will stop when C_0 = C(x). Reduce dt_num, if necessary.

- "SET_pH-CONST": Defines how to calculate pH for PHREEQC.
  - "SET_pH-CONST" equal 0: The pH is normally calculated from the H^+ concentration and the activity coefficient log gamma.
  - "SET_pH-CONST" equal 1: The user overrules all process contributions for pH and sets one constant pH as input for PHREEQC in CoTReM.

- "Value of set pH": Defines the constant value for the pH if "SET_pH-CONST" is 1.

- "Sedimentation rate": Defines the transport velocity of species (solids and solutes), whereas "Flow velocity" affects only aqueous species.

- "pE-Handling": Defines how the pE is initiated in PHREEQC. The depth-dependent background pE will be read from the input PRX file, otherwise its default is 4.0.
  - "pE-Handling" equal 0: The input pE for PHREEQC is never changed from the background values. This case is useful, if measured data are available.
  - "pE-Handling" equal 1: The background pE is used in the first calculation and then substituted by the pE output of PHREEQC. Therefore, pE output is used as input for the PHREEQC calculation in the following time step. This pE is not corrected by the changes of transport and redox reactions in the newer time step. Final pE output into PRX is given as pE output of the last PHREEQC calculation.

- "Boundary": Defines the implementation of the lower boundary of the column. The algorithm uses one extra cell, numbered n+1, below the modeled column. Its concentration C_{n+1} may be calculated with several options. The general option, valid for all species, is chosen here.
  - "Boundary" equal 1: The transmissive boundary condition is defined.
  - "Boundary" equal 2: The impermeable boundary condition is defined.

Annotation: Boundary

The conditions are defined as:

Transmissive boundary (= 1): $C_{n+1} = 2\,C_n - C_{n-1}$

Impermeable boundary (= 2): $C_{n+1} = C_{n-1}$

The transmissive boundary calculates the gradient between the last two cells and uses the same gradient into the extra cell, allowing diffusion/dispersion across the lower boundary. The impermeable boundary sets no gradient between the second last cell and the extra cell, so there is no transport through diffusion/dispersion across the lower boundary.

A third lower boundary condition option may be set species specific in the input *.PRX file and overrules this general setting. It allows to give any species a constant input

concentration. This is more like the type of boundary condition as for the upper boundary (see "C_input" below).

- "LOG K of OH + H = H2O": It defines the logarithm of the dissociation constant for the equilibrium reaction of water. Only non-negative values are valid for input in *.DAT. Due to the reversed equation the value is positive and for standard conditions (T = 25°, P = 1 atm) 14 instead of the more common form log k = -14 for the equation $H_2O = OH^- + H^+$. This parameter is used to apply the temperature and pressure dependence for the water equation. When PHREEQC is used, an equivalent value should to be used (times minus one) in the file PHREEQC.DAT for this equation. This log k setting in *.DAT effects the CoTReM calculations only in three cases. If "INPUT_OPTION" is set to use pH and pOH for representation of input/output concentrations (instead of using H^+ and OH^- directly). If the option "SET_pH-CONST" is used (to define the corresponding OH^- concentration). Finally the most important use for this value is limited to the case, where PHREEQC is not used. Then, a recalculation of H^+ and OH^- according to the above equation follows the redox reactions.

- "INPUT_OPTION": Allows to provide input data (in *.DAT, *S.PRX) in non-standard units and uses them also for output data.
  - "INPUT_OPTION" equal:
    - 0 ===> MOL/L for all species. This is the standard case.
    - 1 ===> MOL/L for all species, except H+ and OH-. These species are used as pH and pOH.
    - 2 ===> All solid species use g / kg of solid. MOL/L for all aqueous species.
    - 3 ===> All solid species use g / kg of solid. MOL/L for aqueous species, except H+ and OH-. These species are used as pH and pOH.

  For INPUT_OPTION > 0 a matrix of conversion parameters is once created during initialization and applied to all input/output data. The standard units of mol/l are always used within CoTReM for calculation purposes.

- "ADD_OUTPUT": Allows new, additional forms of output.
  - "ADD_OUTPUT" equal:
    - 0 ===> Standard, no additional output.
    - 1 ===> PHR_N
    - 2 ===> IRR, TRA, RED, PHR_N
    - 3 ===> IRR, TRA, RED
    - 4 ===> IRR
    - 5 ===> TRA
    - 6 ===> RED

  The abbreviations IRR, TRA and RED mean additional output in the full *.PRX format is provided. These data represent the species distributions after several calculation steps (operator splitting!) within the last timestep. Immediately after the irrigation calculation, the *.IRR output is provided, after the further transport calculations, the *.TRA output is provided and after the redox reaction calculations, the *.RED output is provided.

  The PHR_N option gives an output for all N cells. This style of output is created by PHREEQC and includes important data like saturation indices, activities, dissociations of masterspecies and more. These N files are listed as *.1 - *.N in the directory specified by

the PRN-file-path (cf. COTREM.INI). Like the *.PRX output all these additional forms of output overwrite former similar output files without warning.

2.2.1.2 Species-specific data in *.DAT

Species-specific data include the name, control parameters, sorption parameters and the concentration value at the upper boundary.

- "Species": Simply defines the name of the specific chemical species. It will be edited with the graphic output option /gs. All listed species are necessary for the program compilation, but there is the choice to set a species active or not active. The compilation generally distinguishes between solid and aqueous species. First there is a number of aqueous species and then a number of solid species. All these species, even inactive, are required by a CoTReM compilation. In addition, there are some species, which need special considerations. These are O(0), N(0), H(0), H, OH, particulate and dissolved organic matter OM/DOM. Neither their names nor their number (order) in the species list may be changed except for redefinition of secondary masterspecies (i.e. O(0) to O_zero).

Otherwise species may be exchanged, if:

- Both are aqueous species or both are solid species.
- The new species is listed in the #element column of PHREEQC.DAT or a mineral defined as PHASES in PHREEQC.DAT.
- All species dependent input data in *.DAT, diffusion coefficients in *.PAR, names in *.SI and most notably the reaction formulations in COTREM.STO for the reaction rates are changed accordingly.

If any problems occur with an exchange of species, please contact the developer.

- "Species active": It defines whether a species is an active part of all processes in a simulation run or not. Additionally, it defines whether aqueous species may adsorb or desorb, solid species are excluded from PHREEQC calculations and a species is displayed in the direct DOS-graphic.

The following settings are possible for "Species active":

- 0: The species is inactive.
  Active species are used in hydrodynamical transport and in PHREEQC. Their mass balance in redox reactions is taken into account.
  Inactive species are nevertheless used in redox reactions and cannot decrease defined maximum reaction rates due to unavailability. It is assumed, that an infinite amount of inactive species is available for redox reaction defined with rates > 0.
- 1: The species is active. Aqueous species may adsorb. The species is displayed.
- 2: Like option 1, but the species is not displayed.
- 3: An aqueous species is active and may desorb.
  A solid species is active only for transport and redox reactions, but it is excluded from the PHREEQC calculations. The species is displayed.

- 4: Like option 3, but the species is not displayed.

The species for solid and dissolved organic matter are never "active" within PHREEQC. Their geochemical reactions and kinetics are purely controlled by the redox reaction part of CoTReM.

Annotation: Inactive and active species

Inactive species are indirectly used in the redox reactions. It is assumed, that an infinite concentration of inactive species is available for specified redox reaction rates. Therefore, an inactive species always allows the full maximal redox reaction rate to be used. If a species is switched to inactive, it must be considered that dependent rates using this species as an educt have to be set to zero, too.

For example, if O(0) and OM are inactive and a maximal redox reaction rate for consuming OM by O(0) is set, the products C(4), N(5) and H will, however, be added (if they are active) to their former concentration with a value of: Maximal redox reaction rate times specific stoichiometric coefficient times time step. This process of creating species will not be stopped by the program. If at least one educt would be active, for example O(0), the availability of this educt O(0), if the concentration vanishes, could stop the process. Note that this conditions must be met in each cell individually. So the creating process would not vanish in the first cell (if $C_0(O(0)) > 0.0$), but usually in a deeper cell, if this redox reaction rates are continually set in the column of cells in sufficient values.

Active species are calculated for all processes of concern and the results are written to the output files.

- "Isotherm": Only aqueous species are affected by this control parameter for sorption. It defines whether an isotherm and which type of isotherm is used.

The value list for "Isotherm":

- 0: No isotherm is chosen. Other isotherm parameters are ignored.
- 1: The Henry isotherm is chosen with P1 to equal Kd.
- 2: The Freundlich isotherm is chosen with P1 equal to k, P2 equal to 1/n and Rate 1 equal to the sorption rate.
- 3: The Langmuir isotherm is chosen with P1(P3) equal to $C_{s,max}$, P2(P4) equal to 1/K and Rate 1 (Rate 2) equal to the sorption rate. Values in brackets apply to a second site of the Langmuir isotherm, if used.

Annotation: Isotherm equations

Henry: $C_s = K_d * C$

Freundlich: $C_s = k * C^{1/n}$

Langmuir: $C_s = [C_{s,max} * K * C] / [1 + K * C]$

with $(dm_{(aq)}^3$ = liter):

C_s	adsorbed concentration [mol / $dm_{(aq)}^3$]
C	concentration in the solution [mol / $dm_{(aq)}^3$]
K_d, k	Henry and Freundlich distribution coefficient [1]
1/n	empirical parameter [1]
$C_{s,max}$	maximal adsorbed concentration [mol / $dm_{(aq)}^3$]
K	bonding affinity [$dm_{(aq)}^3$ / mol]

Two site Langmuir isotherms will simply add the contribution for each site to determine C_s. The sorption rates r have the unit of time inverted. They affect the kinetics of the sorption process.

- "C_input": It defines C_0, which is the constant concentration at the upper boundary. This means continuous input into the column by the transport process advection, while diffusion causes in- or output dependent on the gradient.

- "Rate 1", "P1", "P2", "Rate 2", "P3" and "P4":
  These sorption parameters only affect aqueous species and define the values for the variables explained under "Isotherm" (see above).

- "Standardization factor": It means the 100 % value displayed in the graphic output (often set to C_0). If the value is > 1.0 for the species H and OH, their negative logarithm is shown. That approximates (concentrations used) pH and pOH.

- "GFW": The gram formula weight of the species. It is used in the conversion of aqueous concentrations from mol/l (Transport/Redox) to mol/kgw (PHREEQC) to estimate the weight of one liter solution.
  Solid phases "GFW" are standardly not used, except for solid phase conversions (cf. 2.1) applied per "INPUT_OPTION".

The lines for sorption values are not used for solid species. Instead, the "Isotherm" and "P" lines are used for parameters of mineral kinetics ("Rate" lines have still to be written into *.DAT, they are read, but not used).

Annotation: Mineral kinetics

Mineral dissolution kinetics are usually dependent on the deviation of the solution from equilibrium ($SI_{Set} = 0$). Therefore, kinetics for mineral dissolution and precipitation are defined as a function of Ω (or the SI) within CoTReM. The necessary SI-data are taken from the initial calculation of the solution composition (keyword "SOLUTION") within PHREEQC and then the kinetic functions are applied as rate laws. These rates of mineral dissolution DR or precipitation PR are multiplied by the timestep to define the amount of the mineral to be added to or removed from the aqueous solution composition in each cell and timestep with a PHREEQC calculation.

Two forms of rate laws are so far used in CoTReM. The first one was proposed by KEIR (1980) for use with calcite dissolution rates:

$$DR = k_\Omega \cdot (1 - 10^{(-SI_{Set}+SI_{Mineral})})^n \qquad \text{D-Omega law}$$

It was expanded for precipitation rates to

$$PR = k_\Omega \cdot (10^{(-SI_{Set}+SI_{Mineral})} - 1)^n \qquad \text{P-Omega law}$$

Another form of rate law is basically valid for dissolution and precipitation rates:

$$DR = k_{SI} \cdot (SI_{Set} - SI_{Mineral})^n \qquad \text{D-SI law}$$

and

$$PR = k_{SI} \cdot | SI_{Set} - SI_{Mineral} |^n \qquad \text{P-SI law}$$

with

$$SI_{Mineral} = \log_{10} \Omega_{Mineral}$$

and

$$\Omega_{Mineral} = IAP / K_{sp,\,Mineral}$$

where	DR, PR	[mol / (kgw · yr)]	: Dissolution and precipitation rates
	$k = k_{\Omega} = k_{SI}$	[mol / (kgw · yr)]	: Rate constants for diss./prec. and of certain rate law
	n	[-]	: Reaction order
	$\Omega_{Mineral}$	[-]	: Saturation state of the mineral
	IAP	[-]	: Ion activity product
	$K_{sp,\ Mineral}$	[-]	: Solubility product of the mineral, depends on temperature and pressure
	$SI_{Mineral}$	[-]	: Saturation index of the mineral
	SI_{Set}	[-]	: The saturation index of the mineral, which shall be achieved by the mineral kinetics. Usually, SI_{Set} is chosen to be zero and $10^{SI_{Set}}$ equals one.

- "D_Kin_k": Defines the rate constant in case of dissolution.
- "D_Kin_n_th_power": Defines the reaction order in case of dissolution.
- "P_Kin_k": Defines the rate constant in case of precipitation.
- "P_Kin_n_th_power": Defines the reaction order in case of precipitation.

- "Kin_Type": Defines, if, which and how (per PHREEQC keywords) kinetics are applied.

  - "Kin_Type" equal
    - 0 ==> No kinetics applied.
      Calculation to equilibrium with EQUILIBRIUM_PHASES to SI_{Set}.
    - 1 ==> Kinetics with EQUILIBRIUM_PHASES. Only dissolution.
      Kinetics per OMEGA-law.
    - 2 ==> Kinetics with REACTION. Dissolution and precipitation.
      Kinetics per OMEGA-law.
    - 3 ==> Kinetics with EQUILIBRIUM_PHASES. Only dissolution.
      Kinetics per SI-law.
    - 4 ==> Kinetics with REACTION. Dissolution and precipitation.
      Kinetics per SI-law.

    - 11, 12, 13, 14 ==> Like 1, 2, 3 or 4, but these control parameters include depth dependent values for kinetic rate law parameters per *.KIN-file.

How do kinetics per EQUILIBRIUM_PHASES work (only dissolution) ?
With this PHREEQC keyword the kinetic law sets the maximal amount of solid phase, which is available for dissolution. Surplus amounts are held back within CoTReM. PHREEQC calculates towards equilibrium (or the defined SI_{Set}), but stops the dissolution premature, if all available solid phase is dissolved (ending in subsaturation) instead of reaching equilibrium.

How do kinetics per REACTION work ?
The amount of solid phase calculated per kinetic parameters is simply added or removed from the aqueous solution composition. This approach simulates dissolution and precipitation in general correctly. An exception may occur, for example, if too much of the amount of a mineral is calculated to precipitate by the kinetic law and within one timestep a supersaturated solution is changed to a subsaturated solution (or vice versa). This can occur, because with REACTION the calculation does not stop, lowering the added/removed mineral amount, like with EQUILIBRIUM_PHASES, if equilibrium (or the defined SI_{Set}) is reached.

As mentioned above, a depth-dependent variant of the kinetics is used, if "Kin_Type" is raised by 10 (except option zero). It uses depth-dependent rate constants and reaction orders for the rate laws per *.KIN.

NOTE: If no mineral uses the keyword EQUILIBRIUM_PHASES within a simulation, then the keyword has to be removed completely from *.PHR.

2.2.2 Depth-dependent simulation data in *.PAR

The *.PAR file offers the opportunity to define an inhomogeneous depth resolution of the model column and allows to define the parameters dx, α_L, ρ, ϕ, v_a, log gamma, α_x, D_S and D_B independently for each cell. Values from the *.PAR file replace values from the *.DAT file. The *.PAR file is a tabulator separated ascii file and should be edited in EXCEL.

Annotation: Variable thickness of cells

The column "dx" defines the thickness of cells (dx from DAT replaced). It is possible to define cells with different thicknesses. However, it is recommended due to numerical reasons to use sequentially several cells with the same thickness and smooth gradients of thicknesses.

Annotation: PAR_SAV.XLS

The *.PAR file is needed in CoTReM, but it is advantageous to change data for *.PAR in the EXCEL file PAR_SAV.XLS and then save it as tabulator separated ascii file *.PAR. This EXCEL file contains equations for the diffusion coefficient in water D_0 = D_0 (depending on species, temperature and viscosity of water) in the second row. Additionally, the necessary data input $D_S(x)$ in the columns is modified by porosity P. The used equation is:

$$D_S = D_0 / (1 - \ln(P^2))$$

Of course, the user is free to create a *.PAR file without PAR_SAV.XLS.
Important: The included equations for D_0 are only valid for the chosen units of time and space.

Annotation: Bioturbation

The equations only include the molecular diffusion coefficients. Bioturbation coefficients are simply added for solids (and aqueous species), if needed. They should be the same for each species in a cell. Note the WARNING under "Diffusion coefficient" in 2.2.1.1.

Description of *.PAR:

The first three rows in *.PAR contain pure information, no data of these is read into CoTReM.

First row:	Contains temperature, viscosity of water depending of temperature and information about D_0.
Second row:	Contains information about viscosity, all species dependent molecular diffusion coefficients D_0 in water (depending on temperature and viscosity) for aqueous species and chemical formula for solid species.
Third row:	Contains explanations of the data columns. Species names mean, that the diffusion coefficients are listed below.

Description of the data columns:
The number of rows in the data columns is defined with the number N of cells in column one. It defines the necessary N rows in data columns of other data formats like *.UMS, *.AUR, *.PRX and *.SI.

First column: "Depth"
The number N of cells will be defined by this column.
The first depth value x_0 should be the upper edge of the upmost cell (generally zero). It is used with the first "dx" value to define the first depth x_1 for output files (x_1 = x_0 + 0.5*dx_1). Otherwise, this column is primarily information.

Second column: "dx"
The thickness of each cell is defined.
It calculates depth output (x_n = x_n-1 + 0.5*(dx_n+dx_n-1)).

Third column: "Density"
Defines the density ρ as $kg_{(s)}/dm_{(s)}^3$ of each cell. It is standardly not used, except for solid phase conversions, compare 2.1 and "Density ρ" in 2.2.1.1.

Fourth column: "Porosity"
Defines porosity of each cell. It is standardly not used, except for solid phase conversions. Used for the calculation of diffusion coefficients in sediment in PAR_SAV.XLS.

Fifth column: "v_a"
Defines the "Flow velocity" v_a = v_a of each cell. Compare "Flow velocity" in 2.2.1.1.

Sixth column: "Disp."
Defines the dispersivity coefficient α_L of each cell. Compare "Dispersivity" in 2.2.1.1.

Seventh column: "log gamma"
The "log gamma" values are used in the first time step to determine the pH for PHREEQC with the equation pH = - [LOG_{10} (H+) + log gamma]. Further time steps use the "log gamma" output (PHREEQC) of the time step before. These values are overwritten, if PRX-background concentrations are loaded with the batch option /c <Filename>. Therefore, their values can usually be ignored.

Eighth column: "Alpha_x"
"Alpha_x" defines the irrigation coefficients of each cell. Compare "Irrigation" in 2.2.1.1.

Further columns for all species: "Name"
These columns define the "Diffusion coefficient" in sediment (D_S) for each species and each cell. It consists of the molecular diffusion coefficient for aqueous species and the diffusion coefficient of bioturbation D_B. The bioturbation coefficient should be the same for all species (added to the molecular diffusion coefficient). Compare Annotation: Bioturbation and "Diffusion coefficient" in 2.2.1.1.

2.2.3 Reaction rates in *.UMS/*.AUR and reaction formulations in COTREM.STO

Redox reactions are controlled in CoTReM by specifying depth-dependent maximal redox reaction rates for each cell and reaction. The idea of the algorithm with maximal rates is simple. These rates are defined in *.UMS. Note that rates are not defined for species, but for reactions. They are completely used for a reaction, if no negative concentrations of the educts would result, otherwise the algorithm reduces the used reaction rates. The resulting, actually used rates of a simulation run are written to *.AUR as output.

The change $\Delta C_{(species,\ depth)}$ in the concentration of the species is given by the actually (reduced) rate $R_{(reaction,\ depth)}$ of the reaction, the stoichiometric coefficients of the reaction $SC_{(species,\ reaction)}$ and the numerical time step dt_num:

$$\Delta C_{(species,\ depth)} = R_{(reaction,\ depth)} * dt\_num * SC_{(species,\ reaction)}$$

$\Delta C_{(species,\ depth)}$ is used to calculate the new concentration of the species in the specific cell.

The redox reactions are completely new formulated as full reaction equations compared to CoTAM. COTREM.STO defines the necessary stoichiometric coefficients. Also the C/N/P ratio of organic matter ("OM") may be changed by the user. Compare the file RR_LIST.DOC.

Description of *.UMS/*.AUR:

The first three rows are comments. The first row of *.UMS and the third of *.AUR give the number of the redox reaction (RR-No. and RR(n)). *.AUR gives the date and time when the file was created in the first row and the end of the simulation time in the second row. The *.UMS file lists information about the specific reactions in the second and third row. Compare it with the list of included reaction rates in RR_LIST.DOC.

Description of the data columns for both files:
All data columns consist of N rows.

First column: Depth
The depth of the cell is listed.

Second and further columns: Redox reaction rates (defined maximum rates in *.UMS)
These are a number of columns corresponding to the number of redox reactions actually given in COTREM.STO. The user may add further reactions up to a compiled maximum (50). Compare with the annotations in RR_LIST.DOC.

Important: Only positive reaction rates are allowed. See "Description of COTREM.STO".

The files *.UMS and *.AUR are tabulator separated ascii files and should be edited only in EXCEL.

Description of COTREM.STO:

This file contains all stoichiometric coefficients of all implemented redox reactions and the ratio of the C-N-P distribution for particular and dissolved organic matter ("OM" and "DOM"). The coefficients are read into a two-dimensional matrix. The number of redox reactions times the number of implemented species defines this matrix in CoTReM.

Annotation: C_STOECH.XLS

Changes in COTREM.STO by a user are seldom necessary, but possible. However, there is an EXCEL file C_STOECH.XLS with equations for the gram formula weight (GFW) of organic matter (OM) for the case that the Redfield ratio of 106 C / 16 N / 1 P should be changed. It is advantageous to change values of stoichiometric coefficients in EXCEL, too, if new reactions are added or some are exchanged. Therefore, C_STOECH.XLS serves the same purpose for COTREM.STO as PAR_SAV.XLS for *.PAR. Compare Annotation: PAR_SAV.XLS.

The file COTREM.STO is a tabulator separated ascii file and should be edited only in EXCEL, if C_STOECH.XLS is not used.

The first fourteen lines or rows include commentaries and some special data input. Then a number of rows corresponding to the actual number of included redox reactions follows. Information lines may be added, beginning with R (Compare annotations in RR_LIST.DOC).

First row	: Commentary.
Second row	: Version number of the compilation.
Third row	: Definition of organic matter OM, depending on C/N/P ratio.
Fourth to sixth row	: Values for C/N/P ratio.
Seventh row	: Calculated GFW of OM.
Eighth/ninth row	: Numbers of aqueous/solid species, set by a CoTReM compilation.
Tenth row	: Numbers of actual reactions, defined by COTREM.STO.
Eleventh/twelfth row	: Commentary and Chemical formulas of solid species.
Thirteenth/fourteenth row	: Information on the data columns. Species numbers and names.

Data columns:
The first column, the column between aqueous and solid species and the last column:
They list the number of the redox reaction defined in a row. In addition, C/N/P ratio (or x,y,z) depending reactions consist of four rows with the characters x, y and z listed. Other notes are comments. The first numbers/characters in the first column are important for CoTReM to recognize, which redox reaction the row contains. The numbers have to start at zero counting upwards to the actual number of reactions minus one.

Other columns:
They correspond to one species each. The stoichiometric coefficients of the species for the redox reactions are listed as defined by the number in the first column.

Important: Negative coefficients mark educts and positive coefficients mark products of the reaction. Only positive reaction rates are allowed, therefore each reaction included is formulated in a one-way-type.

Most coefficients are taken directly. However, a real stoichiometric coefficient SC(n) of a x-y-z dependent reaction is calculated in four rows as sum of:

$$SC(n) = SC(n = \text{numbered row of the reaction}) + x * SC(x\_n) + y * SC(y\_n) + z * SC(z\_n)$$

With this concept each row (or four rows) is used to provide the necessary data for one redox reaction. Together with the reaction rates in *.UMS for each cell the effect of these reactions is simulated over the whole modeled column.

2.2.4 Setting thermodynamical equilibria conditions in *.PHR and *.SI for PHREEQC

It is required that the *.PHR file has to follow the agreements of PHREEQC. Therefore, most important information on the *.PHR file can be derived from the user's guide to PHREEQC (PARKHURST, 1995).

However, there are some special considerations for the use of PHREEQC within CoTReM. Two CoTReM subroutines are connected to PHREEQC source code. The first one is needed for the initialization of internal structures of PHREEQC and uses the given values in *.PHR. The initiated calculation and their *.PHR input data have no meaning for CoTReM results, but if it is not calculable by PHREEQC, the initialization fails, too. Usually the user fills *.PHR with C_0 concentrations. Such concentrations are usually able to initialize the structures in PHREEQC correctly for CoTReM.

The calculations for all cells and timesteps (= the CoTReM results) are within the second subroutine. This method requires some rules for a CoTReM useable *.PHR.

PHR-File-Rules:

1: "units" has to be mol/kgw. PHREEQC uses this unit. Conversion of concentration units to mol/l is done within CoTReM.

2: "pH" and "pe" need to be specified with values.

3: All active aqueous species, with the exception of "H", "OH" and "DOM", have to be listed with the PHREEQC element name including their appropriate redox state in brackets under the keyword "SOLUTION". These formulations correspond to and differentiate between primary and secondary PHREEQC masterspecies, which define one PHREEQC element. Only pure primary masterspecies need no redox state. "DOM" is never used in PHREEQC. "H" and "OH" are never defined, instead "pH" is defined. "H" and "OH" need always to be active with PHREEQC calculations. In addition, the special species "Zp" and "Zm" have to be added in sufficient concentrations for correct charge balance.

4: All active aqueous species, with the exception of "DOM", have to be listed with their species formula used in the transport and redox modules under the keyword "REACTION" in the correct order defined by the *.DAT file. This formula is NOT the PHREEQC element name, but usually the PHREEQC masterspecies formula. In case of charged species, this formula needs to be balanced with the special species "Zp" and "Zm". In example, the species HCO_3^- (exception: Its PHREEQC primary masterspecies is CO_3^{2-}) with the PHREEQC element name C(4) has to be balanced and noted as HCO3Zp (neutral with respect to charge) under "REACTION".

5: All PHREEQC active solid species, with the exception of "OM", have to be listed with their PHASES-name either under the keyword "EQUILIBRIUM_PHASES" for

A) normal calculations towards a saturation index SI
B) kinetics with "EQUILIBRIUM_PHASES"
or otherwise under the keyword "REACTION" below all active aqueous species (order defined by *.DAT) in case of
C) kinetics per "REACTION".

WARNING !
The PHREEQC options of "alternative formula" and "alternative phase" are not guaranteed to work correctly in case A and case B (A could work out the equilibration correctly, but the source code was not adapted to handle the concentration balances of the solid equilibration phase and an alternative phase/formula). In case C another phase/formula under "REACTION" will work correctly. However, the interpretation has to be changed. See Appendix E.

6: The "REACTION"-keyword block may end with the default unit "1.0 moles" only.

7: The "charge" option should be selected. The option "charge" removes the charge imbalance produced by transport, but the addition/removal of the "charge"-species means an equivalent mass difference within the initial calculations of PHREEQC (keyword "SOLUTION"). The option is recommended and should be applied to charged, but chemically inactive species for the given problem. Use "Na" or"Cl" in marine simulations, otherwise consider also "Mg". The used species needs a sufficient concentration along the whole column.
Using "charge" with pH is not recommended.

IMPORTANT:
Set the diffusion coefficients of the "charge"-species to zero to suppress its transport.

The other possibility is to calculate without the charge option. In this case, the possibly large initial charge imbalance is simply calculated by PHREEQC per "SOLUTION" (use "ADD_INPUT" with PHR_N to display the charge imbalance). PHREEQC calculations do not remove this imbalance without the charge option, they are, correctly, conserved within PHREEQC and modified by transport contributions only. The disadvantage is, that the high level of charge imbalance, compared to the charge option, may cause a little bit less accurate results for other calculations within PHREEQC. If the transport of a "charge"-species is not suppressible (see above; e.g. in case of "Flow velocity" > 0), this "no charge" option could be very useful.
The concentration of the "charge"-species without suppression of its transport may oscillate, indicating numerical problems, due to its transport and its purpose to balance charges. Hint: Always display a charge option species.

8: All listed aqueous species have to be defined with concentrations above 1.0E-14. Otherwise, PHREEQC does not initialize them. 1.1E-14 can be used as minimum value.

Saturation indices SI and the amounts of solid phases need not to be defined for the initialization calculation. Default in PHREEQC is SI = 0.0 and amounts of 10 mol solid phase related to the unit of one kilogram water (kgw) in the solution.

CoTReM calculations use actual calculation data for pE, pH, aqueous and mineral concentrations (at start from *S.PRX). Exception: A minimum of 1.1E-14 mol/l is applied for aqueous species due to initialization needs. The used SI is defined as zero or depth and mineral dependent per *.SI-file (see "SET_SI_Zero").

"density" and "temp" should be defined, otherwise the PHREEQC defaults are used.

Description of *.SI:

The *.SI file allows the definition of depth-dependent SI-values for each mineral according to the prechosen depth resolution. It consists of a comment line first. The version of CoTReM is listed in the second row.

The third row describes the columns. The mineral names follow the order defined by the *.DAT-file and includes even inactive ones and the in this regard unusable "OM".

Data columns consist of N rows:
First column: The depth resolution from *.PAR, but with N cell numbers instead of the depth value.
Further columns: These are the columns according to the number of solid phases in CoTReM. Species and depth dependent saturation indices are listed. These are used in the PHREEQC calculation.

The *.SI file is a tabulator separated ascii file and should be changed only in EXCEL.

2.2.5 Graphic input of measured data in *.EXP

CoTReM provides a way to display measured data of a species on a direct graphic output. The necessary data are contained in the *.EXP file.

Description of *.EXP:

Rows one, two and four are commentary for the data below. Row three contains the standardization factors for the data in columns two and four. These standardization factors should be the same as in the *.DAT file for comparison purposes.

From row five downwards, the measured data are defined in the data columns. The number of data pairs need to be the same for breakthrough curve values and depth distribution values. Data values not in use get a default concentration of -100000 and a time or depth of zero.

Data columns:
First column: Defines time (x-value) for the breakthrough curve.
Second column: Defines concentration (y-value) for the breakthrough curve.
Third column: Defines depth (x-value) for the depth distribution.
Fourth column: Defines concentration (y-value) for the depth distribution.

A maximum number of 500 measured data pairs or rows in the data columns may be shown.

2.2.6 The input and output file *.PRX

The *.PRX file contains the concentrations of all species and adsorbed species (for up to two sites) in each cell. Additionally, the pE and log gamma of H^+ are defined, alkalinity "ALK" and the unit conversion factor "mass_water" (mol/l <=> mol/kgw) are given as output. All are noted depth dependent in each cell. Furthermore, a species dependent lower boundary condition may be set for the concentration in solution. The file can be used as input (name it *S.PRX, see 1.3), if the user wants to start with a given concentration distribution or a fixed boundary condition for specific species or a pe distribution different from PHREEQC default 4.0. The format is also used for the corresponding output file (named *.PRX). Starting a new simulation without *S.PRX creates a PRX-file with the correct format. This can be used as input file for further simulations. Values should be edited in EXCEL and a macro should be run afterwards (see below).

Note: Files used as input are usually named *S.PRX to distinguish between (S for starting) the output files. Output files like *.PRX overwrite former files with the same name regardless of confirmation.

The output is organized in data blocks. There is one data block for each species and the first data block is for the pe, log gamma of "H^+", the alkalinity and the conversion parameter mass_water m_w (C [mol/l] = m_w C [mol/kgw]).

The species boundary condition is controlled by two values in each species data block. It is switched on/off with the first, while the second sets the constant concentration value for the extra cell below the boundary. Compare "Boundary" in 2.2.1.1.

The pe, or "pE" as listed here, and the lgamma H+ values are used as PHREEQC input. Compare "pE-Handling" in 2.2.1.1.

Description of *.PRX:

Two rows are comments. The third row lists the simulation time. Then the data blocks follow.

First data block: "pE"

First row:	Empty.
Second row, first column:	The name "pE".
Second row, further columns:	Column information. See below.
Further N rows:	Data columns.
First column:	Empty.
Second column:	Depth is listed.
Third column:	The "pE" is listed.
Fourth column:	log gamma H^+ is listed.
Fifth column:	Alkalinity output.
Sixth column:	mass_water output.

Fifth and sixth column are not necessary for input.

Further data blocks: Each species has one data block.

First row: Empty.

Second row, first column: "Name of the species" from *.DAT, solid phases use their PHASES names and not the chemical formula.

Third to (N+2)-th row: Data columns.

- First column: Empty.
- Second column: Depth is listed.
- Third column: The concentration of the species is listed.
- Fourth column: The concentration adsorbed at the first site is listed. Zero for solid phases.
- Fifth column: The concentration adsorbed at the second site is listed. If sites are not used, the value is zero. For solid phases is the SI listed in case of kinetics.

(N+3)-th row: Empty.

(N+4)-th row: Species boundary condition.

- First column: Empty.
- Second column: Switch.
  - Zero = Off.
  - One = On
- Third column: Constant concentration in extra cell (N + 1), if switched on.

The *.PRX file ends with the data block of the last included species listed.

The *.PRX file is a tabulator separated ascii file and should be edited and changed only in EXCEL with a special macro used afterwards.

The following FORTRAN formats are used:
All species names use "A21". This gives the maximal length of a species name. Depth is given with "PE11.4" and variables in the "pE" data block and the SI use "E11.4". Time and all concentration in the species data blocks use "PE11.5".

Therefore, editing and changing concentrations, pE or time values for further use in CoTReM requires caution. EXCEL has usually a standard of two decimal places following the decimal point. It will apply this standard if any *.PRX data value is changed in EXCEL. The CoTReM *.PRX file needs five decimal places following the decimal point. Otherwise, an error occurs. Therefore, EXCEL must be forced to use the correct formats, when all changes are done and the file is saved. In addition, the width of EXCEL columns usually disturb this process.

WARNING !!!
EXCEL (or any other used spreadsheet software) needs to use the sign "dot" as decimal point of the double precision numbers in *.PRX (and other formats). A general EXCEL setup using the sign "comma" as decimal point and the sign "dot" to mark the decimal place "thousand" stops the program CoTReM with a (misleading) error message: "*ERR* IO-07 bad character in input field".

Forcing the *.PRX format:
First: The user edits all changes in the file.
Second: The user starts an EXCEL macro (or uses the commands manually).
Third: Then the user saves the file in EXCEL as tabulator separated ascii file with the end of the filename as *.PRX (EXCEL standard suggest *.TXT, the user has to overwrite it).

Annotation: The PRX macro

First command:	Mark the columns B to E (the second to fifth column, which contain all numbers).
Second command:	Open format menu. Choose cells. Choose numbers. Set a user defined format for numbers to "0.00000E+00".
Third command:	Open format menu. Choose columns. Set optimal column width.
Fourth command:	Mark the cell "A2". This is optional and used to unmark the columns.

This set of commands can be recorded and included as macro in EXCEL.

The PRX macro used in the German Microsoft EXCEL version 5.0 is listed as:

```
Sub PRX()
 SpalteListe("B:E").Auswählen
 Auswahl.Zahlenformat = "0,00000E+00"
 Auswahl.GanzeSpalte.OptimalAnpassen
 Bereich("A2").Auswählen
Ende Sub
```

2.2.7 The output file *.PRN

The *.PRN file contains the output data of a breakthrough curve. The data consist of time and the number of exchanged pore volumes on the one hand. On the other hand the concentration at the end of the column and this concentration in relation to C_0 is given for each species.

Description of *.PRN:

The first four rows are commentaries. The fifth row contains the species numbers (for two columns each), starting at zero, whereas the sixth row contains the descriptions for the output data columns.

First column:	The simulation time is listed.
Second column:	The exchanged pore volume is listed.
Further uneven column numbers:	The species concentration at the end of the column is listed.
Further even column numbers:	The species concentration in relation to C_0 is listed.

The number of rows depends of the simulated time and the control parameter "dt". Compare "dt" in 2.2.1.1.

The *.PRN file is a tabulator separated ascii file and should be edited in EXCEL.

Important: The *.PRN output is only written if the command option "/o" is defined by the user in the batch file. This option was chosen, because the output file will grow during the simulation time, producing in some cases gigantic files.

2.2.8 The input file *.KIN

The use of this CoTReM-option is controlled with the solid phase parameter "Kin_Type" (see Annotation: Mineral kinetics for more details).

The *.KIN-file is used to apply depth dependent parameters for mineral kinetics. The path of this file is not controlled by cotrem.ini, instead CoTReM expects to find the *.KIN file under the same path as the *.PAR-file. The format for *.KIN is comparable to the *.PRX-file.

Description of *.KIN:

Two rows are comments. Then data blocks for each solid phase follow.

Data blocks of kinetic parameters: Each species has one data block.
- First row: Empty.
- Second row, first column: "Name of the mineral" from *.DAT (PHASES name). Includes even the unusable OM.
- Second row, second to seventh column: Description of the mineral kinetics parameter for each column (see below).

Third to (N+2)-th row: Data columns.
- First column: Depth.
- Second column: D_kin_k, the dissolution rate constant is listed.
- Third column: D_kin_n_th, the dissolution reaction order is listed.
- Fourth column: D_kin_extra, a dissolution rate law parameter.
- Fifth column: P_kin_k, the precipitation rate constant is listed.
- Sixth column: P_kin_k, the precipitation reaction order is listed.
- Seventh column: P_kin_k, a precipitation rate law parameter.

The extra rate law parameters as well as the pH value are not used in CoTReM rate laws, yet. They are available for additional rate laws, which may be defined using up to three (k, n_th, extra) free parameters (other than the SI and pH). Contact the developer if further rate laws are needed.

The *.KIN file ends with the data block of the last included mineral species listed and is a tabulator separated ascii file which should be edited and changed only in EXCEL.

Appendix A: Principles of CoTReM

A.1 General description

The computer software CoTReM (LANDENBERGER, 1998) is based on the model CoTAM (HAMER AND SIEGER, 1994). Both models are able to model non-steady state conditions by setting the time step variable to an eligible constant value during a current simulation. The simulation of one-dimensional geochemical problems including transport phenomena like sedimentation, advection, dispersion, diffusion, bioturbation, bioirrigation as well as reactions of reoxidation, dissociation, complex-formation, dissolution and precipitation is possible in CoTReM. The incorporation of the model PHREEQC (PARKHURST, 1995) is one key-element of the reaction part.

CoTReM is easily modifiable to a new set of species. Appendix I shows the current standard set of species compiled for use with CoTReM version 2.3.0 (and 2.3.1). Incorporating additional redox reactions or exchanging species is possible for the user with minor restrictions (Appendix J).

The modeling approach solves the General Diagenetic Equation (Eq. A_1, homogeneous one-dimensional case for a cell) as proposed by BERNER (1980) by the technique of operator-splitting. It describes the transport and chemical reactions of species in porous media. Porosity is handled below as a constant factor in each porewater concentration C.

Why can it be handled like that despite time and spatial derivatives? First, even for long time spans modeled, the constancy of porosity in each cell is the usual case. If not, split the modeled time span into several time spans, where the condition "porosity constant" is fulfilled for each cell. Second, the used spatial Taylor series approximations to yield difference terms from the differential terms of the PDE (A_1) depend only on porosities of neighbouring cells. Differences in porosity of adjacent simulation cells are assumed to be negligible in CoTReM. That leads to the independence of porosity in the equation.

Species conc. ↓ Diffusion and Dispersion ↓

$$\partial_t C_i = -\partial_x\left(v \cdot C_i\right) + \partial_x\left(D_i \cdot \partial_x C_i\right) + \alpha_x\left(C_{0,i} - C_i\right) + R_i\left(C_1, \ldots, C_{n_i}\right) \qquad \text{(A\_1)}$$

↑ Sediment advection ↑ Bioirrigation ↑ Reactions

where the unit is mol/(l · a), $i = 1, \ldots, n_i$, C_i is the concentration of the i^{th}-species in porewater (even for solids, cf. Appendices K and L), t is time, D_i is the apparent diffusion coefficient (i^{th}-species; $D = D_{mol} + v_a * \alpha_L$) in sediment (molecular plus dispersion), x is sediment depth, R_i is the reaction rate of the i^{th}-species (source term), v is the sedimentation rate (applied to all species) and/or the flow velocity (v_a applied to aqueous species), $C_{0,i}$ is the input boundary concentration (bottom water in sediment) of the i^{th}-species, and α_x is the exchange coefficient of non-local transport at depth x.

The model separates the model area into discrete numerical steps or cells (with variable thickness). The time-discretization uses a defined time step, which allows non-steady state calculations with CoTReM. Both discretizations have to be chosen with respect to the numeric stability criteria of Courant, Neumann and Peclet (e.g. COLLATZ, 1966; BEAR, 1979; KINZELBACH, 1987). For the numerical calculation all partial differential equations (PDE's)

have to be translated to partial difference equations. CoTReM uses approximations following the Taylor series.

A.2 Operator-splitting
The operator-splitting (OS) approach (e.g. YANENKO, 1971, SCHULZ AND REARDON, 1983) divides the General Diagenetic Equation. The parts are PDE's for the different, independent processes. These less complex PDE's are easier to solve and they are applied sequentially.

A mathematical description uses operators O for the processes, the species concentration matrix C for the status of geochemical system at a defined time and the changes $\partial_t C_{operator}$ to modify the status of the geochemical system:

$$\partial_t C_{operator\ O} = O \cdot C_{before\ using\ operator\ O} \qquad \text{(A\_2)}$$

$$C_{before\ using\ operator\ O} + dt \cdot \partial_t C_{operator\ O} = C_{after\ using\ operator\ O} \qquad \text{(A\_3)}$$

CoTReM's general calculation principle using OS is illustrated in ADLER ET AL. (2000A).

A.3 Transport processes
The process of non-local mixing of solutes (bioirrigation) is applied by:

$$\partial_t C_i = \alpha_x \left(C_{0,i} - C_i \right) \qquad i = 1,\ldots,n_i \quad \text{mol} / \left(1 \cdot \text{a} \right) ;\ 0 \le \alpha_x \le 1 \qquad \text{(A\_4)}$$

This process is applied only to aqueous species.

The dispersion/diffusion/bioturbation and advection/sedimentation processes are applied by:

$$\partial_t C_i = -v \cdot \partial_x C_i + D \cdot \partial_x^2 C_i \qquad i = 1,\ldots,n_i \quad \text{mol} / \left(1 \cdot \text{a} \right) \qquad \text{(A\_5)}$$

With v and D constant in a cell (but $D = f$(porosity $= f$(depths)) different in different cells) for each species. These transport processes are solved simultaneously as linear finite-difference equation system for all cells by a variant of the Thomas algorithm (PRESS ET AL., 1992) with a Crank-Nicholsen difference scheme regarding time discretization.

Boundary conditions
A Cauchy-boundary condition allows advection and diffusion over the sediment - bottomwater boundary. It is applied through fixed bottomwater concentration C_0 for each dissolved species or, similarly, a fixed concentration C_0 reaching the sediment in case of solid species.

The lower boundary condition is given by setting species concentrations into an extra cell (n+1) below the model area. The diffusive behaviour may be chosen generally (the same for all species) as transmissive ($C_{n+1}=2 \cdot C_n - C_{n-1}$) or impermeable ($C_{n+1}=C_n$). Additionally, species-specific concentrations of fixed values may be set in this extra lower boundary cell quite similar to the Cauchy-boundary condition of the upper boundary.

A.4 Chemical reactions

The operators R_i

$$\partial_t C_i = R_i\left(C_1,\ldots,C_{n_i}\right) \qquad i = 1,\ldots,n_i \quad \text{mol}/(1\cdot \text{a}) \tag{A_6}$$

describe the total reaction rate of the i^{th}-species. They may have contributing rates of sorption reactions, of redox reactions and of thermodynamical equilibria reactions (PHREEQC; PARKHURST, 1995).

Sorption reactions

In contrast to the operator splitting approach ad- and desorption processes are not separately calculated in CoTReM. Instead a non-linear modification was used to include isotherm dependent sorption laws with sorption kinetics into the calculation algorithm of diffusive/advective transport. Cf. **"Annotation: Isotherm equations"** within the CoTReM User Guide, SIEGER (1993) and HAMER AND SIEGER (1994).

Redox reactions

The concentration change $dt\cdot\partial_t C_{i\ (\text{species, depth})}$ by redox reactions is calculated by the sum of actual rates $R_{(\text{reaction, depth})}$ of reactions, the stoichiometric coefficients $SC_{(\text{species, reaction})}$ (educt species coefficients are always multiplied by minus one for these calculations) of these full reaction equations and the numerical time step *dt*:

$$dt\cdot\partial_t C_{i\ (\text{species, depth})} = \Sigma_{\text{reaction}}\left(dt\cdot SC_{(\text{species, reaction})}\cdot R_{(\text{reaction, depth})}\right) \tag{A_7}$$

The redox calculations are driven by the concept of maximum reaction rates R_{Max}. These rates are defined depth-dependent for each reaction by the user and they are always positive to define a reaction direction. They translate directly into the actual rates $R_{(\text{reaction, depth})}$, if all total species reaction rates $R_{i,Redox}$ have non-negative concentrations C_i as results. Otherwise, the rates R_{Max} are reduced by the algorithm to avoid negative concentrations. If multiple reactions compete for a educt species, the concentration is distributed between these reactions. Each competing rate R_{Max}, which itself is higher than the corresponding maximal possible total species reaction rate $R_{i,Redox}$, is first reduced to a value leading to zero concentration, if imaginary applied alone. The actual reaction rates $R_{(\text{reaction, depth})}$ are distributed equally from these (new) maximum reaction rates R_{Max}. The species H^+ and OH^- are always formulated as products, thus, their concentrations can increase but never decrease within redox calculations. This inhibits non-realistic R_{Max} reductions for these species.

If a CoTReM calculation without PHREEQC is used, the algorithm adjusts the concentration by the equation:

$$K(H_2O) = C(H^+)\cdot C(OH^-) \tag{A_8}$$

This approximates the H^+ concentration for a pH-calculation. However, brackets refer to concentrations instead of activities in this case and no other species dissociations are calculated. These important calculations for an exact pH remain inherent to CoTReM calculations with PHREEQC.

Thermodynamical equilibria reactions (PHREEQC)

The PHREEQC contributions $R_{i,PHREEQC}$ to the operators R_i are included by incorporating PHREEQC (PARKHURST, 1995) as a subroutine in CoTReM. The calculation actually includes all changes in a timestep for each cell, whether caused by transport, redox reactions or equilibria reactions. The complete condition state of the simulation from the beginning of the time step (saved) is given to the initial calculations of PHREEQC caused by the keyword "SOLUTION". These data are basically all species concentrations, the pH and predefined mineral saturation indices SI_{Set} to equilibrate to (usually $SI_{Set} = 0$). They are written into program structures of PHREEQC. PHREEQC uses ion activities for all species to calculate dissociations and mineral equilibria with real dissociation and solubility constants (NOT apparent constants!!!). The initial part "SOLUTION" calculates the deviation to charge neutrality and balances it optionally by adding/removing a charged species. The calculation output of saturation indices from this initial step is used for determination of sub-/supersaturation of minerals (if dissolution/precipitation kinetics are used; see below). Additional input for the PHREEQC subroutine in CoTReM comes from the database and the input file of PHREEQC. The CoTReM user controls the simulated processes via keywords in the input file. An essential calculation is the addition/removal of elements corresponding to neutral, uncharged element formulas with the keyword "REACTION". This option is necessary to include the changes of species concentrations already calculated by transport/redox when the initial "SOLUTION" step is done. Each species is represented by its corresponding element formula (e.g. species HCO_3^- as formula HCO_3) plus one special element for charge neutrality, if the species is charged. The two special "elements" Zp and Zm were defined in the used PHREEQC database with negligible gram formula weight (10^{-12}). Because they were defined to exist only as ions Zp^+ and Zm^-, they mean essentially a positive and a negative charge used to apply electroneutrality to charged species to yield a neutral formula (e.g. the species HCO_3^- is represented as formula HCO_3Zp, using formula HCO_3 alone neglects the charge and causes errors).

However, the main reason to include the subroutine into CoTReM is the ability of PHREEQC to calculate dissolution or precipitation of mineral phases in relation to defined mineral saturation indices. Usually, the calculation aspires to equilibrium ($SI_{Set} = 0$ defined). The keyword "EQUILIBRIUM_PHASES" defines mineral phases (so far, gas phases are excluded for use with CoTReM) with the desired SI's and their available amounts (related to the solution composition of one kg water; see below). These mineral phases are equilibrated to the solution composition created by the keyword "SOLUTION" (and modified by "REACTION").

Therefore, PHREEQC makes one recalculation of the initial solution composition for the modifications applied by "REACTION" (transport/redox) and "EQUILIBRIUM_PHASES" (mineral equilibria or equivalent kinetic method), which maintains charge conservation. The calculation uses the ion activity product *IAP* in relation to dissociation constants $K_{Species}$ and solubility products $K_{sp,\,Mineral}$ to equilibrate the mineral phases to all ions and complexes in the modeled porewater solution composition.

These PHREEQC calculations (per "REACTION" and "EQUILIBRIUM_PHASES") use amounts (mol) of the aqueous species and mineral phases to describe the quantity, which is added/removed or dissolved/precipitated. However, we are able to interpret this substance amounts effectively as concentrations due to the PHREEQC method to relate the initial solution composition always to one kg of water (for use with CoTReM, this standard unit is

"fixed"). This applies even for the resulting solution composition within CoTReM calculations, because no PHREEQC keyword which evaporates or adds water is used.

This "EQUILIBRIUM_PHASES" concept uses instantaneous equilibration, which means infinite kinetics, and imposes no kinetic restrictions to the reaction (except for mineral availability in case of dissolution). The calculated dissolution and precipitation (and their rates) only depend on the relation between the predefined desired SI_{Set} and the quotient of the ion activity product ($IAP_{Mineral}$) and the solubility product $K_{sp,\ Mineral}$.

Kinetics of dissolution and precipitation reactions in CoTReM
Recent developments for CoTReM allow to perform dissolution/precipitation kinetically modified with PHREEQC. Two methods are available and both use the resulting mineral SI's from the initial calculation by "SOLUTION". The method per "EQUILIBRIUM_PHASES" allows only dissolution kinetics by limiting the available amount of the mineral phase prior to the calculation of the kinetically modified equilibration. This limited phase amount is defined according to the SI from "SOLUTION" and the chosen parameters of the used kinetic rate law. Precipitation will always occur completely without kinetic restrictions with this keyword. The method per "REACTION" uses the same initial calculated SI and kinetic rate law parameters to define prior to the calculation of the kinetically modified equilibration a mineral amount, which is simply added to (dissolution) or removed from (precipitation) the one kgw porewater initial solution composition with this keyword to yield the new kinetically equilibrated solution composition. The method per "REACTION" has the advantage of precipitation kinetics. Its disadvantage is the irrevocable fixed mineral amount to add/remove prior to the new equilibration due to the SI from "SOLUTION", because, due to the modifications in the solution composition per transport/redox reactions of aqueous species (like the mineral equilibration applied after the initial part "SOLUTION"), precipitation may be required instead of the predefined dissolution (or vice versa) in worst case examples. In contrast, the method per "EQUILIBRIUM_PHASES" does not suffer from this problem, because it will stop a dissolution, if the desired SI is reached by dissolving less than the predefined mineral amount (remnants are reapplied to CoTReM's mineral concentrations). This condition revokes in this method the amount defined by the used kinetic rate law, while the order from the rate law cannot be revoked with the "REACTION" method. Nevertheless, the "REACTION" method is more versatile (cf. also Appendix E) and useful for kinetics, because, in a correctly used modeling approach, sufficient small timesteps and many iterations are needed anyway for these calculations and reduce the possible errors inherent to this method to an insignificant order. The "EQUILIBRIUM_PHASES" keyword is still needed for the equilibrium calculations without kinetic restrictions.

While these keywords control the method to implement kinetics into the PHREEQC subroutine of CoTReM, the mineral amount dissolved or precipitated during this kinetically modified equilibration is controlled by the kinetic rate law. Rate laws capable to define non-infinite kinetics for dissolution- (DR) and precipitationrates (PR) are implemented into the PHREEQC subroutine of CoTReM. The rates R [mol/(kgw · a)] define the change in concentration dC [mol/kgw] within a timestep dt [a] as amount [mol] of the mineral phase dissolved to or precipitated from the PHREEQC solution composition of one kilogram water [kgw] according to:

$$dC = DR \cdot dt \quad \text{or} \quad dC = PR \cdot dt \tag{A_9}$$

These precalculated concentration change by the rates R (DR or PR) is applied by the two methods mentioned above. Kinetic rate laws define the rates usually as functions f of the

mineral's saturation state $\Omega_{Mineral}$ (or its saturation index $SI_{Mineral}$) and the desired saturation state $\Omega_{Set,Mineral}$ (or index $SI_{Set,Mineral}$), which is usually the equilibrium.

$$R = f(\Omega_{Mineral}, \Omega_{Set,Mineral}) \quad (A\_10)$$

The **"Annotation: Mineral kinetics"** within the CoTReM User Guide describes the by now two implemented kinetic rate laws and their fit parameters. An extension to further rate laws consistent of fit parameters, pH, the saturation indices from "SOLUTION" and the predefined $SI_{Set,Mineral}$ is easily possible.

Whether kinetical modifications or pure mineral equilibrations are used, the time step ends following these PHREEQC calculations for all cells. The concentrations of the porewater solution and the mineral concentrations are updated in CoTReM.

Appendix B: The transport of solid phases

Solid phases were not considered as species within CoTAM and earlier versions of CoTReM included for them only cell dependent mass balances. The basic idea for solid phase transport is simply to extend the existing transport algorithms for solutes to solids. The advection algorithm is used to regard sedimentation and the diffusion algorithm is used to regard bioturbation of solids. Both processes work due to smaller values for bioturbation coefficients and sedimentation rates on longer time scales than diffusion/dispersion and groundwater advection. However, while these processes important to solid phases are generally simulateable with the same algorithms, several control parameters and changes were necessary to consider the small, but sometimes essential differences. Especially, three species control parameters differentiate between the species, which are applied to processes. If all compiled species are applyable, this is indicated by nTt, nT indicates aqueous species only and nTs indicates solid species only. Additionally, the fixed order of species in *.DAT allows to specify a certain species (see Appendix C).

In the case of bioturbation, the algorithms needed no modifications, but a special consideration has to be made by the user regarding the upper boundary. In general, the bioturbation coefficient is simply added in *.PAR to the molecular diffusion coefficient for solutes (or disregarded, if it is relatively small) and solids (added to zero; essential for bioturbation).

There is an exception: Solid phases should still have a bioturbation coefficient of zero for cells within the water column or responsible for the bottom water/sediment interface. The bioturbation (and diffusion) coefficients within a line in *.PAR are responsible for the transport flux of these processes into the cell described by the line in *.PAR directed from the cell above (or for the first cell from the upper boundary concentrations C_0, which is usually the important case, because (marine) systems are often defined with the first cell as first part of the sediment and apply, thus, bottom water concentrations for C_0). Solid phases cannot be mixed as net effect from bottom water per bioturbation to the sediment (according to a C_0 value for sedimentation of the solid; see below) or, due to the real gradient across the bottom water/sediment interface for solids, vice versa. Nevertheless, the first line of bioturbation coefficients *.PAR is not overwritten due to CoTReM 2.3 with a constant value of zero to inhibit user errors regarding this consideration, because the user may not agree with this idea of bioturbation across the boundary or a simulated model area may be set totally, including

the area directly above the upper boundary, within porous, solid media and not adjacent to water.

WARNING! (summarized from above):
The first line of bioturbation coefficients in *.PAR has to be zero.

Sedimentation causes a bottom water/sediment interface to be transferred with respect to a certain water depth (neglecting position changes of the ocean/atmosphere interface). However, porewater sediment geochemistry is dominated by the relative distance to the bottom water/sediment interface and not to the absolute distance from a water depth. Therefore, the sedimentation causes a change in the usual system of coordinates regarding marine applications (depth zero is the sediment interface, increasing depth into the sediment) and can, thus, be seen and simulated as slow advective transport process into the sediment for sedimenting solid phases (and solutes present in the bottom water enclosed by sedimenting solids, negligible in comparison to molecular diffusion but included in CoTReM).

This sedimentational advection is applied to all species, while groundwater advection according to v_a is applied only to aqueous species. The difference is included into the source code due to different variables for sedimentation w, flow velocity v_a and the species control parameters. The supply of sedimenting solid species is indicated by the upper boundary concentrations C_0, which are sedimented into the first cell according to the advection algorithm. Therefore, use the parameters porosity and density of the first cell for unit conversions of solid phases C_0 (see Appendices K and L).

Pure sedimentation w as transport of solids (without bioturbation) violates the Peclet criterium, because D equivalent to zero causes P_e ($P_e = w \cdot dx\_num / D$) to approach infinity for $\lim D \rightarrow 0$ and the criterium $P_e \leq 2$ cannot be fulfilled. This is even difficult with some bioturbation included. Therefore, sedimentational solid species transport is always subject to high numerical dispersion.

The relative amount of numerical dispersion is also an important property, as well as the mass balance property, for two different Taylor series approximation concepts (transforming differential to difference equations) to include the advection processes. The approach for the diffusion like processes is well covered by the Central-Taylor-Series approximation, which takes both cells adjacent to the calculated cell into account ($\partial C/\partial x\,|_x \cong [C_{i+1}(t) - C_{i-1}(t)] / 2\,\Delta x$), because diffusion like processes work universally to all directions and are in the net effect gradient driven. The same approximation was formerly the only one used in CoTAM/CoTReM to include advective processes. It is successfully used modeling groundwater breakthrough curves due to relatively small numerical dispersion effects and a small Peclet number, but it introduces a deviation in the mass balance (especially clear perceptible and troublesome in solid phase transport), because the advection works toward one prime flow direction and not universally gradient driven. The Backward-Taylor-Series approximation ($\partial C/\partial x\,|_x \cong [C_i(t) - C_{i-1}(t)] / \Delta x$) or "Upwind scheme" (cf. STEEFEL AND MACQUARRIE, 1996) avoids to include into a cell's calculation the cell adjacent in the advective flow direction, which is responsible for the mass differences in the Central-Taylor-Series approximation concept. Due to the varying advantages of both approximation concepts, a choice is introduced in CoTReM for the concept used (cf. "Type of advection" in 2.2.1.1).

The mass balance effect and numerical dispersion is illustrated in the tables BT_1 (central) and BT_2 (backward) below, which start at time step zero with a normalized concentration peak in one cell (others are zero) and show progressive with the calculated time steps in each

line the distribution of the concentration peak as fraction of one caused by pure sedimentation and numerical dispersion. An EXCEL sheet was used for the calculation of the table values and a variable PV for the exchanged pore volumina of the simulated cell per time step (sedimentation rate w times time step dt divided by cell thickness dx; PV = w*dt/dx = 0.2 is used in the tables) was defined. Boundary conditions are concentrations of zero in column A (behaviour of breakthrough curves is applied by concentrations of one) and the starting concentrations in time step zero. The other EXCEL cells contained the formulas for advection calculation according to the approximation concepts and column I contains the sum of the concentrations in the time step (mass balance). The simple explicit time discretization scheme is used for these testing calculations, while CoTReM uses the more complex Crank-Nicholsen-Scheme. Nevertheless, tests with CoTReM yielded, that the qualitative results for the advection calculation concepts depend not on the time discretization scheme. Instead, the explicit scheme is used here, because its formulas are directly understandable. The results of the EXCEL calculation are shown in the tables rounded to four decimal places for cell concentrations and mass balance concentrations, while the calculations themselves were more exact and the summed up mass balance may now deviate from the table contents.

Table BT_1:
Central-Taylor-Series approximation for advection calculation
PV = w*dt/dx = 0.2
The calculation formula in B1 - H6 is: C (t,i) = C(t-1,i) + PV * (C(t-1,i-1) - C(t-1,i+1)) / 2

	A	B	C	D	E	F	G	H	I
Time step t	Cell i-1	Cell i	Cell i+1	Cell i+2	Cell i+3	Cell i+4	Cell i+5	Cell i+6	Mass balance
0	0	**1.0000**	0	0	0	0	0	0	1.0000
1	0	1.0000	0.1000	0	0	0	0	0	1.1000
2	0	0.9900	0.2000	0.0100	0	0	0	0	1.2000
3	0	0.9700	0.2980	0.0300	0.0010	0	0	0	1.2990
4	0	0.9402	0.3920	0.0597	0.0040	0.0001	0	0	1.3960
5	0	0.9010	**0.4801**	0.0985	0.0100	0.0005	0.0000	0	1.4900
6	0	0.8530	0.5603	0.1455	0.0198	0.0015	0.0001	0.0000	1.5801

Table BT_2:
Backward-Taylor-Series approximation for advection calculation
PV = w*dt/dx = 0.2
The calculation formula in B1 - H6 is: C (t,i) = C(t-1,i) + PV * (C(t-1,i-1) - C(t-1,i))

	A	B	C	D	E	F	G	H	I
Time step t	Cell i-1	Cell i	Cell i+1	Cell i+2	Cell i+3	Cell i+4	Cell i+5	Cell i+6	Mass balance
0	0	**1.0000**	0	0	0	0	0	0	1.0000
1	0	0.8000	0.2000	0	0	0	0	0	1.0000
2	0	0.6400	0.3200	0.0400	0	0	0	0	1.0000
3	0	0.5120	0.3840	0.0960	0.0080	0	0	0	1.0000
4	0	0.4096	0.4096	0.1536	0.0256	0.0016	0	0	1.0000
5	0	0.3277	**0.4096**	0.2048	0.0512	0.0064	0.0003	0	1.0000
6	0	0.2621	0.3932	0.2458	0.0819	0.0154	0.0015	0.0001	1.0000

The advantages and disadvantages noted under "Type of advection" in 2.2.1.1 become obvious from these tables, which display an extreme case (PV = 0.2; only one starting concentration peak; pure sedimentation). The bold concentrations are the starting concentrations and the concentrations, which should be of value one for pure sedimentation (PV = 1.0 exchanged). The deviations are caused by numerical dispersion (BT_2) or a mix of smaller numerical dispersion and mass imbalances (BT_1). In table BT_2 is this bold concentration at least the relative maximum, in table BT_1 it has a higher value, but the relative maximum moves slower.

Examinations involving pure sedimentation showed also clearly, that the former concept to include the upper boundary was insufficient for this advection process. The new concentrations in the first cell were calculated only from concentrations of the new time step (indicated by C^+ ; implicit scheme). While this worked mostly for systems influenced by diffusion like processes, the determining equation can be reduced in case of pure sedimentation for the backward concept to $w*C_0 = w*C_1^+$ and in case of the central concept to $w*C_0 = w*C_1^+ / 2 + w*C_2^+ / 2$. This ignores any changes by transport or redox reactions applied in the first cell in the former time step due to total neglection of the old concentrations and led to false results like a fixed C_1^+ equal to C_0 in the backward concept and possibly even increasing C_1^+ in the central concept (if C_2^+ is reduced by solid phase consumption, then mass imbalance occurs at C_1^+, e. g. $C_2^+ = 0.4*C_0$ leads to $C_1^+ = 1.6*C_0$).

The newer, actual calculation concept for the upper boundary follows as far as possible the calculation method applied for cells within the model area (cells 2 - (n-1); cell n influenced similarly by an extra cell n+1 for the lower boundary). It considers according to the Crank-Nicholsen-Scheme of time discretization concentrations of the new time step C^+, therefore an implicit calculation method is necessary to solve it together with the whole difference equation system at once, and of the old time step C. Only this inclusion of the old concentrations C reflects the concentration changes applied in the former time step and avoids the errors of the old calculation concept.

Calculation differences to cells within the model area have only to consider, that the relative cell index i-1 for the first cell exists only as upper boundary concentrations C_0, which are the same in all time steps (leading to $C_{i-1}^+ (i=1) = C_{i-1} (i=1) = C_0^+ = C_0$), and that the distance between C_1 and C_0 is smaller than $(dx_{i-1} + dx_i)/2$, only the half cell thickness of the first cell $dx_1/2$ (C_0 is located at the upper edge of the first cell). This leads to the modified determining calculation equations for the upper boundary very similar to the equations within the model area (cf. SIEGER, 1993; HAMER AND SIEGER, 1994; LANDENBERGER, 1998):

$$G_1 = a_1 C_0 + b_1 C_1^+ + c_1 C_2^+ + W_1 = 0$$

$$W_1 = a_1 C_0 + (b_1 - 2) C_1 + c_1 C_2$$

with the coefficients for the backward calculation concept

$a_1 = - [D\_1 + w/2] * dt / dx_1$ substitute w/2 with w/4 for the central concept

$b_1 = 1 + [D\_1 + D\_2 + w/2] * dt / dx_1$ substitute w/2 with 0 for the central concept

$c_1 = - [D\_2 + 0] * dt / dx_1$ substitute 0 with -w/4 for the central concept

and $D\_1 = D_1 / dx_1$ and $D\_2 = D_2 / (dx_1 + dx_2)$.

The calculation equations with G_1 and W_1 contain in the full formulation also each a term for the isotherm dependent sorption algorithm developed in CoTAM. These sorption terms needed not to be modified and are applied in case of sorption for all model area cells i = 1 - n.

Appendix C: Exceptional species

The User Guide already stated, that a species in CoTReM may be exchanged (regarding several conditions; see "species") with a new species defined by the user. Several species are excluded from these exchange rules. The source code calls sometimes explicitly such a species, because the species is subject of an exceptional handling. The order of species listed in *.DAT is used to assign these species a unique number for this exception handling and inhibits the exchange possibility as for the normal species. The particular exceptions are:

- Organic matter OM and dissolved organic matter DOM are excluded from all PHREEQC calculations. They are only subject to the transport and redox reaction processes. The reasons for this exception is, that no consistent equilibrium constants are available, because organic matter reduction is usually mediated by bioorganisms. Therefore, the concept of the REDOX module is better suited to handle these reductions.
- The species H is needed to calculate the pH, which has to be given to PHREEQC. Also, H and the species OH are returned from PHREEQC with exception handling.
- The gases O_2, N_2 and H_2 have to be doubled in concentration (each has two atoms of the element) during the transfer to PHREEQC, because within PHREEQC they are used as (secondary) masterspecies O(0), N(0) and H(0), which consist only of one atom. The resulting O(0), N(0) and H(0) concentrations are consequently halved, when they are returned to the non-PHREEQC parts of CoTReM.

These exceptional species have to be used in *.DAT, *.PRX, CoTREM.STO etc. at the correct place in the species list. The order of species is given for the CoTReM compilation 2.3.0 in Appendix I. Exceptional species may be substituted by corresponding species, which only redefine an exceptional secondary PHREEQC-masterspecies as independent primary masterspecies (using it per modified PHREEQC.DAT; e.g. O(0) to O_zero; see Appendix F).

Appendix D:
The special elements Zp | Zm and the charge problem in CoTReM

All modeling approaches have to take in account how to handle charged species. CoTReM splits up into the three modules for transport, redox reactions and equilibrium calculation with PHREEQC. Each has a different relation to charged species concentrations within the module. The charge is conserved in closed systems and this law is applied within each cell for the redox and equilibrium calculations. Transport affects the whole model area (all cells) and the model area boundaries. Charge conservation for this open system would only be possible to calculate, if the whole model area and the fluxes of charged species across the model area boundaries could be included. Therefore, charge conservation within particular cells is violated due to the spatial division between positive and negative charges by intercell transport of charged species (different diffusion coefficients and different concentration distributions with depth). This causes deviations from electroneutrality within cells and would lead to an electric field. Electric field forces onto charged species (meaning transport is

modified) are neglected. Instead, it is assumed that the transport of major ion contributors in the solution are modified to maintain electroneutrality for each cell and all timesteps. This is applied, when one uses PHREEQC in CoTReM with an option (keyword "charge") to include the electroneutrality as well in each cell of the simulation. This option "charge" simply adds/removes a chosen charged species, which should be a major ion contributing species. On the one hand, this equilibrates all deviations from electroneutrality. On the other hand, the arbitrariness of the species addition/removal violates in this initial step (keyword "SOLUTION") the charge conservation law and the mass conservation law (only for elements included in the "charge"-species). The chosen species should be chemically inert with respect to the considered processes. Its diffusion coefficients should be set to zero to inhibit its transport. In seawater simulations Na^+ is usually used (Cl^- is another obvious choice).

The use of PHREEQC in CoTReM makes the matter of charges even more complicated. A review about the concentrations updates in CoTReM within each timestep and how to relate the updates to charge conservation and electroneutrality follows.

A simulation may start with any depth distribution of species and applied concentrations. These concentration are separately saved. At this point the electroneutrality in each cell may be applied (A) or not (B). The first changes occur due to transport. As mentioned above these changes usually violate charge conservation and electroneutrality (for A; further violated for B) within cells, while charge conservation (and, hence, electroneutrality (except deviations of B)) is maintained for the model area (plus boundary fluxes). The updated concentrations are considered by the redox module. Concentration changes caused by redox reactions are calculated in each cell separately, thus no intercell violations are possible. All included redox reactions between species are balanced with respect to elements and charges. This rule should always be applied, if reactions are added to the useable list. This means, that the redox module itself follows charge conservation and electroneutrality, but does not negate existing deviations.

The equilibrium calculation module (PHREEQC) starts its initial calculations of activities, dissociation of species and formation of complexes with the saved concentrations from the start of the timestep. The updates of transport and redox module are added later. These initial calculations include the correction to electroneutrality (deviation B) by adding or removing Na^+. Charge conservation within cells is violated only at this point in PHREEQC, but the sum of this deviations along the whole model area (plus boundaries) will theoretically be zero, because they are caused by the transport (see above, except the B of the first timestep). At this point the calculation output of saturation indices (SI) is used, if kinetic considerations are applied.

The sum of changes by the transport and redox module are calculated from the difference of the actual concentrations (following the redox module) and the saved concentrations (start of timestep). These changes are added to the PHREEQC-calculations as species amounts (mol) with the keyword "REACTION". This option allows to add/remove neutral elements. This may happen as any neutral element, as any formula of neutral elements or formula of predefined phases (i.e. the phase Calcite means the formula $CaCO_3$). Therefore, simply adding a charged species like HCO_3^- as formula HCO_3 neglects the charge and causes massive errors. A method is needed to carry the charge within a neutral formula into the calculations. Thus, two special "elements" were defined in the PHREEQC database. The elements Zp and Zm are of neglectable gram formula weight (10^{-12}) and exist only as ions Zp^+ and Zm^-. These ions mean essentially a positive or negative charge, which is used to apply electroneutrality to charged species for use with the keyword "REACTION". I. e., the charged species HCO_3^- is

applied as neutral formula HCO_3Zp. The PHREEQC calculations for this keyword "REACTION" (as well as mineral dissolution/precipitation calculations with it or the keyword "EQUILIBRIUM_PHASES") maintain charge conservation and electroneutrality. Therefore, a positive charge has to be applied to each Zp in the calculation, leaving a corresponding negative charge, which might be associated with the formula HCO_3 as HCO_3^-. This means, that effectively charged species can be added and the charge conservation violation by transport within cells is seen as difference of Zp and Zm in the calculation results. This charge difference is carried into the next timestep through the new updated species concentrations as for situation B and then finally removed within the PHREEQC initial calculation. Zp and Zm have to be added to the initial solution in a sufficient amount (but small in relation to the total ion content, because Zp and Zm affect the activity calculation), because removal of species associated with these "elements" may happen. Transport of the "charge" species Na^+ in this scheme could cause numerical errors by removing all Na^+ (hence, e.g. inhibition of Na^+ transport is achieved by suppressing Na^+ diffusion coefficients as well as v_a to zero).

Alternatively, one may neglect the "charge" option entirely. In this case, the PHREEQC initial calculations will not result in a nearly zero deviation (like it does with "charge") for the electrical balance, because electroneutrality is not given by balancing with Na^+ removal or addition. This electrical imbalance status is fixed in PHREEQC for the further "REACTION" and "EQUILIBRIUM_PHASES" calculations in the timestep and cell, meaning that the imbalance status of the solution is the same before and after the PHREEQC module. The charge conservation violations within cells from the last time step are seen again in the results of the special elements Zp and Zm. Each resulting solution composition of the PHREEQC calculations (initial and final) will be imbalanced (balanced with "charge") within this approach, but only the relative changes of the electrical imbalance in each time step are caused by transport. They are visible only through the Zp/Zm results. Additionally, Na^+ transport (or any other "charge" option species) is normally possible in this approach.

Appendix E: Alternative phases in PHREEQC

The PHREEQC keyword "EQUILIBRIUM_PHASES" normally allows to equilibrate a selected mineral phase to the solution composition. The activities of the ions or complexes (e.g. $[CO_3^{2-}]$ for carbonate) which may react to build this mineral phase are used in connection with the temperature and pressure dependent, non-apparent mineral solubility $K_{Mineral}$ to determine the saturation status $\Omega_{Mineral}$ and its logarithmic expression, the saturation index $SI_{Mineral}$. These values are needed to quantify the equilibration according to (exemplary for calcite):

$$\Omega_{Calcite} = ([Ca^{2+}] \cdot [CO_3^{2-}]) / K_{Calcite}$$

and

$$SI_{Calcite} = \log \Omega_{Calcite}$$

The solution composition is adjusted in the equilibration calculation, removing these ions from the composition by precipitation or adding them by dissolution (and taking care of the secondary condition of the mineral's availability), until the ion activities fulfill the desired saturation index $SI_{Set,\ Mineral}$, which is given as equilibration condition beforehand.

Now PHREEQC enables a calculation option with the keyword "EQUILIBRIUM_PHASES", which allows to calculate the desired saturation index $SI_{Set,\ Mineral}$ with the main mineral, while the equilibration is actually done by precipitation/dissolution of an alternative mineral (option

"alternative phase") or any (neutral) formula (option "alternative formula"). For example, Ca^{2+} needed for a calcite equilibration may be added by dolomite dissolution.

As mentioned above in the **"PHR-File-Rules"**, these options will not work flawless with CoTReM, because no source code structure was adjusted to balance the amount of the alternative phase/formula. It may work without kinetics for the equilibration, but the mineral balance is surely flawed.

In case of kinetics with the "REACTION" method something similar to these equilibration options is available in CoTReM. The calcite (main phase) and dolomite (alternative) example above could simply be simulated by noting "Dolomite" (or any other phase/formula) in the list (cf. **"PHR-File-Rules"**, number 5 option C) under "REACTION" in the *.PHR file, instead of "Calcite". Then, the dolomite formula ions are dissolved to fulfill the $[Ca^{2+}]$ and $[CO_3^{2-}]$ needs, which arise from the initial solution composition saturation index compared to $SI_{Set,Calcite}$ and according to the kinetic options noted under the species "Calcite" in *.DAT. Note, that the mineral balance of the phase is the one of dolomite within PHREEQC (and should be adjusted to dolomite stoichiometrics in COTREM.STO, if the REDOX module is used with this phase). While the interpretation is changed and somewhat unsure and confusing in this calcite/dolomite example, the method may be useful, if small impurities within a mineral are regarded. For example, if calcite is substituted by the formula (CaCO3)0.99(MgCO3)0.01, the mineral balance uses a 1% impurity of Mg^{2+} within calcite correctly in this method. The use of "pure calcite kinetics" is only a formal flaw. The method could be necessary for impurities consisting of rarer elements than Mg.

Appendix F:
Primary and secondary masterspecies in PHREEQC and the pE

Elements in PHREEQC are defined by a database file named PHREEQC.DAT with CoTReM. The standard database file is used for definitions of primary and secondary masterspecies for elements, which exist within the aqueous solution in different redox states, e.g. the primary masterspecies SO_4^{2-} for the definition of the element S and its main redox state S(6) and the secondary masterspecies HS^- for the redox state S(-2). The conversion between redox states for an element in PHREEQC depends on the pE (meaning the activity of electrons) due to the consequent inclusion of the special electron species e^- in all equations describing these conversions per constants similar to pure dissociation or solubility constants. In case of sulfur this reaction equation of conversion is defined as:

$$SO_4^{-2} + 9\ H^+ + 8\ e^- = HS^- + 4\ H_2O \text{ plus } \log k = 33.65 \qquad (F\_1)$$

The definition is derived from the law of mass action and means, that according to this law the activities of the species, "[species]", must fulfill the equation

$$10^{33.65} = \{\ [\ HS^-\ ] * [\ H2O\ ]^4\ \} / \{\ [\ SO_4^{2-}\ ] * [\ H^+\ ]^9 * [\ e^-\ ]^8\ \} \qquad (F\_2)$$

to achieve an equilibrium of these species in the solution. Often the logarithm is applied to the equation and then it is even more clear, why reaction F_2 is derived from equation F_1.

The special species e^- was introduced to be able to use this calculation principle of equilibrations for these redox state conversions. The law of mass action is commonly used for dissociation or complexation equations, where the element is in one and the same redox state.

In the PHREEQC output, all these ions and molecules of dissociations as well as the complexes are listed under the corresponding redox state notation. A definition example of dissociating ions for the redox state S(-2) is

$$HS^- = S^{-2} + H^+ \text{ plus log k} = -12.918 \qquad (F\_3)$$

and the interpretation of the equation equals the redox conversion example above. The same applies to the mineral equilibria, where the solid phases are defined with their solubility constants. PHREEQC includes also gaseous phases, but these are excluded from CoTReM.

Solubility constants of solid phases are only connected to the special species e^- in PHREEQC, if none of the aqueous masterspecies has the same redox state as the element has in the solid phase. An example is pyrite, where the sulfur redox state could be described as minus one (and Fe stays at plus two), with the definition

$$FeS_2 + 2\ H^+ + 2\ e^- = Fe^{+2} + 2\ HS^- \text{ plus log k} = -18.479 \qquad (F\_4)$$

In CoTReM is with the REDOX module another possibility included to convert a element into another redox state. REDOX was mainly developed to include the primary biogeochemically mediated redox reactions reducing organic matter (solid OM, dissolved DOM), a species, where a fixed redox state and "solubility" constants are very impracticable to define (a database file named Wateq4f.dat includes aqueous "Humate" and "Fulvate", but redox dependencies are not given). Consequently, REDOX equations are defined as full reaction equations with possible redox state conversions, but dependencies on pE or thermodynamical constants are ignored, only the mechanism of user defined depth dependent maximum redox rates controls for each reaction the simulated rates. This can lead to difficulties, when secondary (without OM or DOM) redox reaction conversions per REDOX (or other reactions like precipitations, which REDOX is able to simulate) conflict with the thermodynamical "verification" due to the same processes simulated by PHREEQC.

For example, the redox state changes of the reaction $HS^- + 2\ O_2 \Rightarrow SO_4^{2-} + H^+$ per REDOX in the solution composition could be totally reverted within the same time step per PHREEQC, if thermodynamics and pE demand it. Solid phases in secondary reactions are equally affected, if they are allowed to dissolve or precipitate per "EQUILIBRIUM_PHASES" or the added CoTReM specific kinetics in PHREEQC. Especially the pE in PHREEQC is difficult to control, because the control mechanisms in *.PHR under the keyword "SOLUTION", fixed value for the pE or a redox pair determining the pE, affect only the initial solution calculation initiated by "SOLUTION". The solution recalculation following other keywords ("REACTION", "EQUILIBRIUM_PHASES" or simply "REACTION_TEMPERATURE") includes also an independent recalculation of the pE, which is somewhat unclear and, thus, uninfluenceable as well as sometimes unrealistic (e.g. pE calculations dominated by the redox pair O(-2)/O(0)).

A method was found to model redox conversions with REDOX and exclude them in PHREEQC, if the user intends to ignore the thermodynamic constants or mistrusts an involved pE calculation. Redox pairs, which are subject to the problems characterized above, can be disconnected from their pE dependency in PHREEQC, when the affected secondary master species are redefined in the database file as primary masterspecies. These redefined secondary master species have to be changed consistently regarding all appearances of the species formula in the database file, especially in the new element definition noted under "SOLUTION_MASTER_SPECIES", where a new unique string of characters has to be used

for the old secondary master species to act like an own, independent element. The other main redefinition is the removal of the old primary/secondary conversion equation under "SOLUTION_SPECIES", which is substituted by the primary master species definition of the new element.

Two blueprints for the database file PHREEQC.DAT are offered with CoTReM. They are useful to create for each application the database file accordingly and changes like pressure and/or temperature dependent corrections of dissociation or solubility constants (cf. Appendix G) or the redefinitions discussed here should be noted in the header of the blueprint database file. The blueprint file PHR_23.DAT is the standard PHREEQC database file with a few modifications noted in the header for use with CoTReM version 2.3 and excludes all possible redefinitions of secondary master species. The similar file PHR_23_P.DAT includes redefinitions of all secondary master species and consists only of (partly new) primary master species (except for the secondaries O(0) and H(0), which are necessary for the PHREEQC mass- and chargebalance calculations).

The file is compiled under the rule, that the specific element of an old secondary master species gets its redox state appended for the creation of the unique character string. The rule is, first the old element abbreviation, underline, possibly m and underline to indicate negative redox states, and finally the redox state number written in the English word for the number. For example, the secondary master species HS^- with the redox state S(-2) is changed to the independent element name S_m_two with the (primary) master species $HS\_m\_two^-$. For more details refer to the blueprint file PHR_23_P.DAT, it includes the old definitions still as comments.

Appendix G:
Pressure and temperature dependence of solubility and dissociation constants

It is possible to include pressure and temperature dependencies by the following method. Temperature corrections can be taken from the PHREEEQC database file or other sources. For example, the phase Calcite is defined as follows in the database:

```
Calcite
    CaCO3 = CO3-2 + Ca+2
    log_k       -8.480
    delta_h -2.297 kcal
    -analytic    -171.9065    -0.077993    2839.319    71.595
```

Line 3 of the definition applies the standard log_k at 25°C and 1 bar pressure as fixed value. A temperature correction can be applied according to the van't Hoff equation using this standard log_k and the enthalpy delta_h in line 4 for the temperature dependency. Sometimes an analytical fit is available following the keyword "-analytical_expression" (or a keyword modification; line 5). The fit parameters are defined in the PHREEQC User Guide (PARKHURST, 1995) and are independent of the standard log_k. The analytical fit is preferably used by PHREEQC, then the van't Hoff equation is applied and as last option is the standard log_k used as temperature independent value. While these options to apply temperature corrections are fine, if no pressure corrections are necessary, the last option is useful to include both corrections after an external calculation of the appropriate thermodynamical constant.

WARNING!
Note, that these constants need to be real constants in PHREEQC derived from activities and NOT the apparent constants derived from concentrations.

The externally calculated value for the standard log_k should be applied in a new definition line under the phase or dissociation, while the old log_k line as well as the temperature correction lines including delta_h or -analytical are converted to comments by editing a doublecross, " # ", as first character into the definition line. The change should be noted in the header of the blueprint databases PHR_23.DAT or PHR_23_P.DAT offered with CoTReM.

The external calculation suggested consists first of the temperature correction followed by the pressure correction, because thermodynamical data about pressure corrections are usually given only in the isothermal relation between the sought after pressure and the value of the constant at a known pressure and temperature. The EXCEL files k_PT_Min.xls and k_PT_aq.xls are offered with CoTReM and include combined external corrections according to temperature (PHREEQC database file) and pressure for some dissociations constants (k_PT_aq.xls; cf. MILLERO, 1982; MILLERO, 1983; UNESCO, 1987) and CoTReM included solid phases (k_PT_Min.xls; according to the program SOLMINEQ; KHARAKA ET AL., 1989).

Appendix H:
Inside CoTReM: The sequence of important source code operations listed

This overview includes references to the subroutines and files, where the described source code operations actually take place. This is mainly thought as helpful tool for following software developers, but may also be useful to reveal the interna of the "Black Box" CoTReM to interested users. The references usually note "In subroutine / source-code-file:", if several operations are listed and "(subroutine / source-code-file)", if one related operation is noted.

START OF PROGRAM in cotrem.c:

#define NODEBUG or DEBUG for DOS or Win32 compilation
(also necessary in simula.for and f2c_port.for)

In main / cotrem.c:
- Videomodesetup
- Load filenames and file path from cotrem.ini (CLoadIni / cotrem.c)
- Utilization of the command line parameters (*.bat) and setup of unused file formats
- Check of extensions for all file formats (CheckAllExt / cotrem.c)
- Existence check of file formats using file paths and names (AllFilesExists / cotrem.c)
- Saving the actually used file paths and names in cotrem.ini (CSaveIni / cotrem.c)
- Calls the Simulation subroutine

In Simulation / simula.for:
- Definition of the CoTReM version number parameters (within variables declaration)
- Here and below: Many initializations of variables / arrays / matrices
- Loading the input file paths and names into Simulation (FLoadIni / inifile.for)
- Loading the *.DAT file data (DAT_Daten_laden / inifile.for)
- Loading the *.EXP file of measured data (EXP_Daten_laden / inifile.for)
- Renaming of *.DAT data variables inclusive data type conversions
- Setup of the "active" status for each species (Aktive_Masterspezies / simula.for)
- Setup of mineral saturation indices to equilibrate to, if at least one is not zero
  (SI_Daten_laden / inifile.for ⇒ ReadSolid / solid.c)
- Loading of all *.PAR file data and calculation of the compressed coefficient matrix
  [tridiagonal ⇒ (n+2)*3] of the Crank-Nicholsen-scheme, mainly from
  (depth-dependent) *.PAR file data like cell thickness, flow velocity,
  diffusion (each species), irrigation and dispersion coefficients
  (Matrix_G / simula.for)
- Loading of depth dependent kinetic parameters, if (L_)"Kin_Type" > 10
  (Read_Kinetik / files.for)
- Loading of *.PHR and initialization of PHREEQC structures (pqc_ini / pqc.c)

In pqc_ini / pqc.c:
- Recovering necessary numbers of several PHREEQC structures to be
  able to transfer simulation data to and from PHREEQC routines
  (search_outputnumbers / search_inputnumbers / SearchMinOutputNr /
  SearchMinInputNr / all in pqc.c)
- Loading of the stoichiometric reaction coefficients for the reactions of the REDOX
  module from file COTREM.STO (STOECH_INI / redox.c)
- Loading of the depth dependent maximum reaction rates for all the reactions of the
  REDOX module (UMS_Daten_laden / ums.for)

Loading of background concentrations for each cell and species from the file *S.PRX (C_0_setzen / files.for)
Setup of a unit conversion matrix for use with "INPUT_OPTION" (pH_pOH / Calc_URF / Use_URF / all in simula.for)
Preparation of the *.PRN outputfile (Ausgabefile / files.for)
Setting the starting concentration distribution (if *S.PRX is not used) dependent from an analytical transport calculation (Analyt / tracer.for) and sorption (Sorption / simula.for)
DISPLAY: Displaying the simulated concentration distributions and measured *.EXP data in the DOS graphic (Ergebnisausgabe / simula.for ⇒ plotter / plot.for). The simulated concentrations are converted for use with "INPUT_OPTION" before and after each display call (Check_INPUT_OPTION / simula.for). There are several display calls in the source code. They are mentioned below as DISPLAY.
Calculation of the constant elements of the tridiagonal transport matrix DG (DG_const / simula.for)

Beginning of the TIME LOOP and dependent initializations

Actual concentration distribution saved for use with the initial PHREEQC calculation
Calculation of non-local transport (Irrigation / simula.for)
OUTPUT: Concentration output in the *.PRX format for use with "ADD_OUTPUT" named *.IRR (Speicher_PRX / files.for). OUTPUT is like DISPLAY possibly modified by "INPUT_OPTION" conversions (Check_INPUT_OPTION / simula.for). OUTPUT notes further output calls.
Transport calculations of the Crank-Nicholsen-scheme:
Inhomogeneities W (W_calc / simula.for)
Representative functions G (G_calc / simula.for)
Variable, sorption dependent elements of the tridiagonal transport matrix DG (DG_var / simula.for)
Solution of the transport equation system per THOMAS-algorithm (TRIDIAG / simula.for)
The last three transport calculations are iterated per Newton-Raphson-scheme, if used with sorption calculations.

Sorption calculations per Henry-, Freundlich- or Langmuirisotherms and kinetic rates (Sorption / simula.for ⇒ Sorp_L / Sorp_F / both isotherm.for)
OUTPUT: Named *.TRA
Calls the redoxc subroutine

In redoxc / redox.c:

This REDOX module takes the user defined maximum reaction rates from *.UMS and the stoichiometric reaction coefficients from COTREM.STO to change the concentrations of species involved in these reactions. If these rates lead to negative concentrations, an algorithm to decrease the user defined rates to the actual used rates is started. The algorithm guarantees non-negative concentrations. The updated species concentrations are transferred back to Simulation

In Simulation / simula.for:

OUTPUT: Named *.RED

Calls the PQSub subroutine for data transfer to PHREEQC

In PQSub / pqsub.for:

Beginning of the PHREEQC CELL LOOP

Initializations and transfer of depth dependent data to non-depth dependent variables (kinetic parameters, difference of and actual saved concentrations, saved concentrations, pH calculation)

Concentration unit conversion from mol / l to mol / kgw (UnitChange / pqsub.for)

Concentrations of X_2-species doubled, because in PHREEQC they are used as X(0) species (applied for gases H_2, N_2 and O_2 in UnitChange / pqsub.for)

Minimum concentration of aqueous species set to 1.1D-14 and solid species neglect concentrations lower than 1.1D-20 mol / kgw (UnitChange / pqsub.for)

Calls the pqc_run subroutine

In pqc_run / pqc.c:

Initializations necessary due to the transfer from FORTRAN to C

PHR_N: First part of the PHR_N output caused by "ADD_OUTPUT". More parts are written within the PHREEQC subsubroutines called from reactions in mainsubs.c.

Reading again the *.PHR format for the calculation of the actual cell

Transfer of the saved simulation data into the PHREEQC structures explored by pqc.ini for the initial calculation caused by "SOLUTION" (pH, pE, aqueous concentrations)

Initial calculation caused by "SOLUTION" (initial_solutions / mainsubs.c)

Calls the Kinetik subroutine

In Kinetik / pqc.c:

Transfer and calculation of saturation indices / states to equilibrate to (SI_{Set} and Ω_{Set})

Calculation of the needed actual saturation indices $SI_{Mineral}$ for kinetic equilibration from the initial calculation results

Calculation of the mineral amounts to dissolve or precipitate in the equilibration in case of kinetics. The used source code depends on the chosen kinetic rate law (SI and Ω law) and the method (per "EQUILIBRIUM_PHASES" or per "REACTION") to implement these kinetics (see the switch(L_Kin_Type[i]) instruction in Kinetik). Calculation of mineral balances, also for pure equilibration (infinite kinetics). New kinetic rate laws can be added here.

Back to pqc_run

In pqc_run / pqc.c:

Transfer of the concentration difference between actual and saved simulation data into the "REACTION" structures of PHREEQC in mol to add/remove. This is the contribution of the transport and redox reaction modules within the time step to the initial solution result.

Transfer of the mineral amounts to add/remove per "REACTION" in case of kinetics with this keyword

Updated pE input for the following calculations

(reactions / mainsubs.c):

This PHREEQC subroutine (with many other PHREEQC subsubroutines) carries out the calculations initiated by "EQUILIBRIUM_PHASES" and "REACTION".
This means, it calculates the whole new solution composition incorporating the species in-/outflux per transport, the species transformations by REDOX and the (kinetically modified) mineral equilibration in this time step and cell.
The complete results of these cell dependent calculations can be shown per PHR_N output for the last time step of the simulation run.
Back to pqc_run.

Operations to return the simulated data of the cell back to PQSub from PHREEQC structures (pE, pH, pOH, alkalinity, aqueous concentrations, mineral balances)

Back to PQSub

In PQSub / pqsub.for:

Recovering resulting simulated data of this cell into cell dependent FORTRAN data structures (alkalinity, saturation indices of kinetically equilibrated minerals, pE)

Dividing PHREEQC X(0) element concentrations by factor two to yield correct concentrations for X_2 species (H_2, N_2, O_2)

Recovering aqueous and mineral concentrations and transferring them back from mol / kgw to mol / l

Recovering H^+ and OH^- concentrations from PHREEQC dissociation data instead from pH and recovering the H^+ activity correction log gamma for the pH calculation in the next time step

End of the PHREEQC CELL LOOP

Back to Simulation

In Simulation / simula.for:

Checks to stop the simulation and jump out of the TIME LOOP

DISPLAY: For the end of the time step

End of TIME LOOP

OUTPUT: Final species concentration output named *.PRX

Output of the actual redox reaction rates used in the module REDOX from the last time step into file *.AUR (Redox / redox.for)

DISPLAY: For the end of the simulation. Includes in case of some sorption display options more displayed data than during the simulation.

Back to main in cotrem.c

In main / cotrem.c:

END OF PROGRAM

Appendix I:
List of species included in CoTReM version 2.3.0 (37 species):

In the *.DAT file the PHREEQC element names or mineral PHASES names are used. The redox state of the element names are noted in brackets (a plus sign is never used within CoTReM).

Format of dissolved masterspecies (24 species):
Species-No. in CoTReM ; PHREEQC masterspecies; PHREEQC element

0	O_2	O(0)	10	N_2	N(0)
1	NO_3^-	N(5)	11	Ca^{2+}	Ca
2	Mn^{2+}	Mn(2)	12	Mg^{2+}	Mg
3	Fe^{2+}	Fe(2)	13	Na^+	Na
4	SO_4^{2-}	S(6)	14	Cl^-	Cl
5	CH_4	C(-4)	15	H^+	H
6	HCO_3^-	C(4)	16	OH^-	OH in the *.DAT file.
7	PO_4^{3-}	P	17	K^+	K
8	HS^-	S(-2)	18	Fe^{3+}	Fe(3)
9	NH_4^+	N(-3)	19	H_2	H(0)

Note: No PHREEQC element is identified by OH^-.

20	F^-	F	§§§	These §§§-species are not included in the
21	H_3BO_3	B	§§§	CoTReM version 2.3.1, which includes only
22	H_4SiO_4	Si	§§§	32 species and uses the numbers in brackets.
23 (20)	DOM	DOM for dissolved organic matter in the *.DAT file.		
		No PHREEQC element is identified by DOM.		

Format of solid species (13 minerals):
Species-No. in CoTReM ; chemical formula of the solid; a PHREEQC PHASES name

Solid species are used with the names of PHREEQC PHASES, which are used in the *.DAT file and in the *.PHR file. They have to be written in the form noted below.
It is not possible to capitalize all letters, like it is accepted in PHREEQC!!!

24 (21)	OM	OM for solid organic matter in the *.DAT file.	
		No PHREEQC PHASES name is identified by OM.	
25 (22)	$CaCO_3$	Calcite	; Aragonite
26 (23)	$Fe(OH)_3$	Fe(OH)3(a)	
27 (24)	MnO_2	Pyrolusite	; Birnessite, Nsutite
28 (25)	FeS	Mackinawite	
29 (26)	MnS	MnS(Green)	
30 (27)	$FeCO_3$	Siderite	
31 (28)	$MnCO_3$	Rhodochrosite	
32 (29)	$Fe_3(PO_4)_2$	Vivianite	
33 (30)	FeS_2	Pyrite	
34 (31)	$CaMg(CO_3)_2$	Dolomite	
35	$Ca_5(PO_4)_3F$	Fluorapatite	§§§ CoTReM version 2.3.1 includes only
36	SiO_2	SiO2(a)	§§§ 21 dissolved species and 11 minerals

Appendix J: List of REDOX reactions in CoTReM version 2.3

Format:
Reactions-No. in CoTReM ; bracket closed ; comment on the reaction.
Educts ====> products

Water is handled to have a complete reaction formulation, but it is no species in CoTReM.

The formula for solid Organic Matter (OM) means:
$OM = (CH_2O)_X (NH_3)_Y (H_3PO_4)_Z$; Redfield: x = 106 ; y = 16 ; z = 1

The Z-component of reactions 0 - 6 (primary redox reactions) is always:
$(H_3PO_4)_Z = (Z) PO_4^{-3} + (3\ Z) H^+$

This component is not further noted at the products side of the reaction equation !!!

Primary redox reactions:
X- and Y-components for reactions 0 - 6:

0) Oxidation of OM by Oxygen (Product NO_3^-):
*** + $(X + 2\ Y) O_2$ ====> $(X) HCO_3^- + (Y) NO_3^- + (Y) H_2O + (X + Y) H^+$

1) Oxidation of OM by Oxygen (Product NH_4^+):
*** + $(X) O_2 + (Y) H_2O$ ====> $(X) HCO_3^- + (Y) NH_4^+ + (X) H^+ + (Y) OH^-$

2) Oxidation of OM by Nitrate:
*** + $(4\ X / 5) NO_3^- + (Y) H_2O$ ====> $(X) HCO_3^- + (2\ X / 5) N_2 + (Y) NH_4^+$
$+ (2\ X / 5) H_2O + (X / 5) H^+ + (Y) OH^-$

3) Oxidation of OM by Manganese Oxide:
*** + $(2\ X + (3\ Y / 2)) MnO_2 + (X) H_2O$ ====> $(X) HCO_3^- + (2\ X + (3\ Y / 2)) Mn^{+2}$
$+ (Y / 2) N_2 + (3\ X + 3\ Y) OH^-$

4) Oxidation of OM by Iron Oxide:
*** + $(4\ X) Fe(OH)_3 + (Y) H_2O$ ====> $(X) HCO_3^- + (4\ X) Fe^{+2} + (Y) NH_4^+$
$+ (3\ X) H_2O + (7\ X + Y) OH^-$

5) Oxidation of OM by Sulfate:
*** + $(X / 2) SO_4^{-2} + (Y) H_2O$ ====> $(X) HCO_3^- + (X / 2) HS^- + (Y) NH_4^+$
$+ (X / 2) H^+ + (Y) OH^-$

6) Fermentation of OM to Methane:
*** + $((X / 2) + Y) H_2O$ ====> $(X / 2) HCO_3^- + (X / 2) CH_4 + (Y) NH_4^+$
$+ (X / 2) H^+ + (Y) OH^-$

Attention !!!
The complete formula is given only in conjunction with the above mentioned Z-component added. This means $(Z) PO_4^{-3} + (3\ Z) H^+$ must be added to the products.

Further implemented redox reactions:

7) Oxidation of Iron Sulfide:
$FeS + 2.25\ O_2 + 2.5\ H_2O$ ====> $Fe(OH)_3 + SO_4^{2-} + 2\ H^+$

8) Oxidation of Manganese Sulfide:
$MnS + 2.5\ O_2 + H_2O$ ====> $MnO_2 + SO_4^{2-} + 2\ H^+$

9) Oxidation of Iron Carbonate:
$FeCO_3 + 0.25\ O_2 + 2.5\ H_2O$ ====> $Fe(OH)_3 + HCO_3^- + H^+$

10) Oxidation of Manganese Carbonate:
$MnCO_3 + 0.5\ O_2 + H_2O$ ====> $MnO_2 + HCO_3^- + H^+$

11) Oxidation of Methane by Sulfate:
$CH_4 + SO_4^{2-}$ ====> $HS^- + HCO_3^- + H_2O$

12) Oxidation of Methane by Iron Carbonate:
$CH_4 + 8\ Fe(OH)_3$ ====> $8\ Fe^{2+} + HCO_3^- + 6\ H_2O + 15\ OH^-$

13) Oxidation of methane by Manganese Carbonate:
$CH_4 + 4\ MnO_2 + 2\ H_2O$ ====> $4\ Mn^{2+} + HCO_3^- + 7\ OH^-$

14) Oxidation of Methane by Nitrate:
$CH_4 + \ NO_3^- + H_2O$ ====> $NH_4^+ + HCO_3^- + \ OH^-$

15) Oxidation of Methane by Oxygen:
$CH_4 + \ 2\ O_2$ ====> $HCO_3^- + \ H_2O + H^+$

16) Oxidation of Manganese by Oxygen:
$Mn^{2+} + 0.5\ O_2 + H_2O$ ====> $MnO_2 + 2\ H^+$

17) Oxidation of Iron by Oxygen:
$Fe^{2+} + \ 0.25\ O_2 + 2.5\ H_2O$ ====> $Fe(OH)_3 \ + 2\ H^+$

18) Oxidation of Ammonia by Oxygen to Nitrate:
$NH_4^+ + 2\ O_2$ ====> $NO_3^- + H_2O + 2\ H^+$

19) Oxidation of Ammonia by Oxygen to Nitrogen:
$NH_4^+ + 0.75\ O_2$ ====> $0.5\ N_2 + 1.5\ H_2O + H^+$

20) Oxidation of Ammonia by Nitrate:
$NH_4^+ + 0.6\ NO_3^-$ ====> $0.8\ N_2 + 1.8\ H_2O + 0.4\ H^+$

21) Oxidation of Ammonia by Iron Oxide:
$NH_4^+ + 3\ Fe(OH)_3$ ====> $0.5\ N_2 + 3\ Fe^{2+} + 4\ H_2O + 5\ OH^-$

Further reactions:

22) Oxidation of Sulfide by Oxygen:
$HS^- + 2\ O_2$ ====> $SO_4^{2-} + H^+$

23) Oxidation of Sulfide by Nitrate:
$HS^- + 1.6\ NO_3^-$ ====> $SO_4^{2-} + 0.8\ N_2 + 0.2\ H_2O + 0.6\ OH^-$

24) Oxidation of Sulfide by Iron Oxide:
$HS^- + 8\ Fe(OH)_3$ ====> $SO_4^{2-} + 8\ Fe^{2+} + 5\ H_2O + 15\ OH^-$

25) Oxidation of Sulfide by Manganese Oxide:
$HS^- + 4\ MnO_2 + 3\ H_2O$ ====> $SO_4^{2-} + 4\ Mn^{2+} + 7\ OH^-$

26) Oxidation of Iron by Manganese Oxide:
$Fe^{2+} + 0.5\ MnO_2 + 2\ H_2O$ ====> $Fe(OH)_3 + 0.5\ Mn^{2+} + H^+$

Except for using DOM (dissolved organic matter) instead of OM the reactions 27 - 33 in COTREM.STO are similar to the reactions 0 - 6. DOM uses the same C/N/P-ratio defined in COTREM.STO as OM.

Further redox reactions may be added by the user. All species in the reaction have to be included in the CoTReM compilation (cf. the List of species).

How to include a reaction in CoTReM:

1. Add a column for the reaction in the *.UMS file according to the other reaction columns.
2. Add a reaction row with corresponding stoichiometric coefficients in the file C_STOECH.XLS (the general file of stoichiometric coefficients with adjustable C/N/P-ratio and adjustable number of reactions) according to the other reactions and (Important !) change the number of reactions to the new correct value. A maximum of 50 reactions may be included. Additionally, implemented reactions may be overwritten. Further comment lines may be included, if their first sign in the row is the letter "R" and the rows directly above and below are rows with reaction definitions.
3. Save C_STOECH.XLS as a tabulator separated ascii file and name it COTREM.STO.
4. Include this file COTREM.STO into the directory containing the executable CoTReM file.

Appendix K: Units in CoTReM (repetition p. 8)

Fixed units

Substance	:	mol
Volume	:	$l = dm_{(aq)}^3$
Porosity	:	%

Free units

Length	:	cm	(as example)
Time	:	yr	(as example)

Dependant units

Concentration	:	$mol / dm_{(aq)}^3$
Reaction rates	:	$mol / (dm_{(aq)}^3 * yr)$
Velocity	:	cm / yr
Diffusion coeff.	:	$(cm)^2 / yr$
Dispersion coeff.	:	cm
Rate of Sorption	:	1 / yr
Bonding affinity	:	$dm_{(aq)}^3 / mol$
Henry and Freundlich coefficient	:	1

Appendix L: Comments to units (repetition p. 9)

Not used units

Mass	:	kg or g
Flux	:	$mol / (dm^2 * yr)$
Area	:	dm^2
Porosity	:	1

Conversion definitions

Porosity	P [1]	:	$dm_{(aq)}^3 / dm^3$
Density	ρ	:	$kg_{(s)} / dm_{(s)}^3 = g / cm^3$
GFW		:	g / mol

$C [g / kg_{(s)}] / GFW = C [mol / kg_{(s)}]$

$C [mol / kg_{(s)}] * \rho = C [mol / dm_{(s)}^3]$

$C [mol / dm_{(s)}^3] * (1 - P) = C [mol / dm^3]$

$C [mol / dm^3] / P = C [mol / dm_{(aq)}^3]$

$C [mol / dm_{(aq)}^3] = C [mol / l]$

Computer simulation of deep sulfate reduction in sediments of the Amazon Fan

M. ADLER, C. HENSEN, S.KASTEN AND H.D. SCHULZ

University of Bremen, Department of Geosciences, P.O. Box 330 440, Germany

Keywords: Amazon Fan; sulfate reduction; mackinawite; numerical model; operator-splitting; PHREEQC

Corresponding author: Matthias Adler Phone: 0049-421-2183967
Fax: 0049-421-2184321
e-mail: madler@geochemie.uni-bremen.de

Abstract

Pore water concentration profiles of sediments at a site on the Amazon Fan were investigated and simulated with the numerical model CoTReM (Column Transport and Reaction Model) to reveal the biogeochemical processes involved. The pore water profiles for gravity core GeoB 4417-7 showed a distinct sulfate-methane transition zone in which deep sulfate reduction occurs. Only a small sulfide peak could be observed at the reaction zone. Due to high amounts of iron minerals the produced sulfide is instantaneously precipitated in form of iron sulfides. We present a simulation which starts from a steady state system with respect to pore water profiles for methane and sulfate. Furthermore sulfide, iron, pH, pE, calcium and total inorganic carbon (TIC) were included in the simulation. The program calculated mineral equilibria to mackinawite, iron sulfides (more stable than mackinawite), iron hydroxides and calcite via saturation indices (SI) by a module incorporating the program PHREEQC (PARKHURST, 1995). The measured sulfide and iron profiles are obtained in the simulation output by using a constant SI (= 0) for mackinawite and calcite, while a depth dependent SI distribution is applied for the PHREEQC phases "Pyrite" and "Fe(OH)3(a)", representing a composition and the kinetics of different iron sulfides and iron hydroxides. These SI distributions control the results of sulfide and iron pore water profiles, especially conserving the sulfide profile at the reaction zone during the simulation. The results suggest that phases of iron hydroxides are dissolved, mackinawite is precipitated within and other iron sulfides are precipitated below the reaction zone. The chemical reactivity of iron hydroxides corresponds to the rate of sulfide production. The system H_2O-CO_2-$CaCO_3$ is generally successfully maintained during the simulation. Deviations to the measured pH profile suggest that further processes are active which are not included in the simulation yet.

1 Introduction

Deep sulfate reduction by methane is often described in marine sediments (e.g., REEBURGH, 1980; IVERSEN AND BLACKBURN, 1981; HOEHLER ET AL., 1994; BLAIR AND ALLER, 1995; NIEWÖHNER ET AL., 1998). This reaction in marine sediments is an important sink for methane produced in deeper parts of the sediment. REEBURGH AND ALPERIN (1988) give an estimation for the consumption of 5-20% of the global methane flux towards the atmosphere. It was proposed that this redox reaction is consuming equal amounts of sulfate and methane to produce sulfide, bicarbonate and water (DEVOL AND AHMED, 1981). This one-to-one relation was quantitatively confirmed by studies of NIEWÖHNER ET AL. (1998). Nevertheless, the details of this overall reaction are not completely understood, especially the catalyzing microorganisms are not yet revealed. A possible pathway to split the reaction is suggested by HOEHLER ET AL. (1994).

In iron-rich sediments the produced sulfide is usually entirely removed from the pore water by precipitation of iron sulfides. The formation of iron monosulfides (e.g. mackinawite) and pyrite in anoxic sediments is well known and their kinetics are investigated (e.g., BERNER, 1972; RICKARD, 1974; PYZIK AND SOMMER, 1981; CANFIELD ET AL., 1992). In this study we present measured pore water profiles of gravity core GeoB 4417-7 which indicates the sulfide source, the presence of dissolved iron and a limited presence of sulfide. These highly complex conditions are investigated via a numerical simulation with respect to a possible precipitation of iron sulfides and an explanation for the different reaction pathways of sulfur.

Several processes determine the profiles of dissolved pore water species and the distribution of minerals in sediments. These processes include advection, diffusion, redox reactions, precipitation and dissolution as well as further equilibrium reactions and their isolated effects as single process on a geochemical system can be quantitatively calculated. However, the behavior of a complex geochemical system is not easy to understand, because of the interactions of all these processes. In these cases of high nonlinear problems one has to rely on numerical modeling approaches to simulate the system. Determining a solution for the non-linear partial differential equation (PDE) describing the geochemical system is problematic, especially due to different time scales of transport and reaction effects. There are several numerical simulation approaches to model early diagenesis in marine sediments (e.g., RABOUILLE AND GAILLARD, 1991; SOETAERT ET AL., 1996; VAN CAPPELLEN AND WANG, 1996; WANG AND VAN CAPPELLEN, 1996). They differ with respect to the methods applied to

couple effects of transport and chemical reactions and/or the set of studied species. Often, the model is limited by the incorporated species set and focused on the investigation of a particular problem of early diagenesis. For example, the global implicit approach (VAN CAPPELLEN AND WANG, 1996) solves an individual partial differential equation (PDE) by individual algorithms for each species of a limited set. Changes of the transport or the reaction term of a single species result in the necessity to rewrite major parts of the algorithm.

The transport and reaction model CoTReM (Column Transport and Reaction Model; LANDENBERGER, 1998) uses more flexible concepts capable to adapt to all kinds of one-dimensional early diagenetic and groundwater systems. However, the calculation concept of operator-splitting (YANENKO, 1971) may occasionally suffer from less accurate solutions. This can be suppressed by using smaller time steps which requires more calculation time. The program enables us to perform simulations with a chooseable set of dissolved species and mineral species regarding the processes of transport, redox reactions and reactions of thermodynamical equilibria (especially dissolution and precipitation). At present, a set of 27 pre-determined reaction equations is included within the CoTReM software. Furthermore, the user is enabled to add redox reactions for the set of included species (usually at least 30 species, dependent on the compilation). The model CoTReM is available at *http://www.geochemie.uni-bremen.de/cotrem.html.*

2 Methods of pore water retrieval

2.1 Studied core

The geochemical data of gravity core GeoB 4417-7 were collected onboard the research vessel METEOR during cruise M 38/2 from Recife to Las Palmas between March 4 and April 14, 1997. Location details of GeoB 4417-7 are listed in Table 1. The location area is situated on the northern part of the Amazon Fan. In general, the sedimentation on the Amazon Fan changed from terrigenous-dominated material up to a depth of around 35 cm, to carbonate-rich ooze around the change from the last Glacial to the Holocene (KASTEN ET AL., 1998). The lower sections of the core are characterized by iron sulfide minerals (BLEIL ET AL., 1998).

2.2 Sampling methods and extraction of pore water

The gravity core taken was cut lengthwise and one half was used for pore water extraction and analyses, the other half was used for the determination of porosity. The core was kept and processed onboard in the cooling lab at ca. 4° C to obtain the data close to *in situ* conditions.

Table 1:
Location of the station GeoB 4417-7 and main parameters of the core

GeoB station	*4417-7*
Latitude	05°08,3' N
Longitude	46°34,5' W
Water depth	3510 m
Gravity core length	5.49 m
Temperature	2.1 °C
Sedimentation rate (Holocene)	3.5 cm / ka

Pore water samples were taken from the core at each 20 cm and extractions were made by pressure squeezing. Pore water was analyzed immediately after extraction or preserved (with HNO_3 (conc.), at 4°C, analyzed at Bremen University).

2.3 Geochemical analyses

Several parameters were measured directly onboard. First Eh and pH values of the pore water were determined by punch-in electrodes before squeezing. Sulfate and chloride were determined by ion chromatography. Alkalinity was measured by titration with HCl. A gas chromatograph was used to determine methane (cf. NIEWÖHNER ET AL., 1998). Iron was determined by photometrical analysis and sulfide was measured by a potentiometric technique utilizing an ion-sensitive needle electrode. The measurements of both parameters are assumed to have considerable deviations due to given sampling conditions. A more detailed description of sediment sampling and chemical analysis can be found in SCHULZ ET AL. (1994), NIEWÖHNER ET AL. (1998) and NIEWÖHNER ET AL. (1999).

3 Description of the model CoTReM

3.1 General description

The used simulation software CoTReM (LANDENBERGER, 1998) was continuously developed and is based on the former model CoTAM (HAMER AND SIEGER, 1994). Both models were successfully tested for oxic marine environments (HENSEN ET AL., 1997; LANDENBERGER ET AL., 1997; LANDENBERGER, 1998). They are able to model non-steady state conditions using variable, but uniform time steps. Both models, CoTReM and CoTAM, are suitable to simulate one-dimensional transport processes (sedimentation, advection, dispersion, diffusion, bioturbation, bioirrigation) and geochemical reactions (redox reactions and thermodynamical equilibria reactions, the latter via the incorporated model PHREEQC; PARKHURST, 1995).

CoTReM allows to simulate interactions between solid and dissolved phases. All modeled processes are applicable to solid phases if geochemically possible. CoTReM uses a flexible system to calculate the effects of redox reactions on the species distribution. The solid phases may be used fully connected to PHREEQC with several options. Additionally, an algorithm for non-local mixing transport (bioirrigation) is available. It is very important to note that CoTReM can easily be modified by a new compilation to a new available set of useable species (dissolved species or minerals). Incorporating additional redox reactions or exchanging species is possible for the user with minor restrictions.

A complete description of CoTAM/CoTReM is beyond the scope of this paper, see SIEGER (1993), HAMER AND SIEGER (1994), HENSEN ET AL. (1997), LANDENBERGER (1998) for more details. In the following, therefore, only the basic model concept and the main options are described.

The modeling approach solves the General Diagenetic Equation, a partial differential equation (PDE) as proposed by BERNER (1980) by the technique of operator-splitting. It describes the transport and chemical reactions of species in porous media. Equation (1) is written for the homogeneous one-dimensional case, which is independent of porosity and applies to one simulation cell. The use of different cells with separate parameters sets results in an inhomogeneous model area. The equation system for all cells of the model area is solved independently of porosity, but the dependence of diffusion coefficients from porosity is included (cf. Eq. 9). Porosity differences of adjacent simulation cells (Taylor series approximation for difference quotients, cf. 3.3) are assumed to be negligible in CoTReM.

Species conc. Diffusion and Dispersion

$$\partial_t C_i = -\partial_x\left(v \cdot C_i\right) + \partial_x\left(D_i \cdot \partial_x C_i\right) + \alpha_x\left(C_{0,i} - C_i\right) + R_i\left(C_1, \ldots, C_{n_i}\right) \qquad (1)$$

Sediment advection Bioirrigation Reactions

where the unit is mol/(l · a), $i = 1, \ldots, n_i$, C_i is the concentration of the i^{th}-species, t is time, D_i is the diffusion coefficient (i^{th}-species) in sediment (plus dispersion), x is sediment depth, R_i is the reaction rate of the i^{th}-species (source term), v is the sedimentation rate (plus flow

velocity, if applicable), $C_{0,i}$ is the bottom water concentration of the i^{th}-species, and α_x is the exchange coefficient of depth x.

Numerical approaches generally separate time and space of the model area into discrete steps. The discretization in time is worked out sequentially. If a defined time step is used, non-steady state calculations may be possible, like in CoTReM. Otherwise, a convergence criterion can define a steady state and results of sequential iterations can be used to decide whether convergence and steady state are achieved. This method is implemented in the steady state model STEADYSED 1 (VAN CAPPELLEN AND WANG, 1996).

The discretization in one-dimensional space divides the model area into a number of cells. In CoTReM the thickness of each cell can be defined independently. The cell discretization has to fulfill certain criteria. Both discretizations have to be chosen with respect to the numeric stability criteria of Courant, Neumann, and Peclet (e.g., COLLATZ, 1966; BEAR, 1979; KINZELBACH, 1987).

The calculation of processes in a cell depends generally on the entire model area (interaction between all cells). The operator-splitting approach tries to simplify these dependencies by reducing them to adjacent cells (transport) or even no other cell (reactions).

3.2 Operator-splitting

The operator-splitting (OS) approach (YANENKO, 1971; SCHULZ AND REARDON, 1983) divides the complete partial differential equation (PDE) into smaller, easier to solve sub-PDEs and adds up their changing effects. Typically, each process or group of similar processes is modeled by one sub-PDE.

The processes are described by operators O which change the condition of individual cells or the entire model area, represented by the species concentration matrix C. The different operators cause the changes $\partial_t C_{Operator}$ of the cell condition and apply them sequentially to the matrix C of the simulation in each time step. Although the sequence of applied operators is basically arbitrary, the chosen sequence in CoTReM inhibits all major calculating problems which could be introduced by a different sequence. Iterating this operator-splitting approach over a sufficient number of time steps results in a steady state for the modeled area. Non-steady state calculations are possible in CoTReM because a defined uniform time step exists

and therefore correct calculation terms for fluxes and redox reaction rates are implemented. A problem exists, concerning the calculation of the thermodynamic equilibrium reactions by PHREEQC without time dependence. PHREEQC includes no option to apply kinetics and a steady state with respect to the species distribution within a cell is achieved by PHREEQC independent of reaction kinetics. Therefore, the time step is assumed to be sufficiently long to result in this kind of steady state, which is usually true for dissolved species. This is more problematic for minerals, but the PHREEQC option to calculate certain pre-defined disequilibria state using non-zero saturation indices (SI $\neq$ 0) for different mineral phases allows to simulate dynamic equilibria as they would be achieved by application of kinetics. According to this assumption, all results of fluxes and reaction rates reflect a correct dependence on time, so each result for the matrix C after each time step defines results for a non-steady state calculation (and finally ends in a steady state). This assumes, that the initial state (and dynamic) of the modeled geochemical system is exactly represented by the matrix C (and other condition parameters) at the start of the simulation. Often it is not necessary for modeling purposes to apply this concept of steady state/non-steady state to the entire set of modeled species. This concept is especially useful for the set of dissolved pore water species, because their profiles reach (quasi) steady state much faster than minerals (mineral transport limited by sedimentation). The simulation time needed to achieve steady state for minerals with respect to sedimentation in the entire model area will often exceed the time scale for constant conditions which can be applied to the entire model area.

Generally, the operator-splitting method iterates the following two-step calculation:

$$\partial_t C_{operator\ O} = O \cdot C_{before\ operator\ O} \tag{2}$$

$$C_{before\ operator\ O} + dt \cdot \partial_t C_{operator\ O} = C_{after\ operator\ O} \tag{3}$$

All of these two-step calculations or operator-splittings have to be adjusted to the discretization of the model. Therefore, all the splitted partial differential equations are translated into and solved as finite-difference equations. Especially the changes $\partial_t C_{operator}$ are multiplied by the time step dt to adjust them to the new concentrations.

3.3 *Modules of CoTReM*

The operator-splitting steps are described below in order of application within CoTReM. CoTReM's general calculation principle is illustrated in Fig. 1.

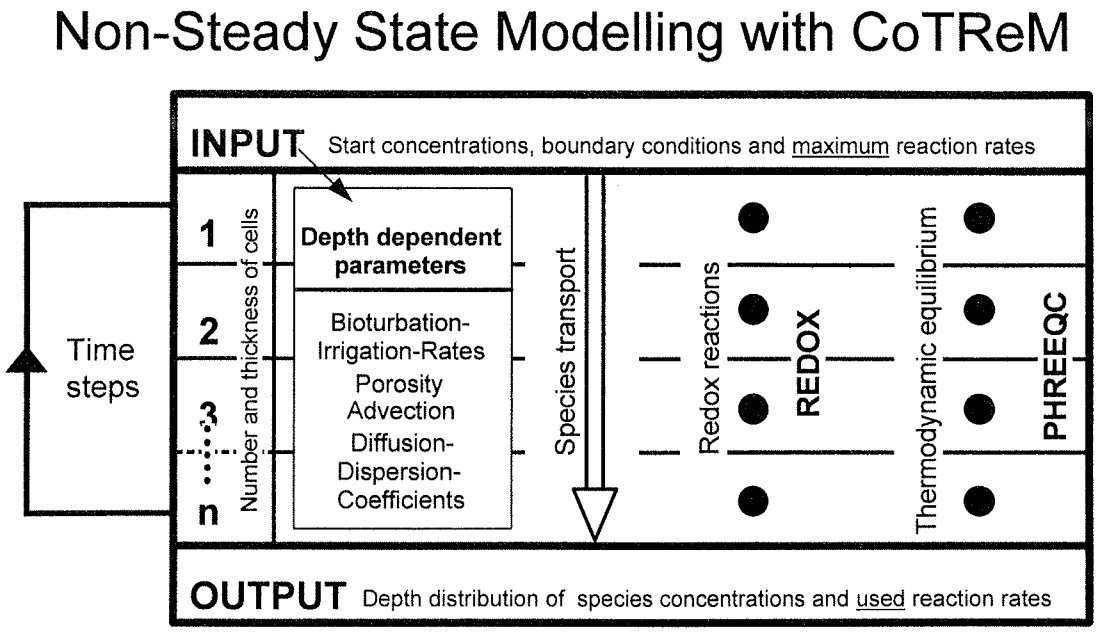

Fig. 1:
Calculation principles of CoTReM (modified after HENSEN ET AL., 1997). First, in each time step the transport is calculated (Eqs (4) and (5)) for the entire model area followed by "cell-by-cell" redox reaction (Eq (7)) and mineral equilibrium calculations by PHREEQC

Transport processes

The first operator splits the process of non-local mixing of solutes (bioirrigation) from the whole PDE (Eq. 1). It solves the simple part:

$$\partial_t C_i = \alpha_x \left(C_{0,i} - C_i \right) \qquad i = 1,\ldots,n_i \quad \text{mol}/(\text{l}\cdot\text{a}) \tag{4}$$

The program requires that $C_i \leq C_{0,i}$, if initial C_i is less than $C_{0,i}$, and vice versa. This application is not used in this study.

The next operator split solves the effects caused by the two transport phenomena groups dispersion/diffusion/bioturbation and advection/sedimentation. The related PDE is:

$$\partial_t C_i = -v \cdot \partial_x C_i + D \cdot \partial_x^2 C_i \qquad i = 1,\ldots,n_i \quad \text{mol}/(\text{l}\cdot\text{a}) \tag{5}$$

where v and D are constant in a cell (different in different cells) for each species. Therefore, they are not affected by the differentials.

These transport processes are solved in a system of linear PDEs simultaneously for all cells. The differential quotients are substituted by difference quotients following the Taylor series approximation. Then the Crank-Nicholsen difference scheme is applied as a method to obtain an equation system depending on concentrations of the old and the new time step (time discretization). Finally, a variant of the Thomas algorithm (PRESS ET AL., 1992) is used to solve the created linear finite-difference equation system.

The upper boundary condition of the transport processes is set as a Cauchy-boundary condition allowing advection and diffusion over the sediment - bottom water boundary. It is applied through the bottom water concentration C_0 for each dissolved species directly above the model area. Solid species are handled similarly, meaning sediment particles are reaching the sediment - bottom water boundary. The lower boundary condition may be defined generally as transmission or impermeable boundary. This describes the behavior in relation to dispersion/diffusion into an extra cell below the model area. Additionally, this extra lower boundary cell may be used species-specific as Cauchy-boundary condition similar to the upper boundary.

Chemical reactions

The third operator split describes the dependence of chemical reactions of R:

$$\partial_t C_i = R_i\left(C_1,\ldots,C_{n_i}\right) \qquad i = 1,\ldots,n_i \quad \text{mol}/(1\cdot \text{a}) \tag{6}$$

where R_i denotes the reaction rate of the i^{th}-species. The operator R consisting of all R_i is a special case. R changes the distribution of chemical species within a cell without being dependent on other cells. The inherent simplification is the main reason for using the operator-splitting approach. R is divided by the operator-splitting technique into contributing rates of redox reactions and of thermodynamical equilibria reactions via the incorporated model PHREEQC (PARKHURST, 1995).

Redox reactions

The change in concentration $dt\cdot\partial_t C_i$ by redox reactions is calculated via a set of full reaction equations. The algorithm is driven by the concept of maximum reaction rates. A matrix with coefficients of redox reactions is used and maximum reaction rates R_{max} have to be chosen depth dependent for each reaction. It is important to distinguish that R_{max} and R (see below) refer to rates of all redox reactions and may therefore contribute to a concentration change for

a species while the operator R in the section above refers to the total rates of concentration changes for a species.

The rates R_{Max} are reduced by the algorithm if any of the educt species are not available in sufficient amounts to fulfill R_{Max}. This avoids negative concentrations. The algorithm uses the total amount of concentration for such a reaction and calculates the actual redox reaction rates R. If the species is an educt of multiple reactions (in the same cell) its concentration is distributed between these reactions. R is equally distributed, if each rate given by R_{Max} is higher than in R. Otherwise, each higher rate in R_{Max} is reduced to the rate in R and then the concentration is distributed with respect to the (new) rates in R_{max}. This distribution is given to an output file as actual reaction rates R.

The concentration change $dt \cdot \partial_t C_{i\ (species,\ depth)}$ of the species is given by the actually (reduced) rate $R_{(reaction,\ depth)}$ of the reaction, the stoichiometric coefficients of the reaction $SC_{(species,\ reaction)}$, and the numerical time step dt:

$$dt \cdot \partial_t C_{i\ (species,\ depth)} = R_{(reaction,\ depth)} \cdot dt \cdot SC_{(species,\ reaction)} \qquad (7)$$

The value of $dt \cdot \partial_t C_i$ is used to calculate the new concentration of the species (i) in the specific cell (depth). The stoichiometric coefficients matrix SC applies the necessary coefficients to the list of full equation redox reactions in CoTReM. The matrix sets educt stoichiometric coefficients of a reaction always to equivalent negative values and product coefficients always to equivalent positive values.

In CoTReM the matrix of redox reaction rates (R_{Max} and R) is always used with positive values, defining the direction of a reaction. The species H^+ and OH^- are always formulated as products, thus, their concentrations can increase but never decrease. For compensation, after all maximum rate-driven calculations are done, the algorithm adjusts the concentration by the equation:

$$K\ (H_2O) = C\ (H^+) \cdot C\ (OH^-) \qquad (8)$$

This sufficiently approximates (brackets refer to concentration instead of activity) the thermodynamical equilibrium for a subsequent PHREEQC calculation.

Thermodynamical equilibria reactions (PHREEQC)

This part of the operator R is included by incorporating PHREEQC (PARKHURST, 1995) as a subroutine in CoTReM. For each cell the complete condition state of the simulation, basically

all species concentrations, the pH, and mineral saturation indices are delivered to the PHREEQC subroutine as input data and written into its own program structures. The PHREEQC subroutine gets additional input data from the PHREEQC database file and the PHREEQC input file. The subroutine performs the thermodynamical equilibria calculations which are keyword controlled by the PHREEQC input file. CoTReM usually uses the keyword EQUILIBRIUM PHASES to achieve mineral equilibria. The results are delivered into the internal structures of CoTReM. This ends the calculation of a time step.

4 Results and Discussion

4.1 Measured pore water profiles

For gravity core GeoB 4417-7 concentration profiles of alkalinity, pH, pE, sulfate, sulfide, methane, iron and chloride were measured. These profiles (except chloride) are plotted in Fig. 2.

One of the most prominent features of the measured profiles is found at a core depth of about 400 cm. At this depth sulfate and methane are both depleted in a reaction zone. The sulfate profile is continuously decreasing with depth and methane is diffusing upwards to this depth from a source below the core bottom. The phenomenon of reducing sulfate by anaerobic methane oxidation is well studied (e.g., REEBURGH, 1980; IVERSEN AND BLACKBURN, 1981; HOEHLER ET AL., 1994; BLAIR AND ALLER, 1995; NIEWÖHNER ET AL., 1998). Such reaction zones are known as deep sulfate reduction by methane producing sulfide and bicarbonate.

Additionally, a distinct concentration peak of sulfide was detected at this depth. The concentration of 25 µmol/l sulfide is, however, three orders of magnitude lower than the sulfate bottom water concentration. The expected release rates of sulfide suggest, however, sulfide concentrations in the pore water system comparable to the scale of sulfate concentration in bottom water. Therefore, a process of sulfide consumption has to be present in the reaction zone of sulfate/methane. However, measuring low sulfide concentrations under shipboard conditions is difficult and the observed peak exists of one data point only. A more exact form and maximum of the peak was, therefore, not deducible, but a peak clearly exists. We consider the highest measured data point to be the maximum of the sulfide peak in the investigation, supported by the fact, that the depth of the measured sulfide data point is similar to the place of the depletion zone of sulfate and methane.

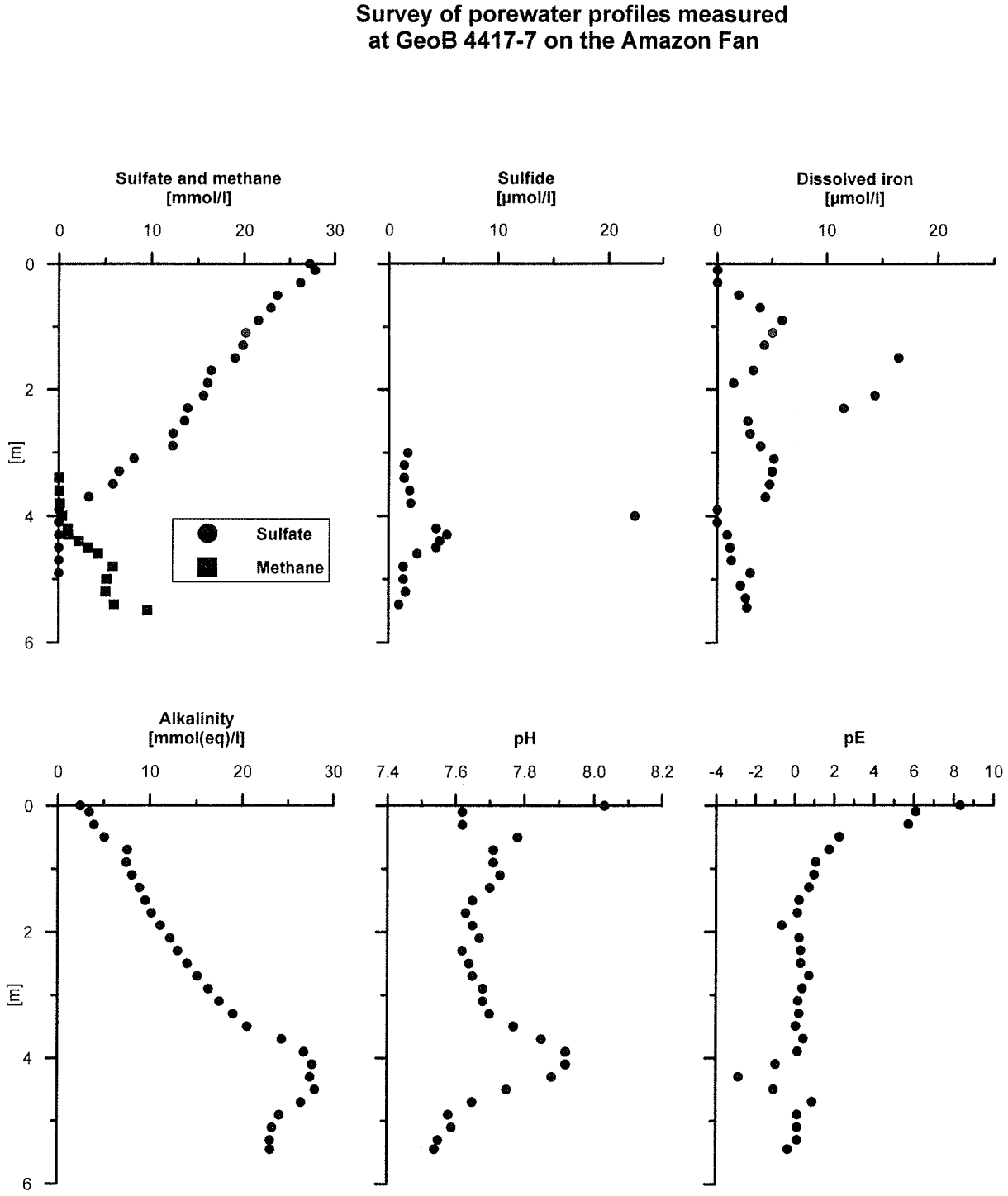

Fig. 2:
Depth profiles of measured data from the gravity core GeoB 4417-7 on the Amazon Fan

Determination of dissolved iron in solution at concentrations below a few micromoles per liter is also difficult to conduct, because large uncertainties arise from reoxidation processes. Therefore, the exact profile is at least uncertain as can be deduced by the scattering data points (Fig. 2). Just below the bottom water interface and at the production zone of sulfide

iron in pore water is depleted. Alkalinity increases with depth to a maximum peak at the reaction zone. This can be explained by the contribution of produced bicarbonate to alkalinity.

Within the first half meter the pH profile shows a decrease, which can be expected due to oxidization of organic matter by oxygen and nitrate, increasing to higher values due to further oxidants and other redox processes. The pE profile shows the transition from oxic sediments with a high pE to more anoxic sediments. The minimum was measured just below the production zone of sulfide.

4.2 Basic input data for modeling

Apart from the measured concentration data the simulation needs a set of parameters, which might be constant or variable over the model area. Data for molecular diffusion coefficients in water D_0 are used for all dissolved species as compiled and given by BOUDREAU (1996B), except for the dynamic viscosity of water (ATKINS, 1978). The diffusion coefficients in sediment D_S were calculated following an empirical equation given by ULLMAN AND ALLER (1982).

$$D_s = \phi^{(n-1)} \cdot D_0 \qquad (9)$$

where D_s is the molecular diffusion coefficient in sediment, D_0 is the molecular diffusion coefficient in water, ϕ is the porosity of the sediment, and n is a correction factor (n=3, if $\phi \geq 0.7$; n=2, if $\phi < 0.7$)

Bioturbation and bioirrigation coefficients in this investigation were assumed to be negligible and set to zero. Thermodynamical equilibrium data like log k values were handled by PHREEQC (PARKHURST, 1995) and its database file including temperature dependence. Saturation indices for mineral equilibria were set as explained below and are listed in Table 2. The model area extends from the sediment - bottom water interface (depth 0 cm) to a depth of 720 cm. The CoTReM option of a different cell thickness was used (cf. Table 2).

4.3 Modeling approach

In a first step the measured sulfate and methane gradients were fitted by a simulation using the redox reaction given by equation (10). Additional data input for this simulation is shown in Table 3.

$$CH_4 + SO_4^{2-} \Rightarrow HS^- + HCO_3^- + H_2O \qquad (10)$$

Table 2:
Distributions of cell thickness and applied saturation indices (SI) for iron hydroxides ("Fe(OH)3(a)") and iron sulfides ("Pyrite") in the simulation

Depth area [m]	Thickness of a cell [cm]	SI of "Fe(OH)3(a)"	SI of "Pyrite"
0.00 - 0.20	20	-1.0	20.0
0.20 - 0.40	20	-3.0	20.0
0.40 - 0.60	20	-5.0	20.0
0.60 - 3.00	20	-6.5	20.0
3.00 - 3.50	10	-6.5	20.0
3.50 - 3.85	5	-6.5	20.0
3.85 - 4.10	5	-7.2	20.0
4.10 - 4.50	5	-7.2	8.5
4.50 - 5.00	10	-7.2	7.5
5.00 - 5.40	20	-7.2	7.5
5.40 - 7.20	20	-7.2	0.0

Table 3:
Starting conditions for the first part of the simulation regarding deep sulfate reduction by methane

Input data	Starting condition
Standard simulation:	16.5 mmol / l ; main parameter to get a fit for
Lower boundary at 730 cm: Methane	the measured profiles of methane and sulfate
Upper boundary:	
Sulfate	28.5 mmol / l fitted to sulfate gradient
Methane	0.0 mmol / l = measured data
Lower boundary: Sulfate	0.0 mmol / l = measured data and transmissive
Maximum reaction rate for $CH_4 + SO_4^{2-}$ in all cells never limiting the reaction	More than necessary: 1.0 mol / (l · a) Meaningful rates are only the actual redox reaction rates R achieved as output (Fig. 3)
Profile distribution of species (not necessary here, but gets faster results)	Similar to measured data
Sedimentation rate	3.5 cm / ka
Time step	1 a
Further simulations:	8.2 and 30 mmol / l; this changes result in
Lower boundary for Methane	other sets of methane/sulfate steady states

The goal is to find the amount of methane diffusing upwards using the option to set a constant concentration in the lower boundary cell as the main fit parameter. The simulation ran until a steady state was achieved. Each tested concentration for methane at the lower boundary cell (720 cm + 20/2 cm for the extra cell) resulted in different steady state profiles for both parameters since the sulfate input concentration is held constant. The fit parameter determines the particular horizon of the depleting zone. We found a concentration of 16.5 mmol/l at 730

cm results in a sufficient fit for the measured distributions ("standard" simulation). In Fig. 3 the modeled species profiles for methane and sulfate are shown.

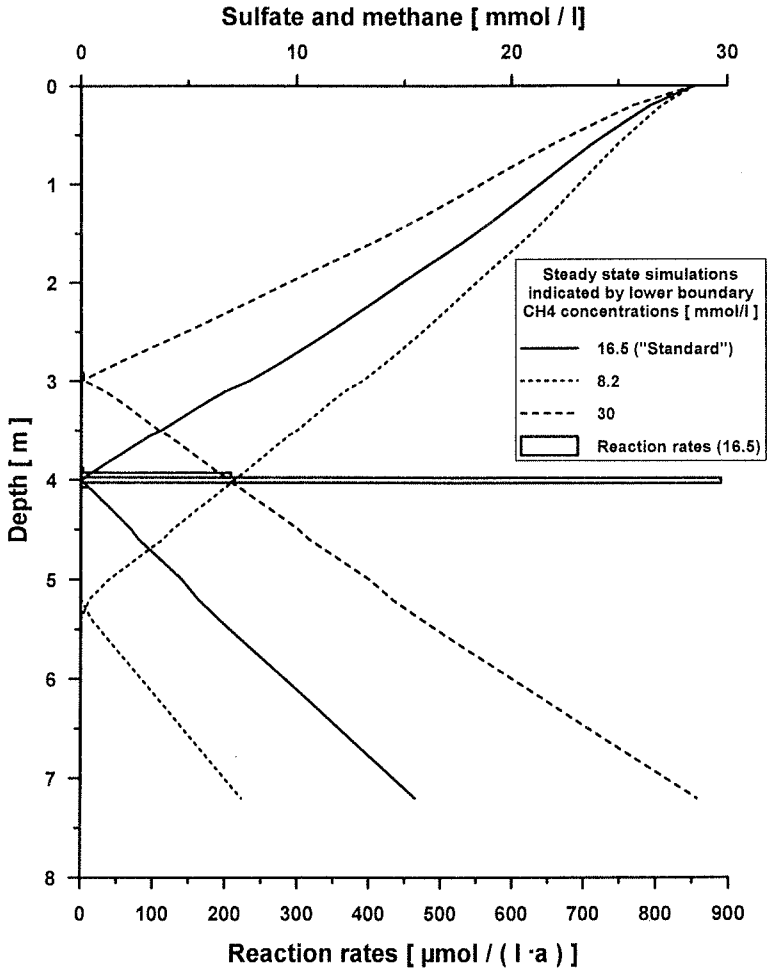

Fig. 3:
Results of three steady state simulations with CoTReM regarding porewater profiles of sulfate (0-4 m) and methane (4-7.2 m) are shown. The steady states are achieved by a redox reaction between CH_4 and SO_4^{2-} producing sulfide and bicarbonate. Their input parameters differ only by different methane concentrations at the lower boundary of the model area. The "standard" simulation represents the conditions at GeoB 4417-7. The rates of the sulfate reduction are shown at the reaction zone for the "standard" simulation with a numerical timestep of 0.005 years

The deviations to exact linear gradients result from depth dependent diffusion coefficients in sediment corrected by porosity. Small boundary and numerical calculation inaccuracies may also be represented. The maximum reaction rates never limit the actual rates in this modeling approach. Therefore, the actual reaction rates are always limited by the available educt species of the reaction. This means, a simulated cell contains either no sulfate or no methane after the redox reaction step, but the PHREEQC calculation removes this sharp and clear separation in the simulated data according to thermodynamic data. This steady state condition is obtained

by reaction rates as shown in Fig. 3 with a time step of 0.005 years. A higher time step of 1 year was used to obtain the steady state concentration profiles (cf. Table 3) which would result in a much wider reaction rate distribution than in Fig. 3, because it allows much more exchange by diffusion within the time step at the reaction zone. However, it is similarly accurate for obtaining steady state profiles. The peak of the sulfate/methane reaction rate limited to a small reaction zone reflects more likely the real situation due to the smaller time step. In contrast, a tendency in the measured methane profile toward a concave curvature with higher methane values than modeled seems to exist between 4 and 4.5 m. This could be the indication for a wider sulfate/methane reaction zone than modeled or for non-steady state conditions, where the reaction zone moves upward due to more methane diffusing upward than consumable by sulfate at this depth. In comparison, the further simulations in Fig. 3 show different steady state profiles caused only by changes of the methane concentration to 8.2 and 30.0 mmol/l at 730 cm. It demonstrates the dependence of the gradients and the depleting zone on this concentration, which controls the upward methane flux.

4.4 Modeling with PHREEQC

We start the PHREEQC simulation with the obtained steady state of the "standard" simulation above. The input data are listed in Table 4. Especially the measured sulfide profile has to be fitted by this second simulation step. The achieved sulfide production rates result in higher sulfide concentrations than those measured. As process to limit the accumulation of sulfide in pore water, we include the solid phases mackinawite and other iron sulfides. The goal is to precipitate sulfide with a rate close to its production rate by sulfate reduction to achieve a steady state for the dissolved species profiles.

To precipitate (or dissolve) solid phases the PHREEQC module within CoTReM is activated. Dissolved iron as reaction partner for precipitation and iron hydroxides as source for dissolved iron are added. The equilibrium to the solid phases is dependent on other species as well, especially the pH. Furthermore, calcite, calcium, pH, pE and total inorganic carbon (TIC) are included. Chloride and sodium are included to achieve the appropriate ionic strength of seawater and to equilibrate the initial charge balance in PHREEQC without disturbing the pH calculation. Furthermore, the time step has to be decreased (0.005 years ≅ 43.8 h); otherwise, numerical stability would not be obtained.

Table 4:
Starting conditions for the second part of the simulation with PHREEQC regarding precipitation of iron sulfides by dissolved iron and sulfide

Input data	Starting condition
Profile distribution of species:	
Methane and sulfate	Obtained steady state from simulation step 1
Sulfide	0.0 mmol / l
Iron	Similar to measured profile
PH	Bottom water value
PE	Measured profile, modified by PHREEQC
Calcium	Approximation: 10.0 mmol / l
Total inorganic carbon	Approximated with measured alkalinity profile
Sodium and chloride	Bottom water concentrations, used for charge balance, activity and seawater ionic strength
Mackinawite and other iron sulfides ("Pyrite")	0.0 g / kg
Calcite and iron hydroxides ("Fe(OH)3(a)")	Constant; differences are shown as results
Upper boundary:	
All dissolved species (except Calcium)	Bottom water concentrations
Calcium	Approximation: 10.0 mmol / l
Calcite and iron hydroxides	Constant
Mackinawite and other iron sulfides	0.0 g / kg
Lower boundary at 730 cm:	
Methane	16.5 mmol / l
All other species	Transmissive boundary condition
Maximum reaction rate for CH_4 and SO_4^{2-}	1.0 mol / (l · a) in all cells; see Table 3.
Sedimentation rate	3.5 cm / ka
Time step	0.005 a ≅ 43.8 h
Simulation run	20 a

The mineral equilibria are determined by the sum of the mineral-log k from the database file and of the chosen saturation index (SI) for the PHREEQC keyword EQUILIBRIUM PHASES. These log k values are constant in a simulation, but we are capable to vary the SI of each mineral depth dependent. A SI of zero results exactly in a mineral equilibrium to the mineral represented by the PHREEQC mineral phase keyword. Therefore, we use the "Calcite" and "Mackinawite" keywords with SI = 0.0 to obtain equilibria to these minerals. We use the mineral phase keywords "Pyrite" and "Fe(OH)3(a)" (an amorph iron hydroxide) to represent a composition and the kinetics of different iron sulfides and iron hydroxides by applying a depth dependent SI distribution (cf. Table 2). These SI distributions are used as important fit parameters to obtain simulation results for sulfide and dissolved iron close to measured profiles. A simple SI distribution of constant values equal zero would result in too

much dissolved iron and virtually no sulfide due to pyrite precipitation. The results for the PHREEQC simulation with variable SI distributions are shown for all included species (except sodium/chloride) in Fig. 4, 5, 6, 7, 8, and 9 after a modeled time period of 20 years.

4.5 Equilibrium of iron and iron hydroxides

The dissolved iron profile is controlled by the SI distribution of iron hydroxides and pH/pE. The iron may precipitate as mackinawite or "Pyrite" with sulfide depending on their ion activity product (IAP) and the SI distribution of the solid phase. During the simulation sulfide accumulates in pore water and iron stays in equilibrium with the iron hydroxides while they are subsaturated with respect to mackinawite and "Pyrite". As soon as they are supersaturated the more supersaturated solid phase precipitates as calculated by PHREEQC, thus reducing sulfide and iron concentrations in the aqueous phase. A source of solid phase iron has to exist around the reaction zone, because the supply of dissolved iron by diffusion to the precipitation zones cannot be sufficient. Iron hydroxides act effectively in the simulation as source of dissolved iron, because the equilibrium between dissolved iron and iron hydroxides is re-applied in each time step by PHREEQC.

The iron hydroxides are represented by different saturation indices in the SI distribution which means an individual chemical tendency to dissolve for each phase due to different properties of the mineral phases with respect to kinetics and thermodynamic equilibrium. An application for mineral kinetics does not exist in PHREEQC, but kinetics would achieve a small disequilibrium toward the mineral in question, because the precipitation/dissolution is a function of super- or subsaturation. This approach of a SI distribution aims at the simulation of the kinetic effects due to calculating toward a defined disequilibrium, which is maintained within a dynamical equilibrium of processes. We explain a substantial part of the SI deviation from SI = 0 for "Fe(OH)3(a)" and "Pyrite" as depth dependent change in the dominating iron hydroxide or iron sulfid phase, but a small part of the SI deviation may be explained as factor maintaining the dynamical equilibrium created by kinetics. However, there is no possibility in this modeling approach to differentiate quantitatively between effects of the SI deviation.

Because older sediments generally lost most of their highly reactive components, we assumed a SI distribution which represents a decrease in the solubility of the iron hydroxides with depth (corresponds to decreasing SI; cf. Table 2). This SI distribution is the main fit parameter for the measured sulfide peak around the methane/sulfate reaction zone. The log k

(≅ 4.9) for "Fe(OH)3(a)" from the PHREEQC database had to be adjusted in the reaction zone with a SI of -7.2 to simulate the measured maximum peak of sulfide. We continued this SI downward. The sum of the log k and SI leads to an iron hydroxide phase present (or reactive with respect to kinetics) in the reaction zone with a log k of -2.3. The remaining SI distribution favors the dissolution of iron (higher SI) and this results in another mackinawite precipitation above the reaction zone. This precipitation stops upward-diffusing sulfide to some degree.

Fig. 4 shows the results for dissolved iron and Fig. 5 the difference for the solid iron hydroxide phases between simulation end and begin.

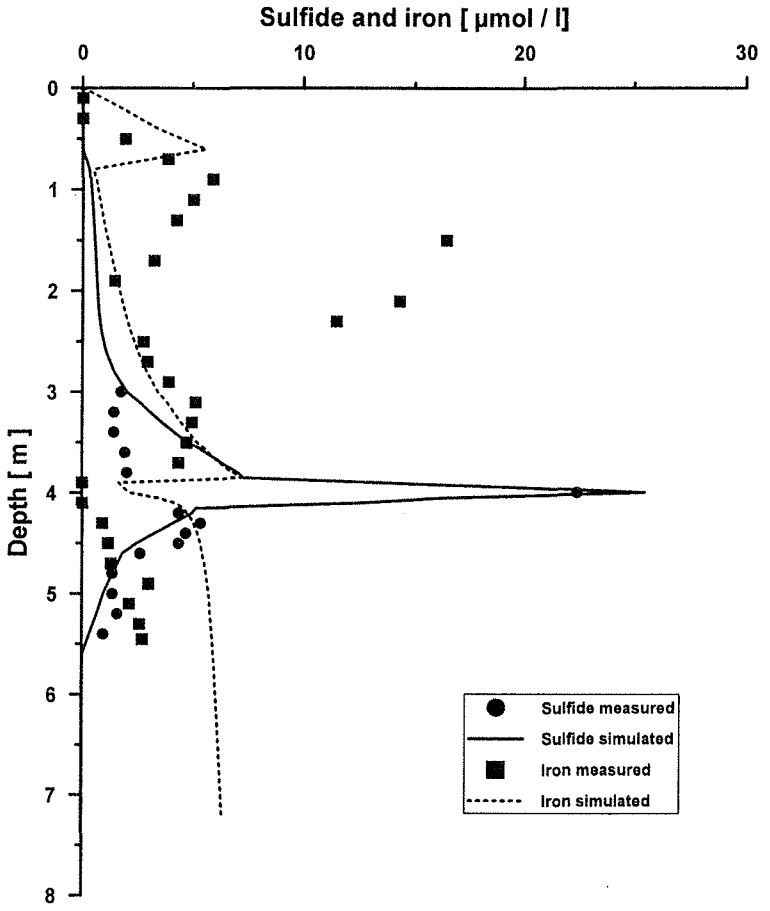

Fig. 4:
The simulated profiles of sulfide and iron are the results of a simulation with PHREEQC and a run of 20 years. The mineral equilibria applied via PHREEQC inhibit a concentration of sulfide in porewater in the range of mmol/l as expected by reaction rates in Fig. 3. Instead, the mineral equilibria result in precipitation of iron sulfides and are capable to fit the measured sulfide data during the simulation run. Dissolved iron is important as the precipitation partner and the concentration results are in the measured range of a few µmol/l

The simulation of dissolved iron deviates partly from the original measurements, but due to the high scattering of data this result was satisfactory. More importantly, the level of some micromoles per liter is obtained, and a smaller concentration in the sulfide production zone is achieved.

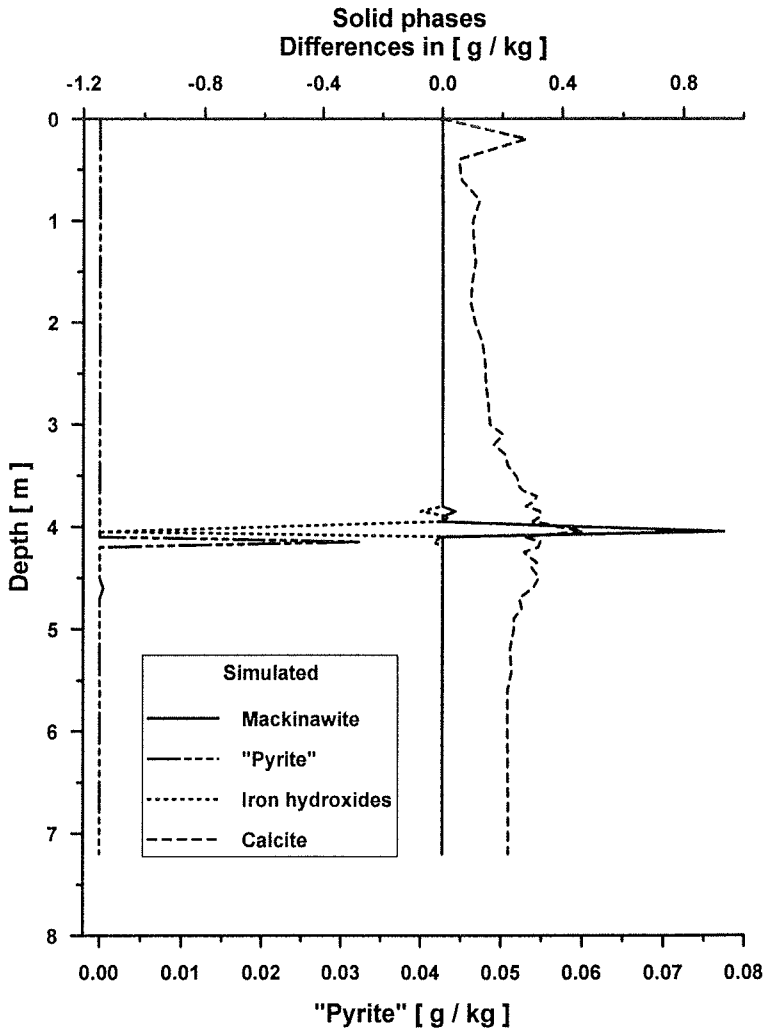

Fig. 5:
Simulated solid phases are shown with the differences of their concentrations between the end and the start of the PHREEQC simulation. Mackinawite is precipitated directly in the sulfate reduction zone and to a smaller extent a few simulation cells above due to upward diffusing sulfide and different saturation indices (SI) for the iron hydroxide phase. Other iron sulfides ("Pyrite") are precipitated at several cells below the reaction zone due to changes of the "Pyrite" SI. Iron hydroxides were dissolved where mackinawite and "Pyrite" were precipitated, because they are the source for dissolved iron consumed by the precipitations. Calcite was precipitated along the core during the run with respect to the H_2O-CO_2-$CaCO_3$-system

Fig. 6 shows the simulated and measured pE. The pE is calculated by the mineral equilibria in PHREEQC and is used in the next time step for the initial species distribution in PHREEQC. It seems that the simulated pE basically reflects the SI distribution of the iron hydroxides. The

distribution determines the relative concentration of the redox couple Fe^{3+} / Fe^{2+} which is used by PHREEQC to obtain the pE in the simulation. Most redox couples are not present in the simulation which contributes to the absolute difference between the measured and the simulated pE. Deviations between measured and calculated pE values are often observed and not yet properly explained (cf. APPELO AND POSTMA, 1996, p. 244). The relative changes in the measured pE profile are, however, obtained by the model.

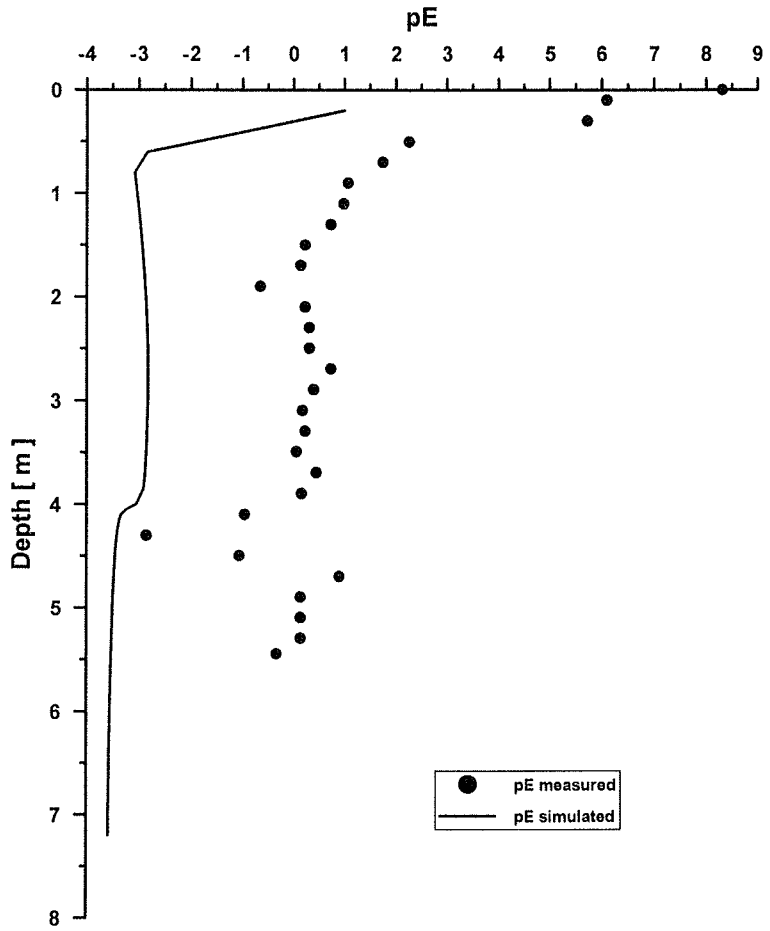

Fig. 6:
The simulated pE was calculated in each time step by PHREEQC. It represents mainly the SI distribution of the iron hydroxides (cf. Table 2) due to the dissolved iron redox couple Fe^{2+}/Fe^{3+}. The measured pE reflects more redox couples and is therefore entirely higher. The form of the pE profile is approximately achieved, but the offset is dramatic

4.6 Equilibrium of sulfide, mackinawite and other iron sulfides

A constant production of sulfide similar to the rates in Fig. 3 can be expected from the methane and sulfate simulation results in Fig. 7. The equilibrium to iron hydroxides (cf. Table 2) and mackinawite (all SI = 0) transforms the most produced sulfide to mackinawite (cf. Fig. 5) in only two cells of the simulation, while limited amounts of sulfide (cf. Fig. 4) with a

simulated similar maximum peak are obtained. This main result of our study demonstrates a dynamical equilibrium over a considerable period of time which is able to explain the existence of small sulfide concentrations in pore water despite high production rates. This simulation for a period of 20 years reflects quasi steady state distributions of aqueous species and is representative for any time period assuming steady state conditions for the sulfate/methane reaction. The solid phase results are given as differences to reflect the dependency on the chosen time period of 20 years.

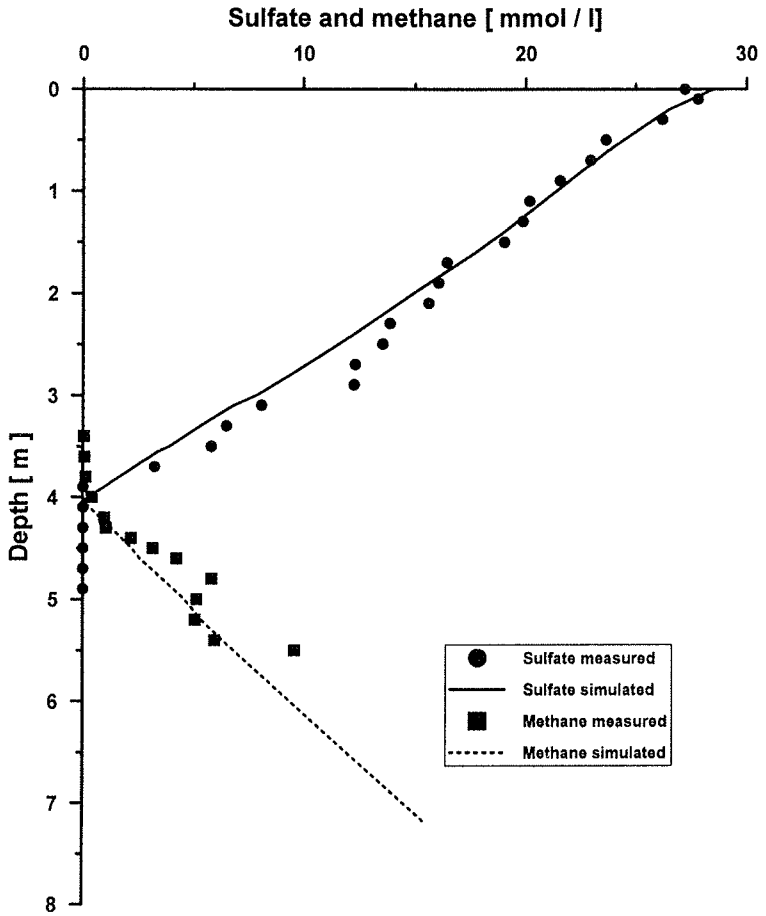

Fig. 7:
These profiles are results of the PHREEQC simulation. Sulfate and methane are in a steady state at GeoB 4417-7 and react in their transition zone according to the rates in Fig. 3 producing sulfide and bicarbonate

The sulfide concentration peak necessary to precipitate mackinawite causes up- and downward diffusion of sulfide, which changes in return the equilibrium calculations in these cells around the sulfide production zone. In our simulation we applied conditions to suppress this problem of recalculating equilibrium as far as possible. The effect of upward-diffusing

sulfide is decelerated by another mackinawite precipitation zone (cf. Fig. 5). This is possible due to variation of the iron hydroxide SI to -6.5 (cf. Table 2), which favors the dissolution of higher amounts of iron (the iron peak in Fig. 4 at ca. 3.8m), thus leading again to a supersaturation with respect to mackinawite. However, this condition cannot totally stop the diffusing sulfide over long time periods. Therefore, the simulated sulfide concentrations in this area fit the measured data only to some extent.

We cannot change the SI for iron hydroxides to a higher SI below the production zone, because deeper sediments should be less reactive. Another point of interest is the redissolution of mackinawite below the precipitation cells, because it is transported downwards by sedimentation. In the simulation the mackinawite can generally not be transported across the lower model area boundary, because the mackinawite would dissolve with respect to concentrations of sulfide, iron and the pH. This problems could be handled by assuming that this is suppressed by the kinetics of mackinawite dissolution.

We decided to cope with this particular problem by incorporating a "Pyrite" equilibrium. In PHREEQC "Pyrite" is simply precipitated directly from dissolved iron and sulfide. It would precipitate with a SI = 0.0 (higher supersaturated than mackinawite) in the simulation, basically removing all sulfide, resulting in no fitted sulfide peak. Therefore, we use "Pyrite" to represent an unknown composition of iron sulfides and assume these "Pyrite" phases are more stable, but their formation is slower than mackinawite due to limitation by kinetics. This is supported by studies which show that pyrite forms via mackinawite (or greigite) or precipitates directly (RICKARD, 1969; RICKARD, 1975; RAISWELL, 1982). According to SWEENEY AND KAPLAN (1973) and GOLDHABER AND KAPLAN (1974) the direct pathway of precipitation will only occur if pyrite is supersaturated, but mackinawite subsaturated. Supersaturation of mackinawite, like in our simulated reaction zone, inhibits direct precipitation of pyrite, despite a possibly higher supersaturation of the latter. Therefore, we inhibit "Pyrite" precipitation from the upper boundary down to one cell below the main mackinawite precipitation zone by applying a SI = +20 for "Pyrite". Below this depth, three areas of "Pyrite"-SI are chosen (cf. Table 2). At each upper cell of these areas (two upmost cells at SI = 0) the simulation result contains precipitated "Pyrite" (cf. Fig. 5, lowest peak too small to see). They suppress the sulfide diffusion downward, providing a sulfide sink into minerals, like the SI change of iron hydroxides does above the reaction zone, and fit the measured sulfide data well.

Iron monosulfides, such as mackinawite, are likely to precipitate first but the entire iron sulfide mineral precipitation is not completely understood at GeoB 4417-7. Especially reaction kinetics, participating minerals, inhibition effects, and secondary reactions such as transformation of mackinawite to other iron sulfides, are simply not known. We recognize that a "Pyrite"-SI distribution is useful to limit the diffusion of the sulfide peak via additional iron sulfide phases and kinetic restrictions for these phases, but cannot explain in detail the missing information about processes and phases. This occurs, because PHREEQC calculates a static mineral equilibrium or a specific disequilibrium (SI≠0) disregarding dissolution or precipitation kinetics and inhibition processes. However, the equilibria with the mineral distributions of mackinawite, "Pyrite" and "Fe(OH)3(a)" result in a simulated sulfide profile comparable to the measured data and estimate sulfide precipitation.

4.7 Calcite equilibrium

Alkalinity and the carbon dioxide system together with the pH are maintained by the calcite equilibrium (referred as H_2O-CO_2-$CaCO_3$ system). The main reason to include these parameters is to get the pH at least roughly due to its effects on distributions and relations of the elements iron and sulfur in aqueous and solid phases. A proper simulation of the calcite equilibrium system needs more processes to consider. Calcite is completely equilibrated with SI = 0 and shown in Fig. 5. Alkalinity, total dissolved carbon (TIC) and calcium are shown in Fig. 8, and the pH in Fig. 9. The starting conditions are listed in Table 4. The alkalinity difference between measured and simulated data was partially caused by the TIC approximation with measured alkalinity. Yet the first PHREEQC calculation resulted in the general form of the calcium, alkalinity, TIC, and pH profile due to precipitating calcite. The shape of the calcium profile is known from other sites with deep sulfate reduction (SCHULZ ET AL., 1994). During the whole simulation run calcite continued to precipitate, especially in the main precipitation zone of mackinawite. Therefore, calcium, alkalinity, and TIC decreased further. The pH showed no further major changes. Across the upper boundary diffusion increased calcium and decreased TIC and alkalinity. All of these simulated data fit only partially to the measured data. This is caused due to neglecting some early diagenetic processes such as, for example, consumption of organic matter within the upper sediment column. The absolute differences in pH measurements and simulations (≈0.6 pH) depend on the solubility constant of calcite. Whereas we used a proper log $k_{Calcite}$ value for pure calcite from the PHREEQC database with temperature corrections, a more exact pH simulation requires modifications concerning log $k_{Calcite}$ variations due to impurities occurring in natural

calcites (e.g., Mg incorporation; MACKENZIE ET AL., 1983). The measured pH peak at 4m depth is not simulated, because it is likely caused by kinetic effects in this reaction zone which is not included in the simulation (cf. ADLER ET AL., in press).

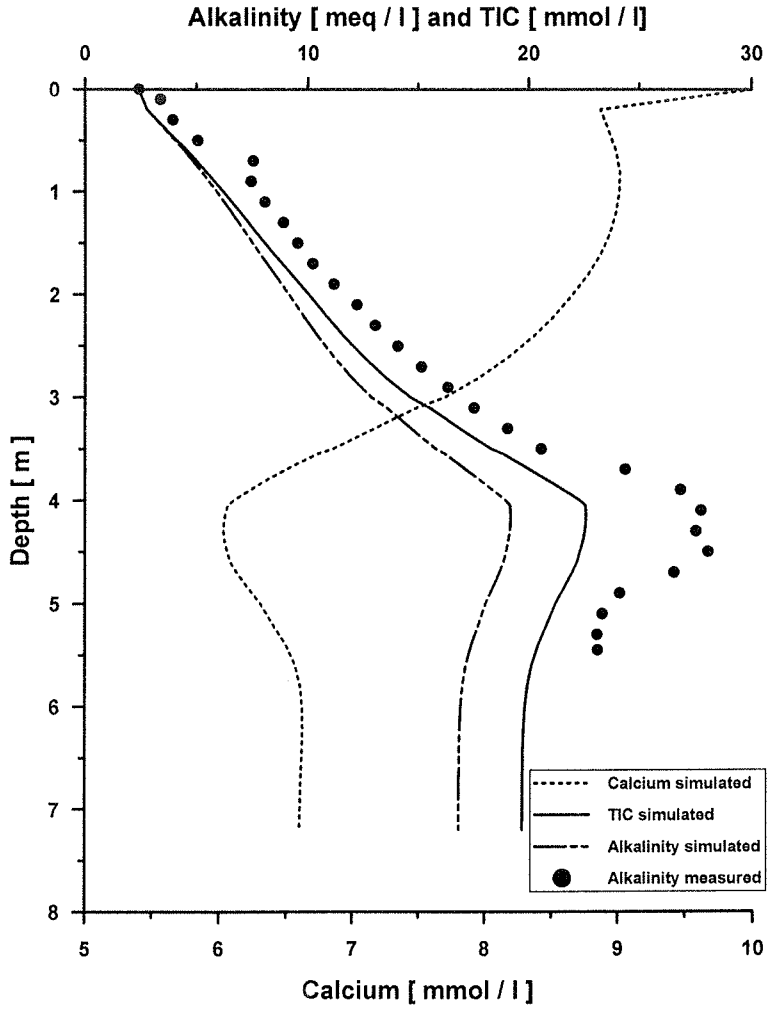

Fig. 8:
The simulated profiles of alkalinity deviate from the measured alkalinity profile due to precipitation of calcite during the simulation, which consumes dissolved carbon (TIC) and calcium. The TIC concentration is also too small. The calcium profile achieved a general form, which is known by other deep sulfate reduction sites off southwestern Africa (SCHULZ ET AL., 1994).

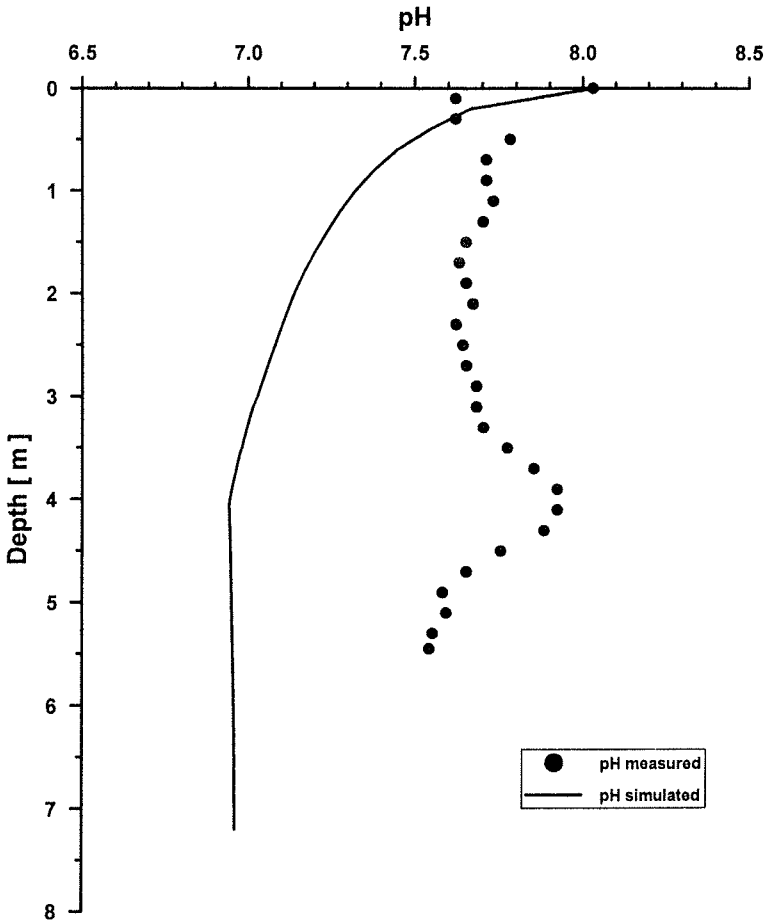

Fig. 9:
The simulated pH shows differences to the measured data caused by the deviations of the H_2O-CO_2-$CaCO_3$-system. Further processes have to be integrated in further simulations

Simulating these species obtained necessary data to use PHREEQC for precipitating sulfide to mackinawite. Further studies should first concentrate on a method to apply a more accurate calculation of pH and pE.

5 Conclusions

Pore water concentration profiles and simulation results show that the flux of sulfate into the sediments is equally consumed by an upward diffusive flux of methane at site GeoB 4417 on the Amazon Fan. The observed sulfide profile has relatively small concentrations (in comparison with sites off southwestern Africa with deep sulfate reduction driven by methane) and is successfully simulated due to the application of several mineral equilibria. A transformation of iron hydroxides with sulfide to mackinawite and other iron sulfides is suggested with rates corresponding to the rates of sulfide production by the deep sulfate reduction in a high reactive zone. The H_2O-CO_2-$CaCO_3$ system was sufficiently simulated to stabilize the pH and obtain a quasi steady state situation of pore water profiles, especially with respect to the sulfide concentration peak, for a simulation run of 20 years. This indicates an at least decade-long stability in this modeling approach, without achieving the problem of an unsolvable thermodynamic equilibrium in PHREEQC. This simulation reveals a possible set of conditions for the geochemical system at GeoB 4417-7, which is actually in a dynamic equilibrium between solutes and mineral phases. With respect to simulation methods, we demonstrated the ability of the model CoTReM to adapt the state of a complex geochemical system and to re-perform its dynamics.

Further studies at GeoB 4417-7 should investigate the reasons for still-existing deviations from measured and simulated data of, for example, pE and pH, and which minerals are exactly formed below the sulfate reduction zone. The program will be modified to incorporate the data of more minerals which can be suspected to be part of the dynamics at this site (greigite, vivianite, goethite, hematite) and methods to incorporate kinetics for precipitation and dissolution in PHREEQC will be examined.

Acknowledgments

We thank the captain and the crew on cruise M 38/2 of the RV Meteor. We thank S. Hinrichs and K. Enneking for the great assistance of shipboard geochemical analyses. This research was funded by the Deutsche Forschungsgemeinschaft and was supported by the SFB 261 (The South Atlantic in the Late Quaternary: Reconstruction of material budget and current system) and by the "Graduate College of Material Flux in Marine Geosystems" at the University of Bremen.

Modeling of calcite dissolution by oxic respiration in supralysoclinal deep-sea sediments

M. ADLER[1], C. HENSEN[1], F.WENZHÖFER[2], K. PFEIFER[1] AND H.D. SCHULZ[1]

1 University of Bremen, Department of Geosciences, P.O. Box 330 440, Germany

2 Max Planck Institute for Marine Microbiology, Celsiusstr. 1, D-28359 Bremen, Germany

Corresponding author: Matthias Adler Phone: 0049-421-2183967
Fax: 0049-421-2184321
e-mail: madler@geochemie.uni-bremen.de

Abstract

Pore-water profiles of CO_2, pH, Ca^{2+} and O_2 *in situ* concentrations were measured at two stations on the upper continental slope off Gabon. The present study evaluates these measurements concerning their implications for the calcium carbonate system in deep-sea sediments. The model CoTReM, which was used to simulate the dynamics of this complex geochemical system, revealed a strong dependence of calcite dissolution on oxic respiration at both sites. All simulated calcite dissolution kinetics reached a dynamic equilibrium with almost equal calcite dissolution rates, but different subsaturation states and pH values. The latter are mainly dependent on boundary conditions and kinetic rate law parameters. Boundary conditions are of immense importance. They define which pH deviations between measured data and the simulated equilibration (instantaneous kinetics) have still to be fitted by kinetic restrictions per rate law for the equilibration. These pH deviations set up the range of possible values for rate constants in a given rate law to yield a well simulated pH. A failure in the implementation of these boundary conditions may lead to non-linearly flawed rate constants, which fit only one (usually the maximal) pH deviation well. The whole depth distribution of pH deviations has to be fitted very well by a kinetic rate law. Only this procedure secures that the used boundary conditions and rate laws/constants are acceptable. Nevertheless, several kinetic rate laws may be used for good pH fits, featuring clear differences in parameter values for rate constants and reaction orders. The connection between these rate laws with different parameters is examined and the dependence of the rate constant on the given form of the rate law is demonstrated. This study achieves rate constants of 0.038 and 18 %/d for a dissolution rate law of 4.5^{th} reaction order and subsaturation dependence from the term ($1 - \Omega$). These results are well within the range of rate constants obtained during former field studies for the same form of the dissolution rate law.

Keywords: Calcite; dissolution kinetics; numerical model; operator-splitting; PHREEQC

1 Introduction

Deep-sea sediments are one of the major sinks for inorganic and organic carbon on earth. Most of the biogenic particles reaching the seafloor are, however, recycled by respiratory decomposition and dissolution processes generating a benthic reflux of dissolved organic and inorganic carbon back to the water column. The diagenetic reactions are most intense at the sediment-water interface and within the upper centimeters of the sediment column where the most labile components are rapidly mineralized. The dissolution of calcium carbonate in deep-sea sediments is controlled by two major factors, the degree of subsaturation of the deep ocean waters overlying the sediments with respect to calcite and aragonite, and the reaction with metabolically produced carbon dioxide (EMERSON AND BENDER, 1981).

The effects of respiration on calcite dissolution in marine sediments have received attention only recently (ARCHER AND MAIER-REIMER, 1994). In the last decade, increasingly more *in situ* techniques have been developed to overcome sampling artifacts that obscured profiles and made it impossible to properly analyze the processes. Until today, various studies have been performed with benthic chambers and profiling lander systems, determining total fluxes of dissolved species across the sediment-water interface and pore-water microprofiles of oxygen, pH and pCO_2. Quite a number of these recent investigations revealed that significant amounts of calcium carbonate are dissolved in response to oxic respiration close to the sediment-water interface (ARCHER ET AL., 1989; BERELSON ET AL., 1994; CAI ET AL., 1995; HALES AND EMERSON, 1996, 1997A; HALES ET AL., 1994; JAHNKE ET AL., 1997; MARTIN AND SAYLES, 1996). In contrast, it is still under debate which kind of dissolution kinetics offers the best explanation for the measured profiles. The most widely accepted and applied rate law is the one suggested by MORSE (1978) and KEIR (1980):

$$DR = k \cdot (1 - \Omega_{Calcite})^{n} \qquad \text{(Eq. 1)}$$

where DR is the calcite dissolution rate, k is the calcite dissolution rate constant, $\Omega_{Calcite}$ is the saturation state and n the reaction order. In most studies the value applied for the reaction order n is 4.5 for calcite and 4.2 for aragonite. The rate constant k varies greatly. Laboratory experiments of KEIR (1980) indicate a value of about 1000 %/d for k (cf. section 3.4 for [mol / (kgw · yr)] as unit) for suspended particles, whereas values two orders of magnitude lower are characteristic of sedimented carbonates (KEIR, 1983). Field observations often require even lower values for k. In different model calculations for *in situ* microelectrode data derived from various locations in the Pacific and Atlantic Oceans, the rate constant k varies by several orders of magnitude from 0.01 to 150 %/d (ARCHER, 1991; BERELSON ET AL., 1990A, 1994;

CAI ET AL., 1995; HALES AND EMERSON, 1996, 1997A). The reason for this discrepancy is not clearly known. Important and regionally variable factors, however, may be the grain size and thus the surface area of calcium carbonate crystals in the sediments, or adsorbed coatings like phosphate ions protecting calcium carbonate grains from corrosive pore waters (HALES AND EMERSON, 1997A; JAHNKE ET AL., 1994). In contrast, HALES AND EMERSON (1997B) found evidence that *in situ* pH measurements in pore waters of calcite-rich, deep-sea sediments are more consistent with a first-order than with a 4.5^{th} order dependence. The first-order approach reduced the differences of required k_Ω values in their field studies to less than one order of magnitude compared to the 4.5^{th} order model.

In the present study we address the problem of calcite dissolution kinetics in sediments on the continental slope off Gabon with overlying bottom-water supersaturated with calcite (WENZHÖFER ET AL., subm.). Different kinetics as formulated in Equation 1 are applied and compared to previous results. In order to evaluate the coupling of calcium carbonate dissolution to oxic respiration and related redox processes we applied the numerical model CoTReM (Column Transport and Reaction Model;

http:\\www.geochemie.uni-bremen.de/cotrem.html

LANDENBERGER, 1998) to *in situ* measurements of oxygen, pH, pCO_2, and calcium.

2 Material and Methods

2.1 Studied sites

The sites examined in this study are GeoB 4906 and GeoB 4909 at the continental slope off Gabon (cf. Table 1). Shipboard data were collected onboard the research vessel METEOR during cruise M 41/1 from Malaga to Libreville between February 13 and March 15, 1998 (SCHULZ ET AL., 1998). *In situ* data were gained by means of a profiling lander (WENZHÖFER ET AL., subm.). Site GeoB 4906 is located within an area of equatorial upwelling, while site GeoB 4909 reflects more oligotrophic conditions (Fig. 1). This is, for example, reflected by the penetration depth of oxygen at both sites (cf. Table 1 as measured by WENZHÖFER ET AL., subm.).

2.2 Measured concentration profiles

In situ measurements were carried out for CO_2, pH, Ca^{2+} and O_2 with microelectrodes and optodes (see WENZHÖFER ET AL. (subm.) for detailed description). Further parameters were obtained by multicorer sampling and pore-water extraction as is extensively described by

SCHULZ ET AL. (1994) or HENSEN ET AL. (1997). Nitrate and alkalinity were determined onboard the ship. Sulfate, sodium, chloride, potassium, magnesium and manganese were determined in acidified samples, by using an inductively coupled plasma emission spectrometer (ICP-AES) at Bremen University.

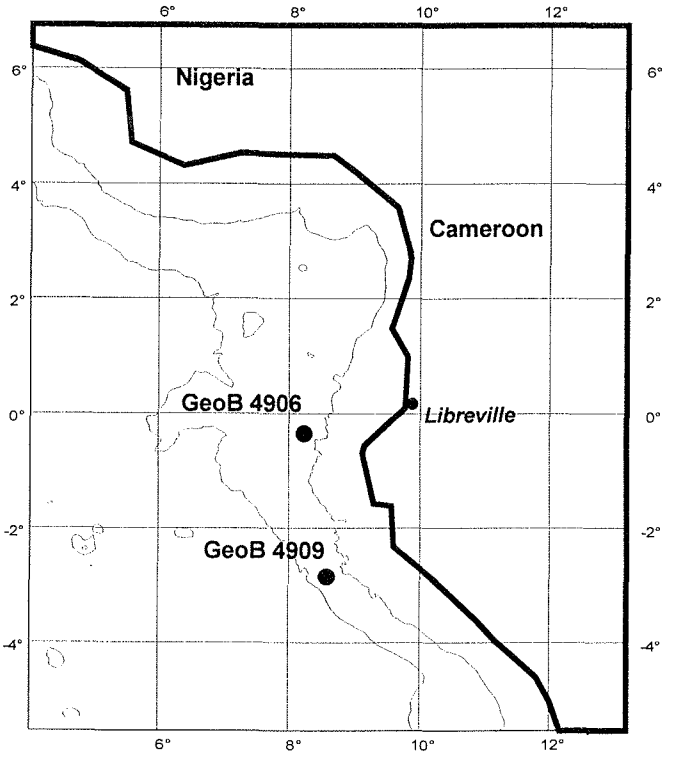

Fig. 1:
Location map of the eastern equatorial Atlantic.

Table 1:
Location of the stations GeoB 4906 and GeoB 4909 and the main characteristics of these sites.

GeoB station		*4906*	*4909*
Latitude		00°41.17 S	02°04.35 S
Longitude		08°22.94 E	08°37.54 E
Water depth		1251 m	1317 m
Temperature		4.5 °C	4.5 °C
Bottom water:	pH	7.81	7.92
	O_2 [µmol / l]	184	184
	$SI_{Calcite}$	+ 0.03	+ 0.04
Oxygen penetration depth (OPD)		15.5 mm	25.0 mm

3 Modeling approach

3.1 Presumed processes

The uppermost sediment layer where organic matter degradation and calcite dissolution occur, was investigated with the simulation model CoTReM. The mathematical model area is divided into a column of cells and simulates the sediment layer. These cells of the model area consider the following processes and geochemical reactions:

I. Diffusive transport for all aqueous species within the model area plus certain boundary settings (cf. 3.3).

II. Redox reactions for organic matter (OM) degradation by oxygen and nitrate. The organic matter is assumed to be characterized by the Redfield ratio (elements C:N:P = 106:16:1 = x:y:z) and defined within this study as:

$$OM = (CH_2O)_x (NH_3)_y (H_3PO_4)_z \quad \text{(Eq. 2)}$$

The redox reactions for the OM degradation are:

$$OM + (x+2y)\,O_2 \Longrightarrow x\,HCO_3^- + y\,NO_3^- + y\,H_2O + (x+y+3z)\,H^+ + z\,PO_4^{-3} \quad \text{(Eq. 3)}$$

and

$$OM + 0.8x\,NO_3^- + y\,H_2O \Longrightarrow x\,HCO_3^- + 0.4x\,N_2 + y\,NH_4^+ + 0.4x\,H_2O + (0.2x+3z)\,H^+ + y\,OH^- + z\,PO_4^{-3} \quad \text{(Eq. 4)}$$

III. General thermodynamic equilibrium reactions are calculated by PHREEQC (PARKHURST, 1995). They consider mass balance, concentration, activity and dissociation of species (pH), ionic strength, temperature, density and charge balance of the solution as well as the saturation indices of minerals in the solution.

IV. Adjustment of the calcite equilibrium for each time-step and simulated cell: Either calculation to exact equilibrium (instantaneous kinetics) or calculation considering calcite dissolution kinetics driven by the deviation from equilibrium.

3.2 General model description

The numerical model CoTReM (**Co**lumn **T**ransport and **Re**action **M**odel; LANDENBERGER, 1998), based on the former model CoTAM (HAMER AND SIEGER, 1994), was developed for the simulation of the one-dimensional transport of solute and mineral phases and their interactions as dictated by bio-geochemical reactions and thermodynamic equilibria in natural environments. It can even be applied to non-steady state conditions and to an inhomogeneous model area. Simulations including sedimentation, advection, dispersion, diffusion, bioturbation, bioirrigation as well as reactions of reoxidation, dissociation, dissolution and precipitation are possible with CoTReM. The coupling to the model PHREEQC (PARKHURST,

1995) enables CoTReM to simulate the thermodynamic equilibrium reactions. The modeling approach solves the General Diagenetic Equation (cf. in Appendix Eq. A.1; e.g. BERNER, 1980) with a method of operator-splitting (OS). A finite difference method is used for the transport of the various species, which carries out the simulation of a column of n cells as the model area. Then, due to OS, the effects of the chemical reactions are calculated for these isolated cells. CoTReM's general calculation principle is illustrated in Fig. 2.

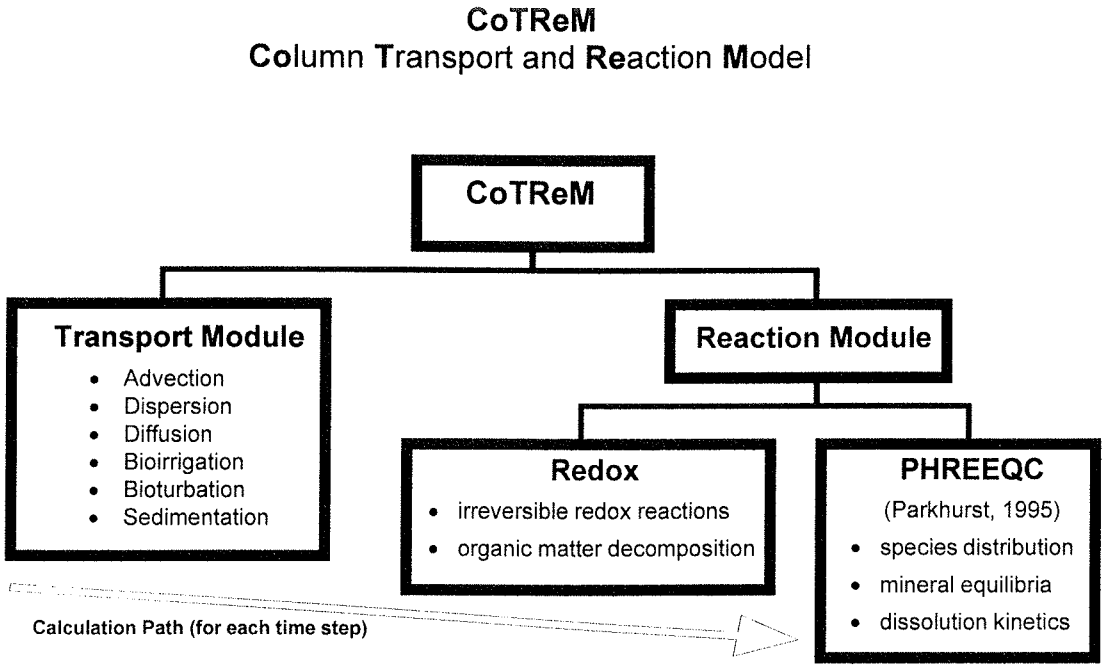

Fig. 2:
Calculation scheme of CoTReM. In each time-step the transport effects are first solved (Appendix: A.2/A.3) for the entire model area followed by "cell by cell" calculations for redox reactions (A.5) and mineral equilibrium kinetics (PHREEQC).

This approach allows the modeler to divide the General Diagenetic Equation into several parts (Appendix: Eq. A.2-A.5 plus PHREEQC), which are easier to solve and which are applied sequentially. A linear difference equation system (developed for all cells from Eq. A.3 with Taylor series approximations and the Crank-Nicholsen difference scheme) is solved for the transport by a variant of the Thomas algorithm (PRESS ET AL., 1992).

A Cauchy-boundary condition for the sediment bottom-water boundary is applied by fixed bottom-water concentrations for each species ($C_{0\_Species}$). The lower boundary condition is set with an extra cell (n+1) below the model area, which may be transmissive ($C_{n+1}=2 \cdot C_n - C_{n-1}$) or impermeable ($C_{n+1}=C_n$), or fixed, depending on the species (similar to Cauchy).

The total reaction rate (cf. in Appendix Eq. A.4) of a species is split into components caused by redox reactions (Eq. A.5) and by thermodynamical equilibria reactions. The redox reaction rates are defined as depth-dependent for each reaction using zero-order kinetics. The equilibria reactions are executed by incorporating PHREEQC (PARKHURST, 1995) as a subroutine in CoTReM, which receives as input all species concentrations, the pH and the mineral saturation indices (SI_{Set}) to be achieved. Saturation indices obtained from the initial equilibration of the solution are further used for determining effects of dissolution kinetics. The final results from the equilibrium calculation end the time-step and include the effects of adding/removing mineral amounts (limited by supply or kinetics) by dissolution or precipitation to the solution in a cell. More details about CoTReM and its mathematical background are given in the Appendix A and in the CoTReM User Guide (ADLER ET AL., 2000B; http:\\www.geochemie.uni-bremen.de/cotrem.html).

3.3 Boundary conditions for the simulation runs

A model simulation requires some conditions to be fixed for the runtime. The time-step for the simulations was $1 \cdot 10^{-5}$ yr. An inhomogeneous discretization of the model area was used for site GeoB 4909 (cells of 0.5 mm for the range 0-3 cm; cells of 1.0 mm for the range 3-3.9 cm), while cells of 1.0 mm were used for site GeoB 4906.

The interaction between bottom-water and the sediment is implemented by using the fixed concentrations $C_{0\_Species}$ as upper boundary conditions for the topmost cell. These $C_{0\_Species}$ are usually set according to bottom-water measurements (cf. Table 2). In these simulations the lower boundary (LB) is defined for all species concentrations as impermeable to diffusion (the last cell's concentrations are used for the extra LB-cell). Exceptions are fixed values for NO_3^- and HCO_3^-(except first runs) at site GeoB 4909 and for Mn^{2+} and HCO_3^- at site GeoB 4906 (listed under C_{LB} in Table 2).

Porosity and species-dependent sediment diffusion coefficients D_S are assumed to decrease with depth. Porosity was set according to Eq. 5 given by RABOUILLE AND GAILLARD (1991) as

$$P = P_{Min} + (P_{Max} - P_{Min}) \cdot \exp(-Depth / k^*) \qquad \text{(Eq. 5)}$$

where P is the porosity of a cell in the sediment, P_{Max} (= 95%) is the maximum porosity at the sediment bottom-water interface, P_{min} (= 85%) is the minimum porosity at the end of the sediment column, Depth refers to the depth of the cell in cm and k^* (= 3.5 cm) is the depth constant for the porosity decrease.

Table 2:
Upper and lower boundary concentrations $C_{0\_Species}$ and $C_{LB\_Species}$ of the simulated model areas at both sites. The lower boundary values for HCO_3^- (or TIC) depend on the applied conditions.

Boundary Concentrations		GeoB 4906	GeoB 4909
Upper boundary $C_{0\_Species}$:			
PH		7.81	7.87
O_2	[µmol/l]	179	181.5
NO_3^-	[µmol/l]	30.92	32.03
HCO_3^-	[mmol/l]	2.44	2.15
Ca^{2+}	[mmol/l]	10.30	10.353
SO_4^{2-}	[mmol/l]	30.169	28.5
Mg^{2+}	[mmol/l]	50	50
Na^+	[mmol/l]	483	479
Cl^-	[mmol/l]	550	550
K^+	[mmol/l]	9.60	9.60
Mn^{2+}	[µmol/l]	0	-
Fe^{2+}	[µmol/l]	0	-
PO_4^{3-}	[µmol/l]	2.0	-
HS^-	[µmol/l]	0	-
NH_4^+	[µmol/l]	0	-
H_2	[µmol/l]	0	-
Lower boundary $C_{LB\_Species}$:		at 6.05 cm	at 3.95 cm
HCO_3^-	[mmol/l]		
Log $K_{sp,\ Calcite}$			
	= -8.222	4.0 Fig. 8	3.7 Fig. 5a
	= -8.180	-	4.0 Fig. 5b
	= -8.180	-	3.8 Fig. 5c
Mn^{2+}	[µmol/l]	42	-
NO_3^-	[µmol/l]	-	1.0

Molecular diffusion coefficients for all dissolved species, D_0, are taken from BOUDREAU (1996B), except for the dynamic viscosity of water (ATKINS, 1978). The diffusion coefficients in sediment, D_S, which are dependent on porosity, are calculated according to BOUDREAU (1996 B).

$$D_S = D_0 / (1 - \ln(P^2)) \qquad \text{(Eq. 6)}$$

where D_s is the molecular diffusion coefficient in sediment, D_0 the molecular diffusion coefficient in water and P the porosity of a cell in the sediment. Bioturbation and bioirrigation effects were not measured and are neglected in this study.

Thermodynamical equilibrium constants were calculated by PHREEQC (PARKHURST, 1995) including corrections for bottom-water temperature. Pressure dependence was included for the dissociation of water and carbonic acid (MILLERO, 1983) as well as for the solubility product of calcite $K_{sp,\ Calcite}$ according to data from SOLMINEQ.88 (KHARAKA ET AL., 1989). The logarithm of $K_{sp,\ Calcite}$ was calculated to be $log\ K_{sp,\ Calcite}$ = -8.222 (T = 4.5°C; p = 130 bar). The supersaturation of the bottom-water solutions relative to $log\ K_{sp,\ Calcite}$ = -8.222 is listed in Table 1. All presented simulations examine the calcite dissolution and include the number of species listed in Table 2 to simulate seawater conditions (ionic strength, activities, aquatic species distribution) within the PHREEQC subroutine.

The oxygen distribution in pore-water was not calculated with PHREEQC since equilibrium calculations are not appropriate for a microbially mediated process.

3.4 Calcite dissolution rate laws in CoTReM

Mineral dissolution kinetics usually depend on the solution's deviation (according to Newton's law of actio = reactio) from the equilibrium (SI_{Set} = 0). Therefore, kinetics for calcite dissolution are defined as a function of Ω (or the SI) within CoTReM. $SI_{Set} \neq 0$ could be used to modify the equilibrium condition, which is set up with a general, fixed value of $log\ K_{sp,\ Calcite}$ in the PHREEQC database, for cell specific corrections. These may be secondary depth-dependent corrections due to existing temperature or pressure gradients within the model area or due to cell dependent set up of the specific mineral (characterized by the solubility product) to dissolve or precipitate (cf. ADLER ET AL., 2000A).

The main function used for calcite dissolution rates in CoTReM is analogous to those proposed by KEIR (1980):

$$DR = k_{\Omega} \cdot (1 - 10^{(-SI_{Set}+SI_{Calcite})})^{n} \quad \text{(Eq. 7)}$$

with $$SI_{Calcite} = \log_{10} \Omega_{Calcite} \quad \text{(Eq. 8)}$$

and $$\Omega_{Calcite} = IAP / K_{sp,\,Calcite} \quad \text{(Eq. 9)}$$

where	DR	[mol / (kgw · yr)]	:	Dissolution rate
	$k = k_{\Omega}$	[mol / (kgw · yr)]	:	Dissolution rate constant (of the Ω-law)
	n	[-]	:	Reaction order
	$\Omega_{Calcite}$	[-]	:	Saturation state of calcite
	IAP	[-]	:	Ion activity product
	$K_{sp,\,Calcite}$	[-]	:	Solubility product of calcite, dependent on temperature and pressure
	$SI_{Calcite}$	[-]	:	Saturation index of calcite
	SI_{Set}	[-]	:	The Saturation index of calcite, which shall be achieved by the calcite kinetics. Usually, SI_{Set} is chosen to be zero and $10^{SI_{Set}}$ equals one.

note that k [mol / (kgw · yr)] = k [% / d] · 365 [d / yr] · ρ · (1 - P) · 0.01 [1 / %] / (P · m_w · $GFW_{Calcite}$) (Eq. 10)

where	ρ	[g / dm^3]	:	Density = 2600 g / dm^3
	m_w	[kgw / dm^3]	:	Mass of water in one dm^3 of solution
	P	[-]	:	Porosity [Fluid volume / Total volume]
	$GFW_{Calcite}$	[g / mol]	:	Gram formula weight of Calcite = 100.09 g / mol

With an averaged porosity of P = 0.9 and a approximately cell-constant mass of water m_w = 0.965 [kgw / dm^3] the conversion within this study is:

$$k \text{ [mol / (kgw · yr)]} = k \text{ [\% / d]} \cdot 365 \cdot 2600 \cdot 0.1 \cdot 0.01 / (0.9 \cdot 0.965 \cdot 100.09)$$
$$= k \text{ [\% / d]} \cdot 10.917 \quad \text{(Eq. 11)}$$

further valid is: $1.0 \cdot \%_{Calcite} = 2.991 \cdot 10^{-2} \cdot \text{mol}_{Calcite} / \text{kgw}$ (Eq. 12)

Unless the unit [% / d] is noted, [mol / (kgw · yr)] is used below for k and DR.

A different law used for the determination of calcite dissolution rates DR is:

$$DR = k_{SI} \cdot (SI_{Set} - SI_{Calcite})^{n} \quad \text{(Eq. 13)}$$

where $k = k_{SI}$ [mol / (kgw · yr)] is the dissolution rate constant of the SI-law. The difference of both groups (parameters k and n) of rate laws is given by the dependence on Ω or log Ω. The meaning of this difference is examined in 4.4.2. Due to the exclusive use of $SI_{Set,Calcite}$ = 0 in this study, Eq. 7 reduces to $DR = k_{\Omega} \cdot (1 - \Omega_{Calcite})^{n}$ and Eq. 13 to $DR = k_{SI} \cdot (- SI_{Calcite})^{n}$.

4 Results and Discussion

4.1 Fit of the oxygen profile in case of oxic respiration

The oxygen profile for site GeoB 4909 was modeled with the transport and reaction modules of CoTReM under the following four assumptions:

I. The measured oxygen reflects a (dynamic) steady-state profile.
II. Oxygen input across the sediment bottom-water boundary into the model area occurs by diffusion according to the coefficients in section 3.3.
III. Oxygen is consumed by organic matter (OM) degradation (Eq. 3) only. The consumption equals the oxygen input from transport (II.).
IV. The oxygen profile is simulated independently of any thermodynamic equilibrium conditions.

The initial oxygen concentrations for the simulation approximate the measured concentrations within all cells. This concentration distribution is seen as the "true" oxygen profile. Delta_O_2 (Fig. 3a) is calculated as the difference between the model simulation and the "true" profile exclusively due to the transport during one time-step, dependent on the exact amount of C_{0_Oxygen}. C_{0_Oxygen} controls the topmost two millimeters of delta_O_2. Otherwise, the results show that the oxygen input is positive and on average decreases with depth. Less expected are the few negative values of delta_O_2 (more diffusion out than into the cell). Assumption III cannot be used with negative delta_O_2 (meaning creation of OM instead of degradation). Therefore, the delta_O_2-values were averaged before they were used to calculate depth-dependent OM degradation rates, in order to fulfill assumption III. This means, on the other hand, that assumption I. is not exactly fulfilled, because the slightly different distribution of rates (not the sum of rates) results in small deviations of the calculated profile from the "true" profile. These deviations of the calculated profile are sufficiently accurate to define the "true" profile, and the method gives better fitted rates than any fit made by eye.

For simulation purposes, C_{0_Oxygen} is the concentration exactly at the bottom-water sediment boundary below a diffusive boundary layer (DBL), while the bottom-water concentration above the DBL in general equals 184.0 µmol/l (cf. WENZHÖFER ET AL., subm.). According to the measured data, a C_{0_Oxygen} of 181.5 µmol/l is used in this study.

The precise implementation of C_{0_Oxygen} is very important for the simulation because C_{0_Oxygen} mainly defines delta_O_2 in the first few cells and, thus, the oxygen OM consumption rates in these cells. Figure 3a describes this strong influence of C_{0_Oxygen} on delta_O_2 in relation to

different values for C_{0_Oxygen} with only very small deviations from 181.5 µmol/l. For example, the consequence of using the value of 184.0 µmol/l from above the DBL would require much higher OM degradation rates in the first few cells than in any cell below. As we will see later, the effect of such high rates on the pH value is very difficult, or even impossible, to simulate with any calcite dissolution kinetics.

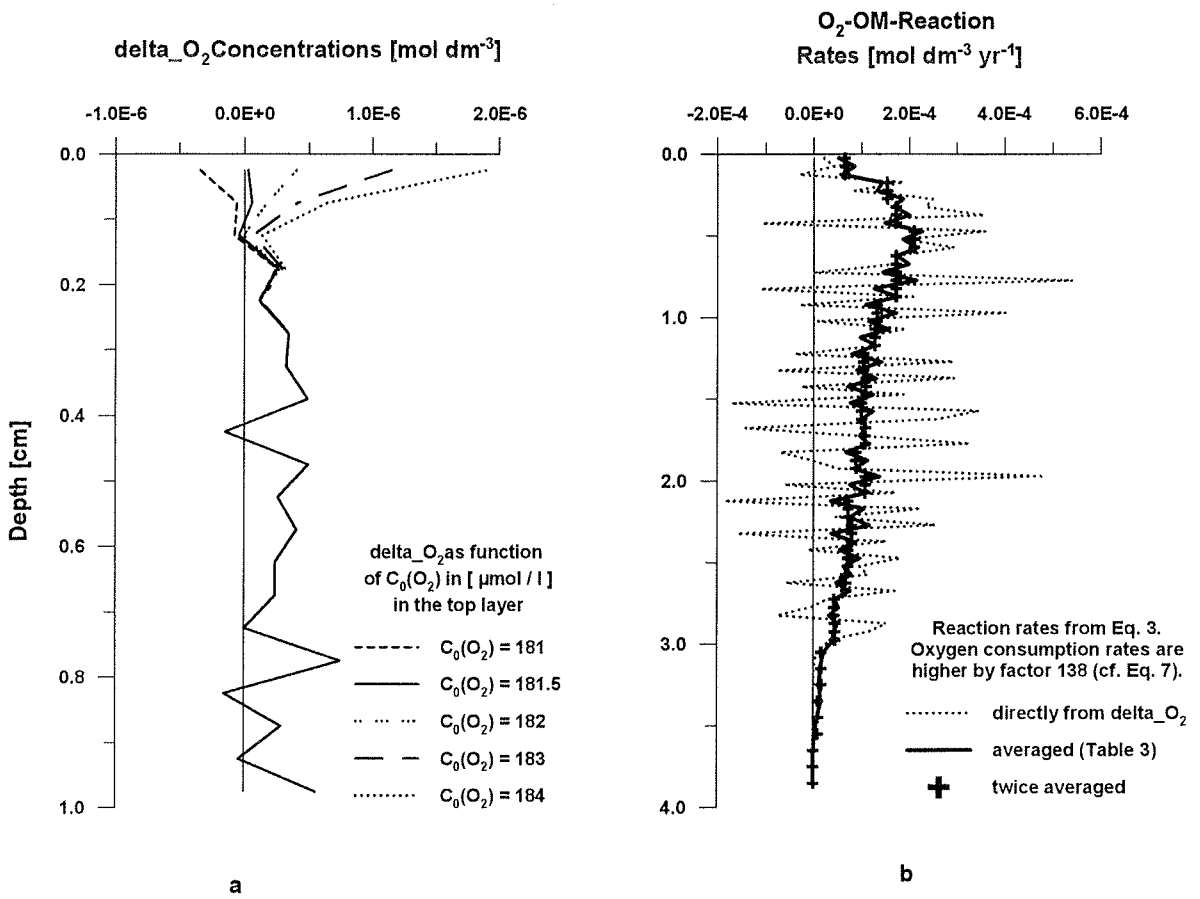

Fig. 3:
Figure 3a shows the sensitivity of delta_O_2 (= change of O_2-concentration within one time-step $dt = 10^{-5}$ yr) close to the sediment surface, with respect to the boundary concentration C_{0_O2} for site GeoB 4909. Bottom-water values for C_{0_O2} (i.e. 184 µmol/l) would produce unlikely large delta_O_2 and oxygen OM reaction rates in this area. Figure 3b shows these oxygen OM reaction rates which were directly calculated from delta_O_2 according to Eq. 3 and Eq. 14 and subsequently averaged.

Figure 3b shows three profiles of OM degradation rates (C_{0_Oxygen}=181.5 µmol/l) according to the equation

$$\text{Degradation rate OM [mol / (l} \cdot \text{yr)]} = \text{delta\_O}_2 / (138 \cdot dt) \qquad \text{(Eq. 14)}$$

The profile shown as a dotted line is obtained directly from delta_O_2 and includes negative values. The solid-line profile displays the resulting rates of a running weighted average

(Table 3). The profile of cross symbols shows the rates applied in further simulations and represents a simple mean of the solid-line profile results for groups of three cells each.

Table 3:
This table describes the number of units that a cell from (n - 6) to (n + 6) contributes to the running weighted average of cell n in the conversion of delta_O_2-concentration results (Eq. 3/Eq. 14/Fig 3a) to O_2-OM-reaction rates (Fig. 3b) . The first column shows the standard case. Some modifications are necessary for the six uppermost cells, because cells with n < 1 are not available. Since oxic respiration is finished well within the model area, the lower boundary cells need no modification. All columns include 20 units (5% of a cell's delta_O_2-concentration per unit) and each cell itself contributes 20 units (diagonal) in the whole process of average calculation.

Cells n	Standard case	6th	5th	4th	3rd	2nd	1st
n + 6	1	1	1	1	1	1	1
n + 5	1	1	1	1	1	1	1
n + 4	1	1	1	1	1	1	1
n + 3	1	1	1	1	1	1	1
n + 2	2	2	2	2	2	2	2
n + 1	2	2	2	2	2	2	2
n	4	5	6	7	8	10	12
n - 1	2	2	2	2	2	2	-
n - 2	2	2	2	2	2	-	-
n - 3	1	1	1	1	-	-	-
n - 4	1	1	1	-	-	-	-
n - 5	1	1	-	-	-	-	-
n - 6	1	-	-	-	-	-	-

4.2 Other implemented redox reactions

The ex-*situ* data show a nitrate increase (relative to $C_{0\_Nitrate}$) around one cm depth due to nitrification and a nearly complete consumption around three cm depth. The measured nitrate profile is difficult to fit, because the simulated increase of nitrate due to the degradation of OM with oxygen is too low under steady-state conditions (diffusion inhibits the buildup of a nitrate peak). This difference between the observed nitrate peak and nitrate simulations is well known, but the problem is still open to discussion (cf. BERELSON ET AL., 1990B; CAI ET AL., 1995; HAMMOND ET AL., 1996; HENSEN AND ZABEL, 1999; HENSEN ET AL., 1998; MARTIN AND SAYLES, 1996). Therefore, these data were only fitted with respect to the measured nitrate penetration depth (cf. Fig. 4). Denitrification produces additional H^+ in the lower part of the modeling area where oxygen consumption is negligible. The production of nitrogen and ammonia are not further included in the simulation.

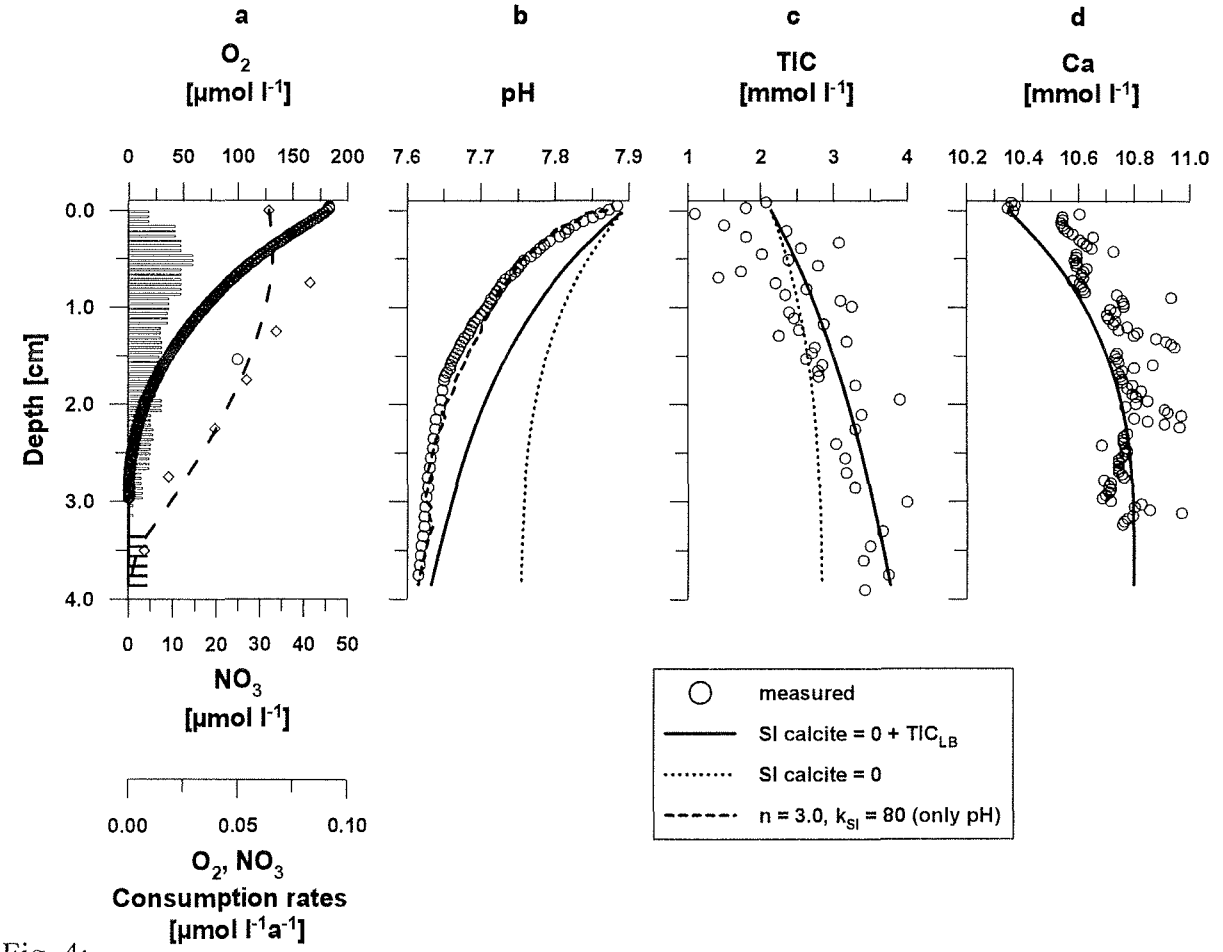

Fig. 4:
Simulated profiles, *in situ* profiles of O_2 (solid line/circles), pH, Ca^{2+} and CO_2 (converted to TIC) measured with microsensors, and shipboard NO_3^- measurements (dashed line/diamonds) at site GeoB 4909 are shown. The two simulated profiles (without TIC_{LB} and with TIC_{LB} = 3.8mM) use a log $K_{sp,\ Calcite}$ = -8.18 (cf. Fig. 5c), are calculated exactly to calcite equilibrium ($SI_{\ Calcite}$ = 0), and show differences only in pH and TIC. Bar charts show consumption rates of O_2 and NO_3^- (filled).

At site GeoB 4906, the consumption of oxygen is simulated by OM degradation and by the reoxidation of manganese (cf. 4.5). The effects of suboxic and anoxic processes are much more intense at this site of the equatorial upwelling than at site GeoB 4909. Investigations by PFEIFER ET AL. (in prep.) reveal the importance of reoxidation of anoxic species at site GeoB 4906.

4.3 Calcite equilibrium

So far, with transport and respiration, we have considered the processes, which can cause a disequilibration of the calcium carbonate system. The degradation of OM causes calcite subsaturation within the sediment, despite the transport of supersaturated bottom-water (with respect to calcite at both sites; WENZHÖFER ET AL., subm.). The system should respond to the

subsaturation with calcite dissolution, which is indeed indicated by the measured calcium profiles (Fig. 4; Fig. 8). These effects of CO_2 release by means of OM degradation are investigated by PHREEQC-calculations.

The first PHREEQC simulation was calculated to an equilibration condition of $SI_{Set,\ Calcite} = 0$ at site GeoB 4909 (cf. Fig. 4 for a similar case, but with a different *log* $K_{sp,\ Calcite}$). The resulting pH profile displays a strong deviation from the measured data (Fig. 5a, case $SI_{Set,Calcite} = 0$, compare HENSEN ET AL., 1997). It is unlikely to approximate this pH profile simply by kinetics, because the oxygen OM consumption rates form a depth-dependent distribution (high rates at the top, small rates at the bottom; see Fig. 4) and, due to H^+ generation, lead to a quite similar distribution of subsaturation (see 4.4.2). Indeed, the kinetics permit lowering the values in the pH profile. This achievement of a pH difference between pure equilibrium and kinetics occurs according to the subsaturation, but the examined pH profile of this equilibrium case has constantly high pH deviations over the whole model area between simulated equilibrium and measured pH values. These pH deviations cannot be fitted consistently with one law of kinetics, the pH deviations could only be corrected by a constantly high homogeneous subsaturation in the model area, which does not exist at this site (even, if another method to obtain the oxygen OM consumption rates is used, the "needed" high consumption rates at the bottom are generally questionable). Consequently, simulations with the single boundary condition of $SI_{Set,Calcite} = 0$ fail to fit the measured pH.

To circumvent this problem, a diffusive flux of bicarbonate across the lower boundary is assumed, which is likely to occur due to the generation of HCO_3^- by sulfate reduction and fermentation processes in the deeper sediment layers. Thus, an effective concentration gradient of HCO_3^- should exist and the problem of the first simulation run was partly solved by applying a fixed bicarbonate concentration to the lower boundary. Under this condition, the simulated TIC/HCO_3^--profiles are much better within the range of measured data (Fig. 4, similar case with another *log* $K_{sp,\ Calcite}$).

Upon applying exact equilibrium to calcite, the resulting pH profile (Fig. 5a, case $SI_{Set,Calcite} = 0 + TIC_{LB}$ of 3.7 mmol/l) matches the measured profile in the lowest part of the model area. The resulting pH deviations between this equilibrium simulation and the measured profile nearly show the same distribution as the oxygen OM consumption rates, which is a helpful relation. This relation does not exist when TIC_{LB} is not used. In the

following section different kinetics are tested to approximate the pH, which is the most sensitive parameter.

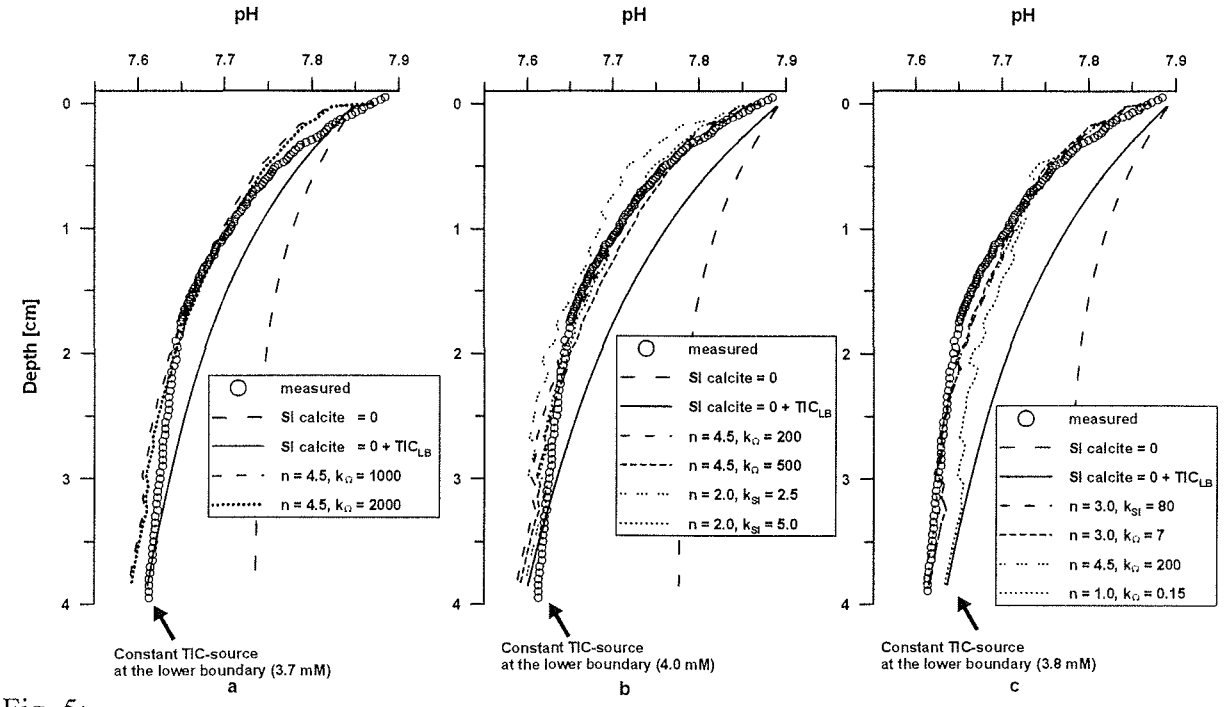

Fig. 5:
pH profiles at site GeoB 4909 resulting from different kinetics after applying the Ω-law (Eq. 7) and the SI-law (Eq. 13, marked with (SI)) as well as from calculations of the calcite equilibrium ($SI_{Calcite} = 0$) under three conditions (log $K_{sp,\ Calcite}$ = -8.222 in Fig. 5a and -8.18 in Fig. 5b/5c. All have different TIC_{LB} sources at the lower boundary. The conditions reflected by Fig. 5c yield the best overall results.

4.4 Kinetics of calcite dissolution rates

The dissolution rate law dependence according to section 3.4 leads to several correlations within each cell: Rates and kinetics of calcite dissolution cause the deviation of the H^+ profile from the profile when calcite is in a state of equilibrium, and they depend on Ω themselves by definition, whereas Ω mainly depends on the cell's H^+ production complying to the laws of calcite dissolution and H_2CO_3 dissociation, and finally H^+ production mainly depends on the cell's oxygen OM consumption rates (as long as only OM consumption by O_2 and NO_3^- are considered from the redox reactions). Therefore, modified by transport, the laws of calcite kinetics have to result in a depth distribution of calcite dissolution rates which reflect the oxygen OM consumption rates.

4.4.1 Comparison of different kinetics regarding boundary conditions and calcite rate constants

The starting conditions for the calculations with different dissolution kinetics are obtained from the equilibrium case C_{LB_TIC} = 3.7 mmol/l (Fig. 5a). The simulated profiles of total inorganic carbon (TIC) and calcium are shown only once (for conditions C_{LB_TIC} = 3.8 mmol/l and $K_{sp,\ Calcite}$ = -8.222, Fig. 4) with a C_{LB_TIC}, because in simulations including kinetics they are approximately equal for one starting condition. Even under different starting conditions they remain qualitatively equal and quantitatively quite similar (showing differences mainly near the bottom due to the difference in C_{LB_TIC}). Oxygen and nitrate profiles (Fig. 4) are valid for all simulation runs.

Two examples of simulation runs made under these conditions show results (Fig. 5a) of the Ω-kinetics law with a reaction order of 4.5, as it is commonly used (see Introduction). With a rate constant of k = 1000, the measured profile fits very well between 1.1 and 1.9 cm depth. Above and below, less calcite is dissolved than is necessary for an exact fit (equivalent to a higher subsaturation) resulting in a negative pH deviation, as compared to the pH data measured *in situ*. More calcite seems to be dissolved in relation to the higher rate constant k = 2000, but calcite is not dissolved simply twice as much as before, because the simulated system responds by calculating a lower subsaturation than with k = 1000. In fact, as it is further demonstrated below, the dissolved amount of calcite or the dissolution rate (*DR*), has approximately the same depth-dependent fixed value regardless of the kinetics used as soon as the applied kinetic law has reached its dynamic equilibrium. These considerations assume that the H^+ production in the course of OM degradation is constant over time, the latter driving the solution system permanently out of its equilibrium. The real benefit of the higher k value is the lower subsaturation needed to obtain the same *DR*. This lower degree of subsaturation produces a higher simulated pH, which is the expected result. Instead of interpreting a kinetic law by asking how much calcite (*DR*) can be dissolved by its application, it seems more reasonable to consider which subsaturation state of the solution does a dissolution kinetics law allow in the dynamic equilibrium of processes (while the solution consists of static concentration distributions in thermodynamical disequilibrium). However, the interpretation of rate laws on the basis of dissolution rates still remains useful. Since a lower rate constant k (compared for the same law and the same reaction order) corresponds to a static concentration distribution with lower pH, the overall amount of calcite, which is dissolved to reach this state of disequilibrium (starting from the equilibrium

calculation) is lower than with a higher rate constant. A higher rate constant acquires a static concentration distribution more similar to the concentrations in the equilibrium case (k approaches infinity). In time, equivalent dissolution rates DR of a fixed value are achieved for all rate constants, thus, the difference in overall calcite dissolution is caused during the dynamic phase at the beginning of the new calculation. In this phase, higher rate constants lead faster to higher dissolution rates approaching finally the fixed value of the rate in dynamic equilibrium.

The better fit with $k = 2000$ produces smaller pH deviations (now positive and negative) than with $k = 1000$. However, all simulations under these conditions, even the calculations to equilibrium, show systematically negative pH deviations in the topmost cells between 0-0.2 cm depth. The same problem exists in the deepest cells. The problem is that there is no possibility to avoid these deviations with any kinetics, since the pH must decrease in comparison to the results of the $SI_{Set,Calcite} = 0 + TIC_{LB} = 3.7$mmol/l simulation run. The pH decrease occurs, since the kinetics buffer the H_2CO_3 production from OM degradation (with O_2 (top) or NO_3^- (bottom)). Therefore, extremely high rate constants would certainly asymptotically approach the equilibrium simulation run, but simultaneously would fail to fit the pH. Instead, it is more likely that the boundary conditions of the coupling between pH and TIC are inappropriate. Two possibilities exist to overcome this problem: Changing the TIC concentration at the model boundaries (C_{0_TIC} and C_{LB_TIC}), or changing $log\ K_{sp,\ Calcite}$ to adjust the pH in return.

Two sets of conditions are presented using a combination of these methods (Fig. 5b/c). C_{0_TIC} was not changed, because the bottom-water value measured *in situ* allows no deviation. Therefore, all further simulation runs related to site GeoB 4909 use a slightly different value of $log\ K_{sp,\ Calcite}$ (-8.18) to circumvent this problem. This small variation can easily be justified considering the uncertainties of temperature and/or pressure corrections (KHARAKA ET AL., 1989; PARKHURST, 1995) or by differences in the $log\ K_{sp,\ Calcite}$ for natural forms of calcite. The basis for correcting temperature and pressure is the standard $log\ K_{sp,\ Calcite}$ of -8.48 at 25°C for pure calcite, but natural calcites have a wide spectrum of $log\ K_{sp}$'s due to varying amounts of impurities (solid solution with Mg; MACKENZIE, 1983).

Simulated pH profiles using kinetics with the condition $\log K_{sp,\ Calcite} = -8.18$ and $C_{LB\_TIC} = 4.0$ mmol/l are presented in Fig. 5b. Examination of the (new) equilibrium calculation runs

($SI_{Set,Calcite}$= 0 and $SI_{Set,Calcite}$= 0 + TIC_{LB}) reveals the changes which are due to the log $K_{sp,\ Calcite}$ adjustment. They are larger positive pH deviations between the equilibrium simulations and the measured pH data in all cells. This selection of $K_{sp,\ Calcite}$ takes into account that the measured solution is subsaturated at the upper boundary (C_{0_pH} = 7.87) and a fit in case of $SI_{Set,Calcite}$= 0 should result in a higher pH than C_{0_pH}. Equilibrium calculations considering the solubility product log $K_{sp,\ Calcite}$ = -8.222 (Fig. 5a) started near the surface with measured pHs, forcing applied kinetics to yield consistently too small pH under this condition, resulting in a worse fit in this area than the equilibrium case.

When C_{LB_TIC} is set to 4.0 mmol/l pH values are produced that are even lower than those measured at the lower boundary, but yielding good fits within the oxygen penetration zone (0-25 mm). Partly neglecting the goodness of the fit below the oxygen penetration depth (OPD) might be justified, since this area is most likely affected by sub-/anoxic processes, the reoxidation of reduced species affecting the calcium carbonate system. This run reflects calcite dissolution entirely driven by oxic respiration.

As for pH values, the Ω-rate law (Eq. 7) with a reaction order of n = 4.5 yields results in a balanced mix of negative (down to 0.6 cm, highest O_2 rates) and positive deviations (ca. 1.0-2.0 cm, moderate O_2 rates) from the measured values. This phenomenon is, more or less, generally observed in all simulation results. An important difference under the new conditions is the rate constant k. While a rate constant of k = 1000 does not yield any positive pH differences under the earlier conditions (Fig. 5a), this is now already the case for a rate constant decreased to k = 200 (Fig. 5b). The conclusion is that the boundary settings are very important for determining correct rate constants.

Certainly, the rate constant depends even more on the kind of dissolution law and reaction order applied. This is demonstrated by two more results which are shown in Fig. 5b, in which fits apply the SI-rate law (Eq. 13) with a reaction order of n = 2 and significantly smaller rate constants. In case of k = 2.5 this SI-law generates too small DR (or as the alternative interpretation suggests, the rate law achieves a too large subsaturation of the solution producing large negative pH deviations). This does not mean that this combination of law (SI) and reaction order (n = 2) is definitely worse than the former law (Ω, n = 4.5), because applying a different rate constant (k = 5) leads to an acceptable fit with qualitatively the same flaws as observed in the Ω-rate law (n = 4.5).

However, certain differences can be observed. First, as explained above, the rate constants are not directly comparable for different laws. Second, the SI-law (k = 5) with the smaller reaction order shows lower pH values than the Ω law at a depth of 0.6 cm, and higher pH values at a depth of 3.5 cm. The qualitative differences in the pH deviations from the equilibrium between both laws mean a difference in their ability to dissolve calcite in dependence of the distribution of subsaturations. Therefore, the important comparison between different kinetic laws is given by their relative differences in pH deviations from the equilibrium case as a function of subsaturation. Third, changing a rate constant by a fixed factor has different effects on different rate laws. An indication for this conclusion is given by the example of the different kinetic laws shown in Fig. 5b. While changing the rate constant by a factor of 2.5 in the Ω-law yields only small differences, the change of the rate constant by a factor of 2.0 in the SI-law causes a large difference between the two fits. These observations are further examined below (see 4.4.2) using the calculated subsaturation (SI) which depends on the depth for the next set of conditions.

The conditions log $K_{sp,\ Calcite}$ = -8.18 and C_{LB_TIC} = 3.8 mmol/l yield the best overall pH simulations presented in this study (Fig. 5c). The "best" rate constants for each law and reaction order were chosen from several fits. Each fit had a maximum in the deviations of the pH, when compared to the measured profile. The goodness of the fit was judged by selecting the fit with the smallest value of these maxima deviations. Three combinations of rate laws, reaction orders and rate constants, although highly different in the parameters, achieve good and similar fits. Nevertheless, there are systematical deviations (pH too low in the range 0 to 0.6 cm, too high in the range 1 to 2.5 cm) in all simulations. It is not possible to correct them, because, e. g., subsaturation SI = -0.055 (SI-law) is calculated for a depth of about 0.15 cm and 1.50 cm, but contrary corrections of the rate constant are needed to yield a better pH fit in these depths. Any rate law formulated in Eq. 7 or Eq. 13 and not depending on the depth, cannot achieve both. The first order Ω-law simulation (k = 0.15) results in extreme pH deviations and shows that this combination of dissolution law and reaction order will always fail for these conditions, because its relation between subsaturation and dissolution rates is clearly not consistent in different depth horizons.

We conclude that it is possible to fit the pH under these conditions by applying different kinetics, although not all forms of dissolution rate laws are useful. Especially, we cannot support the suggestion of HALES and EMERSON (1997B) that the first order Ω-law will lead to

acceptable results in any case. The reason why certain kinetics are more suitable than others at any given site needs, however, more examination than by mere judgment of the resulting pH profiles.

4.4.2 Comparison of different kinetics regarding calcite dissolution rates, saturation state and reaction order

The direct dependencies between oxic respiration, subsaturation and calcite dissolution rates are illustrated in Figures 6 and 7. It is obvious that oxic respiration rates cause nearly exactly the same dissolution rates in all kinetics, as suggested by the examination of the pH results depicted in Fig. 5a. Subsaturation profiles differ for different kinetics, but are also correlated to the respiration rates.

While dissolution rates are equal for different rate laws, a difference between the rate laws is seen in the subsaturation, which is expressed by the pH deviations from the equilibrium case (Fig. 5c). The three good fits in Figs. 5c and 6 display only small deviations for the pH as well as for the SI. In contrast, the poor first- order fit of the pH is caused by its very different SI profile. The dissolution rates shown in Fig.7 explain this from another point of view. The best overall fit (SI: $n = 3$; $k = 80$) is shown together with two other fits, which differ from the best fit only due to small modifications of the rate constant ($k = 60$ and $k = 100$). These modified fits are well acceptable fits themselves and nearly envelope all good fits. In contrast, the first-order fit shows significant differences. The good fits are shown up to maximum subsaturation in each case, limiting the dissolution rate for all fits to a nearly constant maximum. Fig. 7 illustrates why the very different parameters of the well fitted cases may lead to fairly equal results (=*DR*), especially in the subsaturation range of interest (SI = -0.040 to -0.075).

Upon comparing the cases of the best fit and $n = 4.5$, it shows that an intersection point exists at a subsaturation of roughly SI = -0.05. Such a graphical intersection means that two rate laws respond to this particular subsaturation, by achieving nearly the same pH, due to exactly the same *DR*. If the difference to this intersectional subsaturation increases, the differences in the pH will also increase, as a result of the diverging rate laws. This comparison describes which differences in pH can be expected to result from different rate laws, i.e. the enveloped kinetic laws shown in Fig. 7 lead to enveloped pH plots.

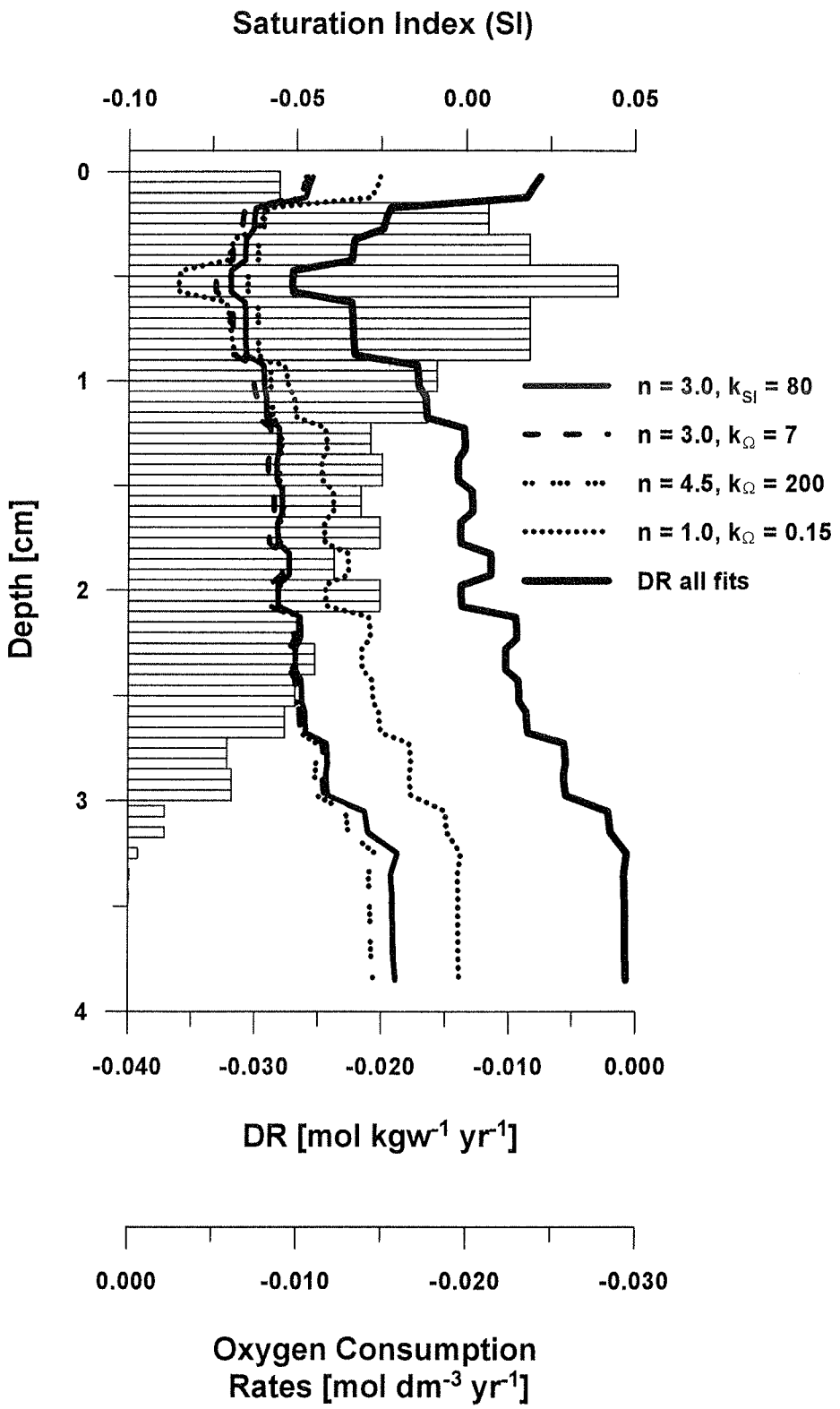

Fig. 6:
Comparison of saturation indices ($SI_{Calcite}$), the rates of calcite dissolution according to the kinetic rate laws, and oxygen consumption rates (bar charts) at site GeoB 4909 for all kinetics shown in Fig. 5c. The differences in the saturation indices mainly cause the differences in the pH profiles (Fig. 5c) relative to the equilibrium calculation with TIC_{LB}. All kinetics practically result in the same dissolution rates *DR*, which are strongly correlated with the rates of oxygen consumption.

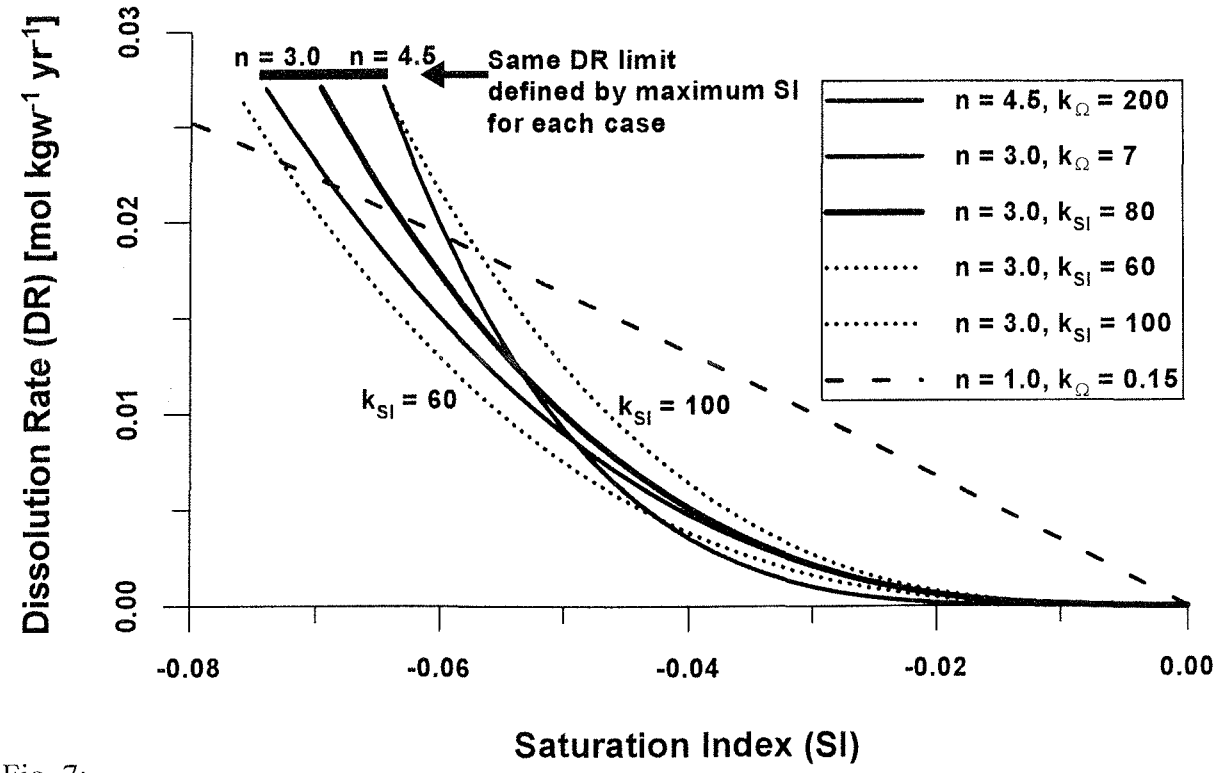

Fig. 7:
The dissolution rates for the kinetic laws applied in Fig. 5c (GeoB 4909) are shown as a function of the saturation index. The rate law with the best fit (SI-law, n = 3.0, k_{SI} = 80) is enveloped by two plots which differ only in the rate constant and also lead to acceptable pH fits. Any fit produced by an arbitrary rate law, which would achieve a curve-plot enveloped by these both plots within the subsaturation range of interest (SI = -0.040 to -0.075), would lead to good pH results, due to the nature of the rate law dependence shown. The first order law deviates clearly from the other laws, leading to a worse pH fit as compared to other kinetics.

Conversely, the rate constant for a kinetic law can be calculated from a different kinetic law at these intersection points. It is good practice to obtain a useful rate constant for a new applied law from a known good fit despite different kinetic parameters. However, these intersection points should occur close to the point of maximum subsaturation, i. e., we can conclude from the good SI-law fit that according to

$$DR_{Max} = k_{SI} (SI_{Max})^3 = 80 \cdot (|-0.07|)^3 = k_{\Omega} \cdot (1 - 10^{-0.07})^{4.5}$$

$$k_{\Omega} = 80 \cdot (0.07)^3 / (1 - 10^{-0.07})^{4.5} = 145 \qquad \text{(Eq.15)}$$

the rate constant for a Ω-law with a reaction order of n = 4.5 should be in the order of 10^2. This is a very helpful method to quickly obtain useful values for rate constants of kinetic laws without simulation. Why bother with a different rate law if good results are already achieved? Improvements are almost always available for these pH fits and the usefulness of rate laws can be judged only by their ability to achieve a good pH fit simultaneously in all cells. Inappropriate rate laws (for a particular site) fail terribly in this regard, but any rate law, even

an inappropriate one, achieves the necessary distribution of dissolution rates to balance oxic respiration (and transport) effects in a dynamical equilibrium of processes. In addition, an exact pH fit in at least one cell (for one necessary dissolution rate) can always be determined by the choice of the rate constant. Obviously, rate laws have to achieve the fixed maximum value of the dissolution rate with their own maximum subsaturation (cf. Fig.6 at 0.6 cm and the horizontal limit in Fig. 7), and we imagine an inappropriate rate law achieving this. This means that the correct pH is achieved at the laws' own maximum subsaturation, but nowhere else (per definition of "inappropriate rate law"). Then, figures such as Fig. 7 may help to determine which rate laws could be capable of yielding better fits by means of visualizing, if another rate law needs more or less subsaturation (and vice versa pH) to dissolve the necessary calcite. Thus, a rate law may be derived from a *DR*/SI-figure, which achieves a correction of the inappropriate rate law and leads to a better pH fit. However, the pH fit can be improved by iterating this process, utilizing the method above, until the reliability of the measurements or the conceptual limits of one rate law are reached for all cells.

4.5 Dissolution kinetics at site GeoB 4906

Figure 8 shows differently simulated pore-water profiles at site GeoB 4906, including the pH for two different dissolution kinetics. Again, an Ω-law with reaction orders n = 1.0 and n = 4.5 is used to compare the rate constants with previous studies. Since different chemical processes are presumed to occur at site GeoB 4906, the simulation is more complex as compared to site GeoB 4909. Apart from the degradation of organic matter coupled to oxygen and nitrate, iron- and sulfate-reduction occurs in deeper layers which results in a number of reoxidation processes (cf. PFEIFER ET AL., in prep.). This study focusses on the top layer of the model area (2.0 cm), where the dominating processes equal those at site GeoB 4909, with the exception of manganese reoxidation in the presence of molecular oxygen:

$$Mn^{2+} + 0.5\ O_2 + H_2O \Longrightarrow MnO_2 + 2\ H^+ \qquad \text{(Eq. 16)}$$

Manganese diffuses upward from the source of its creation and across the lower boundary (cf. $C_{LB\_Manganese}$ in Table 2). In Fig. 8 the simulated pH shows a minimum at around 1.5 cm within the manganese reoxidation zone promoting this effect by H^+ production (Eq. 16). The simulated TIC and Ca^{2+} profiles show the typical curved and theoretically expected increase with depth, which are qualitatively similar to the increases in Fig. 4. The measured Ca^{2+} increase may be underestimated in this case, because it seems clear, that the OM-degradation effects "needs" to be balanced by more CO_3^{2-} release due to calcite dissolution, which would release in response more Ca^{2+} than indicated by the measurements (compare to simulation

results; Fig. 8). Otherwise, this problem could be solved by another source releasing CO_3^{2-}, which releases in response no or at least relatively less Ca^{2+} than calcite. In contrast, a good candidate was not found in the quantity of solid phases to add a fraction in the CO_3^{2-} release assumed to be driven purely by calcite dissolution. Profiles for pH, TIC and Ca^{2+} are presented only down to 2 cm, because the expected pH increase below results from the reduction of SO_4^{2-} and $Fe(OH)_3$ coupled to OM, and its associated effects on calcite equilibration are generally simulated. However, the detailed distribution of processes is still under investigation (cf. PFEIFER ET AL., in prep.).

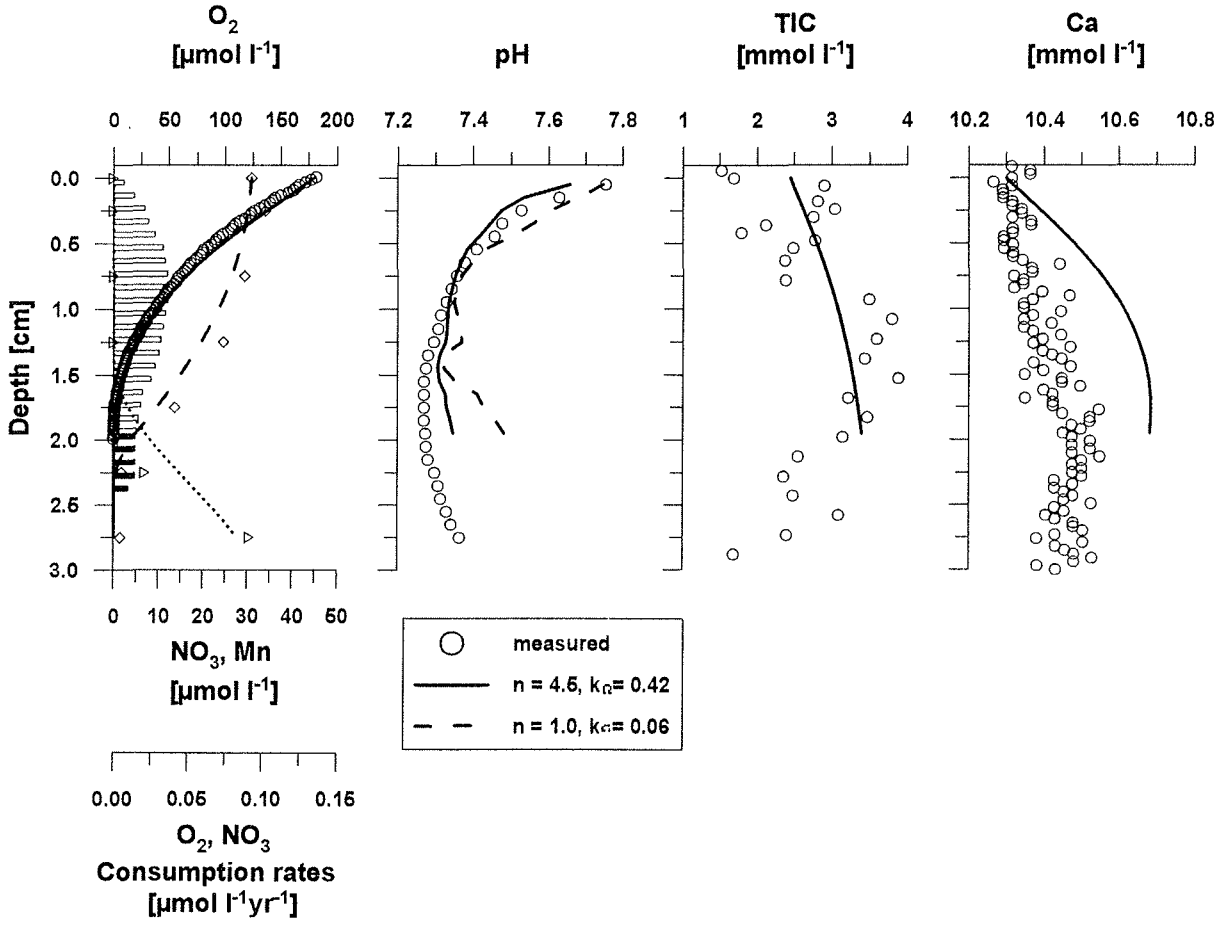

Fig. 8:
Simulated profiles, *in situ* profiles of O_2 (solid line/circles), pH, Ca^{2+} and CO_2 (converted to TIC) measured with microsensors, and shipboard NO_3^- (dashed line/diamonds) and Mn^{2+} (points/triangle) measurements are shown for site GeoB 4906. The simulated profiles show the top layer results from a run with applied kinetics (Ω-law, n = 4.5, k_Ω = 0.42). Additional pH results (Ω-law, n = 1.0, k_Ω = 0.06) are included. Bar charts show consumption rates of O_2 and NO_3^- (filled).

An examination of dissolution rates, subsaturation, and oxic respiration for the simulated pH profiles leads to similar explanations as for site GeoB 4909 (Fig. 9). Both kinetic laws reached a quasi equal distribution of dissolution rates with depth (with maximum rates around 0.033 mol / (kgw · yr) for site GeoB 4906 compared to 0.027 mol / (kgw · yr) for site GeoB 4909). The SI distribution, however, differs again for the first-order kinetics, with too low subsaturations and too high pH values, especially in the lower model area. Dissolution rates correlate with the degradation rates.

An important distinction between these sites is the difference in the absolute value of the subsaturation. The range of subsaturation of interest is now SI = -0.1 to -0.37 (4909: -0.04 to -0.075). This is accompanied by decreasing rate constants (n = 4.5: k = 200 → 0.42; n = 1.0: k = 0.15 → 0.06) as expected when different SI ranges but similar dissolution rate ranges for both sites are considered. These very different rate constants and subsaturations for equal rate laws and reaction orders indicate different qualities of calcite at these sites. Calcite at site GeoB 4906 with the lower rate constants is more difficult to dissolve, because much greater forces (defined by the subsaturation) are needed to yield roughly the same dissolution rates.

The kinetic laws used for site GeoB 4906 and several other kinetic laws are shown in Fig. 10. The intersection point of the kinetics used is around the maximum subsaturation (SI ≅ -0.35) as expected. The result of very different pH profiles in Fig. 8 is no surprise due to these different rate laws defining the pH response according to subsaturation as a function of depth.

4.6 General properties of kinetic rate laws

According to the last statement above, each rate law forms its own distribution of pH deviations from calcite equilibrium as a function of depth. Nevertheless, the question arises, why does the first-order Ω-law specifically produce worse fits at both sites. Is there a specific reason why the particular kinetics are inappropriate, or is there a site-dependency as to which rate laws and reaction orders lead to suitable results?

The comparison of rate laws with different properties (reaction order and term of subsaturation dependence) is strictly correct only for a fixed rate constant. A k of 0.06 was chosen to demonstrate the Ω-law with reaction orders up to 4.5 and the SI-law with 1st and 2nd reaction order (Fig. 10). The response of the linear SI-law can be compared with the law applying to a spring's elastic force.

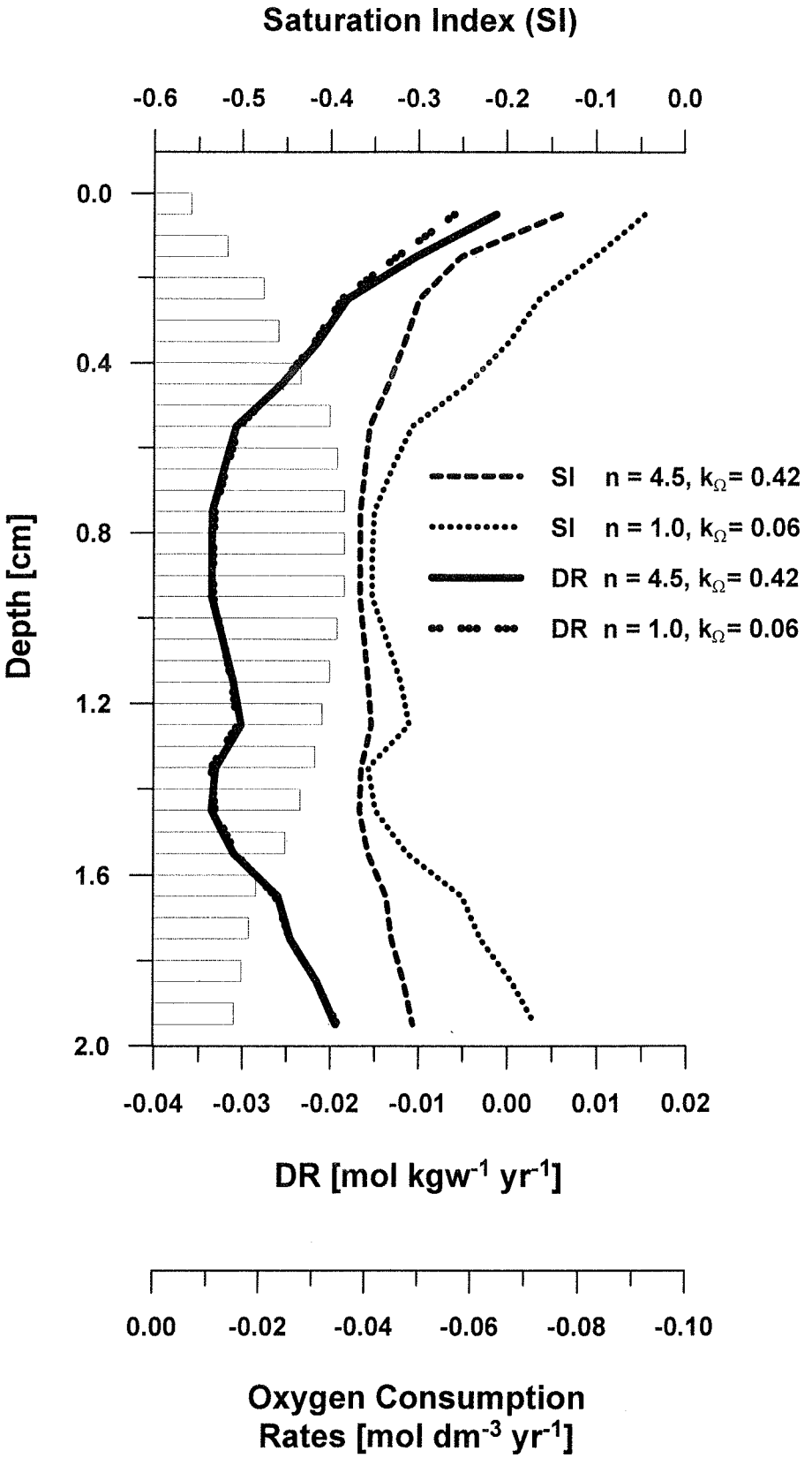

Fig. 9:
Comparison of saturation indices ($SI_{Calcite}$), calcite dissolution rates according to the kinetic rate laws and O_2-and NO_3^--consumption rates (bar charts) for both kinetics tested at site GeoB 4906. The different SI profiles are mainly responsible for the differing quality of the pH fits in Fig. 8. The dissolution rates *DR* are nearly the same for both kinetics, as is to expected from Fig. 6. Correlation with the oxic respiration rates differs on account of Mn^{2+} oxidation (1.5 to 2.0 cm).

A disruption leading away from equilibrium is achieved by a constant force (pulling the spring or due to oxic respiration producing H^+ in the solution) resulting in a dynamic equilibrium of forces in both systems (disruption force and its response). This corresponds to a disequilibrium relative to the principle of energy minimization (spring with an elongated length or a subsaturation to calcite for the solution). The response to the disruption force is a force inherent to the system and working towards the equilibrium of minimized energy (spring's elastic property and the solution's capacity to buffer added H^+ per calcite dissolution). Therefore, the dissolution rate may be identified as the retrieving force of the solution. The elastic response or force is given by linear first order dependence from the measure of disruption in the law of the retrieving force (like in the spring's elastic law: $F_R = - D \cdot x$; disruption elongation with measure length x, spring's constant D (comparable to the rate constant), retrieving force F_R). While an elastic force law displays no curvature (SI-law, $n = 1$) in the graphic plot of the retrieving force ($F_R = DR$) as function of the disruption status (subsaturation), we use, starting from SI = 0, the terms "superelastic" for a right-turning curvature (like the SI-law with $n = 2$) and "subelastic" for a left-turning curvature.

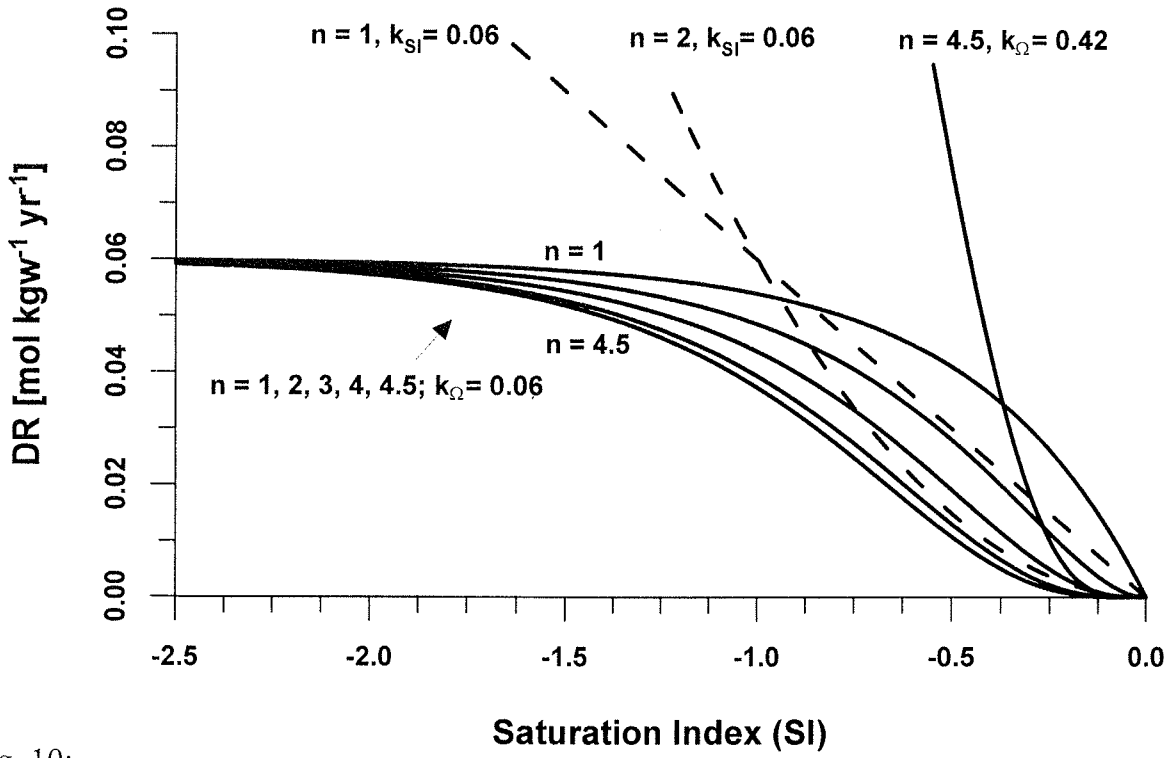

Fig. 10:
The dissolution rates for the kinetic laws applied to site GeoB 4906 (Ω-laws: $n = 4.5$, $k_\Omega = 0.42$ and $n = 1.0$, $k_\Omega = 0.06$) are shown as a function of the saturation index. Both clearly show a different behavior for subsaturations between SI = -0.1 and -0.37, explaining the differences in the resulting pH fits. For a more general discussion several other rate laws are shown down to a high degree of subsaturation, with a rate constant of $k = 0.06$.

It is possible to assume different measures for the quantity of subsaturation, which expresses the disruption. We apply again the saturation index as measure and this leads to the *DR*/SI-plot shown in Fig. 10 as relation between disruption status and retrieving force. We hold that the retrieving force in a solution is at least elastic. This means that there is not any subelastic turn to the left in the curvature. The necessary curvature depends only on the form and the reaction order of the rate law, the rate constant is only able to stretch the curvature. Naturally, as far as the measure SI is concerned, all SI-laws with reaction orders $n \geq 1$ are at least elastic, but what is the response of the Ω-laws in this regard? They differ and are SI-dependent (cf. Fig.10) in their response.

Very high subsaturation (SI $\leq$ -1.5) in Ω-laws leads to dissolution rates which are asymptotically limited by the value of the rate constant. Such high subsaturations are unlikely, but the SI-laws are more suitable in this regard, because their dissolution rates are never limited as a function of subsaturation. Starting from this extreme end in the area which is controlled by subelastic response, the Ω-laws show, with decreasing subsaturations, changes from the subelastic response to quasi-elastic and, finally, for $n > 1.0$ to a clearly superelastic response. The subsaturation at which the response is exactly elastic (no curvature) is only a function of the reaction order (no rate constant influence) and increases in the event of higher reaction orders (Fig.10).

The well fitted examples in Fig. 7 and Fig. 10 show even superelastic responses for the site-dependent subsaturation range of interest. Contrarily, the inappropriate first-order Ω-law fit always has subelastic response. With the term (1 - Ω) as a measure for subsaturation, this rate law would produce exactly elastic response. However, this implies no contradiction to our demand, because we expect a useful dissolution rate law to be at least elastic for all useful subsaturation measures (SI and (1 - Ω), maybe even others), which is fulfilled for SI-laws with $n \geq 1.0$.

The examples indicate a superelastic response and that several laws (type SI or Ω, orders $n >$ 1.0) should be appropriate to fit a system well, if all of them show a similar response for $DR = f(\mathrm{SI})$. Additionally, demanding an elastic response may be sufficient in the subsaturation range of interest, because all rate laws of good fits show a quasi elastic response in this range as shown in Fig. 7 and Fig. 10 (k = 0.42). However, approximating these laws in this way

with an elastic dependence would result in a negative dissolution rate at SI = 0, which is certainly the wrong boundary condition.

4.7 Comparison of rate constants with other studies

Table 4 shows our simulated results of rate constants expressed in the units [mol / (kgw · yr)] and [% / d] for the Ω-law and reaction orders n = 1.0 and n = 4.5, converted according to Equation 11. The first-order results are not very reliable due to their poor fitting properties, but they are included for reasons of comparison. As described in section 4.5 a comparison of rate constants is strictly valid only for the same form of the rate law. A conversion according to Equation 15 might be possible but the results should be used considered caution.

Table 4:
Resulting rate constants k_Ω of both sites applying the Ω-law (Eq. 7) with reaction orders n = 4.5 and n = 1.0. The constants are converted by the factor 1 / 10.917 (Eq. 11) to the unit [% / d] for comparisons to other studies.

GeoB site and reaction order n		k_Ω mol / (kgw · yr)	k_Ω % / d
4906	n = 4.5	0.42	0.03847
	n = 1.0	0.06	0.005496
4909	n = 4.5	200	18.32
	n = 1.0	0.15	0.01374

In case of a fixed subsaturation, higher rate constants mean faster calcite dissolution. Therefore, the calcite at site GeoB 4909 dissolves faster, or easier, than calcite at site GeoB 4906. The reaction order n = 4.5 has been used to predict a range of 0.01 to 150 %/d for the rate constant (cf. Introduction) in previous studies. Our rate constant results for n = 4.5 are well within this range for both sites and demonstrate once more the site-dependence of the rate constant.

For calcite-rich sediments, HALES AND EMERSON (1997B) obtained a better fit to *in situ* pH profiles with the first-order dissolution Ω-law. Their reestimation of Keir's laboratory results (KEIR, 1980), using the same ion concentration product (ICP), but a different method to define the apparent calcite solubility $K'_{sp,\,Calcite}$, led to the high rate constant, considering n = 1, of 38 %/d. However, their field studies at Ontong Java and Ceara Rise sites yielded as best fits rate constants of approximately 0.0004 and 0.0112 %/d. Our first order law fits, despite achieving inferior results compared to fits of higher reaction orders, produce comparable rate

constants. Nevertheless, an explanation for the contradiction between both studies, regarding the question which reaction orders are useful in the Ω-law, or even the best, is unclear. Their results lead to the first-order law as the best possibility, while our investigations, including some general considerations, lead to the preference of higher reaction orders. However, the given site may be the decisive factor in this discussion.

5 Conclusions

In situ measurements provided the basis for simulating depth-dependent profiles of all relevant constituents in the system of subsurface calcite dissolution in deep-sea sediments. The model CoTReM demonstrated its capability to reproduce the dynamics of such a complex geochemical system. Several important insights were revealed within the process of our investigations:

- Dependence of oxygen transport rates and oxygen OM consumption rates in the topmost sediment layer on the concentration of (bottom-water) oxygen below the DBL (Fig. 3a).
- Correlation of calcite dissolution rates and oxygen OM consumption rates (Fig. 6 / Fig. 9). The calcite dissolution rates are almost identical for all applied kinetics in dynamic equilibrium.
- pH deviations between kinetic simulations and comparable equilibrium ($SI_{Set} = 0$) simulations depend on the distribution of obtained subsaturation (Figs. 5/6 and Figs. 8/9). This distribution of subsaturation states especially depends on the form of the rate law (SI- or Ω-law and n), while the rate constant determines the necessary maximum value of dissolution rates for a kinetic simulation in a dynamic equilibrium.
- Importance of boundary conditions in all simulations. The application of oxygen OM consumption rates, calcite solubility, TIC_0 (etc.), and TIC_{LB} substantially determines, whether a kinetic law enables a suitable pH fit at all (Fig. 5). The rate constants vary widely, if they depend on poorly constrained boundary conditions.
- Several rate laws with quite different parameters result in similar dissolution rates (Fig. 7), therefore, all these rate laws may produce useful fits.
- Exact comparability of rate constants is valid only for the same form of the rate laws (Fig. 7). The method presented in Equation 15 may partially circumvent this non-comparability of rate constants for the differing forms of rate laws.
- The investigations support higher reaction orders on kinetic rate laws.

Further studies should always include comparisons between Ω-law simulations with reaction orders n = 1.0 and n = 4.5, until a clear decision is possible whether the results are site-dependent or a general preference for some form of rate law exist. In addition, the SI-law form should be considered as a useful alternative and an extension to a similar precipitation law will be easier to obtain. Additionally, the concept of one rate law equation for a depth-dependent simulation may be not flexible enough. Applying depth-dependent rate constants (same form of rate law) may help to overcome this problem. A correlation to different calcite fractions with different properties will then be easily possible.

Acknowledgments

We would like to thank the captain and the crew on cruise M 41/1 of the RV *Meteor*. We thank S. Hinrichs, S. Siemer and K. Enneking for the assistance in shipboard geochemical analyses, S. Meyer for lander deployment assistance, A. Krack for equipment preparation and G. Eickert, V. Hübner and A. Eggers for well constructed microsensors and calcium measurements. We thank R. A. Jahnke and an anonymous reviewer for their helpful contributions. This research was funded by the *Deutsche Forschungsgemeinschaft* (DFG) and was supported by the SFB 261 (*The South Atlantic in the Late Quaternary: Reconstruction of material budget and current system*) and by the "*Graduate College of Material Flux in Marine Geosystems*" at the University of Bremen.

Appendix: Principles of CoTReM

The simulation model CoTReM (LANDENBERGER, 1998; LANDENBERGER ET AL., 1997) is based on the model CoTAM (HAMER AND SIEGER, 1994). Both models are developed for non-steady state calculations using Fick's second law of diffusion. The operator-splitting (OS) algorithms in CoTReM solve the General Diagenetic Equation (Eq. A.1, homogeneous one-dimensional case; BERNER, 1980), which describes transport and chemical reactions of species in porous media.

Species conc. Diffusion and Dispersion

$$\partial_t C_i = -\partial_x\left(v \cdot C_i\right) + \partial_x\left(D_i \cdot \partial_x C_i\right) + \alpha_x\left(C_{0,i} - C_i\right) + R_i\left(C_1,\ldots,C_{n_i}\right) \quad i = 1,\ldots,n_i \quad \frac{\text{mol}}{\text{l}\cdot\text{a}} \quad \text{(A.1)}$$

Sediment advection Bioirrigation Reactions

with:	C_i:	concentration of the i^{th}-species	t:	time
	D_i:	sum of diffusion (of the i^{th}-species) and dispersion coefficient	x:	sediment depth
			R_i:	reaction rate of the i^{th}-species (source term)
	v:	sedimentation rate (plus flow velocity, if applicable)	$C_{0,i}$:	bottom-water concentration of i^{th}-species
			α_x :	exchange coefficient of depth x

The partial differential equations (PDE's) are translated in partial difference equations using the Taylor series approximations. The OS method (YANENKO, 1971; SCHULZ AND REARDON, 1983) allows to divide the General Diagenetic Equation according to the calculation scheme in Fig. 2.

The transport processes are splitted into non-local mixing of solutes (bioirrigation)

$$\partial_t C_i = \alpha_x \left(C_{0,i} - C_i \right) \qquad i = 1,\ldots,n_i \quad \text{mol} / \left(1 \cdot \text{a} \right) ; \; 0 \le \alpha_x \le 1 \tag{A.2}$$

and the processes of dispersion/diffusion/bioturbation and advection/sedimentation

$$\partial_t C_i = -v \cdot \partial_x C_i + D \cdot \partial_x^2 C_i \qquad i = 1,\ldots,n_i \quad \text{mol} / (1 \cdot \text{a}) \tag{A.3}$$

with v and D constant within a cell. The total reaction rate R_i of the i^{th}-species is not used explicitly in CoTReM, because

$$\partial_t C_i = R_i \left(C_1,\ldots,C_{n_i} \right) \qquad i = 1,\ldots,n_i \quad \text{mol} / (1 \cdot \text{a}) \tag{A.4}$$

is divided into a redox reaction rate equation (A.5) and the PHREEQC calculations, which use external input (rate constants and reaction orders) for kinetics. The reaction rate equation

$$dt \cdot \partial_t C_{i\ (\text{species, depth})} = \Sigma_{\text{reaction}} \left(dt \cdot \text{SC}_{(\text{species, reaction})} \cdot \text{R}_{(\text{reaction, depth})} \right) \tag{A.5}$$

uses the concentration change $dt \cdot \partial_t C_{i\ (\text{species, depth})}$, the sum of actual rates $\text{R}_{(\text{reaction, depth})}$ of reactions and the full reaction's stoichiometric coefficients $\text{SC}_{(\text{species, reaction})}$. The actual rates $\text{R}_{(\text{reaction, depth})}$ are developed from depth-dependent, user defined maximum reaction rates R_{max}. Within PHREEQC, the solution distribution is calculated first, including the correction for charge neutrality and the mineral saturation indices output, which is used for the kinetic laws. Then, changes by transport/redox are calculated using a PHREEQC algorithm to add/subtract species concentrations. Simultaneously, the capability of PHREEQC to calculate towards a preselected saturation index of a mineral phase is applied. Equilibrium calculations may either be applied obtaining an instantaneous equilibrium for the mineral in question, or kinetics determine the effective dissolution, initially decreasing it. The PHREEQC calculations use the ion activity product IAP in relation to dissociation constants K_{Species} and the applied solubility

products $K_{sp,\ Mineral}$ to equilibrate the mineral phases to all ions and complexes in the modeled pore-water solution.

Dissolution or precipitation rates R are defined by the kinetics of the concentration change dC [mol/kgw] within a time-step dt, as amount [mol] of the mineral phase dissolved in, or precipitated from, the solution of one kilogram water [kgw], according to

$$dC = R \cdot dt \tag{A.6}$$

and the kinetic law used, which defines the rates R (cf. 3.4). Including this concentration change, as well as those from transport and redox reactions, PHREEQC recalculates the concentration distribution of different species in all cells and achieves the final results of the time-step.

The incorporation of PHREEQC required different name conventions for the species used by CoTReM, i. e. transport (diffusion coefficient) and redox reaction module (element/molecule formula for stoichiometrics) refer to HCO_3^- as the name of one C-species, which is represented in PHREEQC as element C(4) (CH_4/C(-4) stands for another, but it is not used in this study). This PHREEQC element C(4) means all dissociations and complexes directly achievable from the chosen PHREEQC master species of CO_3^{2-} for this element. In this particular case the transport/redox formula HCO_3^- is equivalent to the total inorganic carbon (TIC), a term used in this study when operating with PHREEQC. This is necessary, because the master species of CO_3^{2-} is different from the transport/redox formulation HCO_3^- in this case. Therefore, a transport/redox formulation corresponds to the formulation of one PHREEQC element. If such an element as C(4) is distributed between several dissociation/complexes, the PHREEQC dissociation of HCO_3^- is only a fraction of the transport/redox species HCO_3^- (usually chosen to be the major fraction due to one diffusion coefficient existing for the whole distribution of the element).

Conclusions

The further development of CoTReM (**Co**lumn **T**ransport and **Re**action **M**odel) based on SIEGER (1993) and LANDENBERGER (1998) achieved a well rounded set of results within this work. First, the simulation program itself is now properly equipped with all the components and processes necessary for successful modeling of combined biogeochemical reactions and transport in porous media in case of one-dimensional problems. The User Guide and the former dissertations about the CoTAM/CoTReM development explain extensively the concrete use of the program and all necessary data files as well as each used modeling concept with the corresponding mathematical and numerical background for all the concerned processes of physical transport and chemical reactions. While the program is still expandable, the program's potential to describe and solve questions in this geochemical field of research is by far not exhausted. Second, the applicability of CoTReM is successfully tested by two studies with very different geochemical questions resulting in important insights about the examined systems. Additionally, these studies themselves describe and show apart from their own scientific results methodical ways to go for proper modeling with CoTReM, because the setup of assumptions, boundary conditions and the qualitative "modeling" is well described.

CoTReM is as far as I know unique for a coupled transport/geochemical model regarding the equilibrium calculation due to PHREEQC. None of the other geochemical transport models invests a comparable exactness and calculating power regarding this complex of determining the composition of the solution in each time step and each cell. In contrast, PHREEQC and other equilibration programs (mainly zero-dimensional based) contain certainly not the transport abilities of CoTReM. Even more, a successful transport/geochemical model needs the option to overrule the constraints of equilibration constants to include "bio"-chemically mediated reactions (REDOX) or kinetically slowed reactions including solid phases. Indeed, regarding the chemical program components, only this mix of modeling abilities, following the constraining approach of exact calculation justified by thermodynamic constants on the one hand and the more arbitrary approach to define reaction rates or kinetic parameters due to a decision of the model user (who should really know due to geochemical knowledge, what is initiated in the simulation by the decision) on the other hand, makes CoTReM a powerful modeling tool. This touches another important point regarding CoTReM, the advantage to model with all the complex program options is connected to the disadvantage that the user has to invest much time to be know how to model with CoTReM properly. Further massive

development of CoTReM may change the program to more dimensions as mentioned in the introduction. A smaller change may end the assumption of constant porosity between the calculated and the adjacent cells. LANDENBERGER (1998) has given the proper formulas to include this change, if it seems really necessary. Otherwise, further development has primarily to follow the needs and qualitative considerations of the user.

General insights due to the first study covered the modeling of redox reaction zones, the importance of a simulation setup to balance a steadily ongoing process (sulfide production) with a steady ability to convert its effects even further (availability of iron from solid phase equilibration for sulfide precipitation), the essential depth-dependability of important parameters within the modeled area (solubility constants of ironhydroxides) and the advantage to compare as many simulated species concentrations as possible to measurements (the complex of iron and sulfur contains more measurements and is more successful simulated in this study than the complex about calcite, DIC and pH).

The new insights of the second study cover useful methods in the whole modeling approach, e.g. first approximating the measurements by applying the assumption of pure calcite equilibration followed by further fitting due to the kinetic options and visualizing the dependence between oxic respiration rates and calcite dissolution for all kinetic simulations in the plot of SI and rates over depth, as well as the conclusions and results about the different applied calcite equilibrium kinetics. This success in the otherwise seldom modeled area of equatorial upwelling achieved even comparable results to former studies (in non-upwelling areas) regarding the calcite kinetic parameters. Additionally, the immense importance of boundary conditions was revealed and demonstrated. Especially the central pH simulation is under these circumstances an important point, which allows for an optimistic view to model other complex questions with CoTReM successfully in the future.

References

(includes references in files, which are offered with CoTReM 2.3)

ADLER, M., C. HENSEN, S. KASTEN, H.D. SCHULZ (2000A): Computer simulation of deep sulfate reduction in sediments of the Amazon Fan.- Int. Journ Earth Sciences **88**, 4, 641-654.

ADLER M., HENSEN, C. AND SCHULZ, H.D. (2000B): CoTReM - Column Transport and Reaction Model, User Guide, Version 2.3. http://www.geochemie.uni-bremen.de/cotrem.html.

ADLER, M., C. HENSEN, K. PFEIFER, H.D. SCHULZ (in press): Modeling of calcite dissolution by oxic respiration in supralysoclinal deep-sea sediments.- In press at Marine Geology.

APPELO, C.A.J. AND POSTMA, D. (1996): Geochemistry, groundwater and pollution.- A.A.Balkema, Rotterdam.

ARCHER, D.E. (1991): Modeling the calcite lysocline.- J. Geophys. Res., 96, 17,037-17,050.

ARCHER, D., EMERSON, S., REIMERS, C.E. (1989): Dissolution of calcite in deep-sea sediments: PH and O_2 microelectrode results.- Geochim. Cosmochim. Acta 53, 2831-2845.

ARCHER, D.E. AND MAIER-REIMER, E. (1994): Effect of deep-sea sedimentary calcite preservation on atmospheric CO_2 concentration.- Nature, 367, 260 - 263.

ATKINS, P.W. (1978): Physical Chemistry.- Oxford University Press, Oxford.

BALL, J.W. AND NORDSTROM, D.K. (1991): WATEQ4F - User's manual with revised thermodynamic data base and test cases for calculating speciation of major, trace and redox elements in nature waters.- U.S. Geological Survey Open - File Report 90-129, 185 p.

BEAR, J. (1979): Hydraulics in groundwater.- McGraw-Hill Book Company, New York, 567 p.

BERELSON, W.M., HAMMOND, D.E., AND CUTTER, G.A. (1990A): In situ measurements of calcium carbonate dissolution rates in deep-sea sediments.- Geochim. Cosmochim. Acta, 54, 3013 - 3020.

BERELSON, W.M., HAMMOND, D.E., O'NEILL, D., XU, X.M., CHIN, C. AND ZUKIN, J. (1990B): Benthic fluxes and pore water studies from sediments of central equatorial north Pacific: nutrient diagenesis.- Geochim. Cosmochim. Acta, 54, 3001-3012.

BERELSON, W.M., HAMMOND, D.E., MCMANUS J., AND KILGORE, T.E. (1994): Dissolution kinetics of calcium carbonate in equatorial Pacific sediments.-Global Biogeochemical Cycles, 8, 219 - 235.

BERNER, R.A. (1972): Sulfate reduction, pyrite formation and the oceanic sulfur budget.- In: Dryssen, D. and Jagner, D., eds.: The Changing Chemistry of the Oceans.- Wiley & Sons, New York, pp. 347-361.

BERNER, R.A. (1980): Early Diagenesis - A Theoretical Approach.- Princeton University Press, 241 p.

BLAIR, N.E. AND ALLER, R.C. (1995): Anaerobic methane oxidation on the Amazon Shelf.- Geochim. Cosmochim. Acta, 59, pp. 3707-3715.

BLEIL, U., ET AL. (1998): Report and preliminary results of METEOR cruise 38/2 Recife - Las Palmas, 04.03.-14.04.1997. 126 p., Ber. FB5, 95, Univ. Bremen.

BOUDREAU, B.P. (1996A): The diffusive tortuosity of fine-grained unlithified sediments.- Geochim. Cosmochim. Acta, 55, 145-159.

BOUDREAU, B.P. (1996B): Diagenetic Models and Their Implementation - Modelling Transport and Reactions in Aquatic Sediments.- Springer, Berlin Heidelberg New York, 414 p.

CAI, W.-J., REIMERS, C.E., SHAW, T. (1995): Microelectrode studies of organic carbon degradation and calcite dissolution at a California continental rise site.- Geochim. Cosmochim. Acta, 59, 497-511.

CANFIELD, D.E., RAISWELL, R., BOTTRELL, S. (1992): The reactivity of sedimentary iron minerals toward sulfide.- Am. J. Sci. 292: 659-683.

COLLATZ, L. (1966): The numerical treatment of differential equations.- 3rd ed., Springer, Berlin Heidelberg New York, 568 p.

DEVOL, A.H. AND AHMED, S.I. (1981): Are high rates of sulfate reduction associated with anaerobic oxidation of methane?- Nature, 291, pp. 407-408.

EBERT, M., J. HENCKE, M. ISENBECK-SCHRÖTER (1995): Modellierung von Transportprozessen dargestellt am Beispiel Chrom (III) / Chrom (VI). - Z. dt. geol. Ges. 146: P. 138-145

EMERSON, S. AND BENDER, M. (1981): Carbon fluxes at the sediment-water interface of the deep-sea: calcium carbonate preservation.- Journal of Marine Research, 39, 139 - 162.

GOLDHABER, M.B. AND KAPLAN, I.R. (1974): The sulfur cycle.- In: Goldberg, E.D., ed.: The Sea, 5.- Wiley & Sons, New York, pp. 569-655.

HALES B. AND EMERSON S. (1996): Calcite dissolution in sediments of the Ontong-Java Plateau: In situ measurements of pore water O_2 and pH.- Global Biogeochemical Cycles, 10(3), 527 - 541.

HALES B. AND EMERSON S. (1997A): Calcite dissolution in sediments of the Ceara Rise: In situ measurements of porewater O_2, pH, and $CO_{2(aq)}$.- Geochimica et Cosmochimica Acta, 61(3), 501-514.

HALES B. AND EMERSON S. (1997B): Evidence in support of first-order dissolution kinetics of calcite in seawater.- Earth Planet. Sci. Letters, 148, 317-327.

HALES, B., EMERSON, S., ARCHER, D. (1994): Respiration and dissolution in the sediments of the western North Atlantic: Estimates from models of in situ porewater oxygen and pH.- Deep-Sea Res. 41, 695-719.

HAMER, K. (1993): Entwicklung von Laborversuchen als Grundlage für die Modellierung des Transportverhaltens von Arsenat, Blei, Cadmium und Kupfer in wassergesättigten Säulen. 147 p., Diss., Ber. FB5, **39**, Univ. Bremen.

HAMER, K. AND R. SIEGER (1994): Anwendung des Modells CoTAM zur Simulation von Stofftransport und geochemischen Reaktionen. 186 p.: Verlag Ernst & Sohn, Berlin

HAMER, K., R. SIEGER, M. ISENBECK-SCHRÖTER, H.D. SCHULZ (1992): Transport of heavy metals in saturated columns - Experiments and modelling. In: Hötzl, H. and Werner A. (eds.): Tracer Hydrology. Balkema, Rotterdam, pp.423-438.

HAMER, K., R. VON LÜHRTE, M. ISENBECK-SCHRÖTER (1994): Transport of Cd and Cu in a zone of calcite dissolution: Column experiments and modeling. In: Transport and Reactive Processes in Aquifers. Editors: T.H. Dracos, F. Stauffer. P.105-110: A.A. Balkema, Rotterdam Brookfield

HAMMOND D. E., MCMANUS J., BERELSON W. M., KILGORE T. E., AND POPE R. H. (1996): Early diagenesis of organic material in equatorial Pacific sediments: stoichiometry and kinetics.- Deep-Sea Research II, 43(4-6), 1365-1412.

HENSEN C., LANDENBERGER H., ZABEL M., AND SCHULZ H.D. (1998): Quantification of diffusive benthic fluxes of nitrate, phosphate and silicate in the Southern Atlantic Ocean.- Global Biogeochemical Cycles, 11, 193-210.

HENSEN, C., LANDENBERGER, H., ZABEL, M., GUNDERSEN, J.K., GLUD, R.N., AND SCHULZ, H.D. (1997): Simulation of early diagenetic processes in continental slope sediments off Southwest Africa: The Computer model CoTAM tested. In: Marine Geology 144. P.191-210. Amsterdam (Elsevier).

HENSEN C. AND ZABEL, M. (1999): Early Diagenesis at the Benthic Boundary Layer: Oxygen and Nitrate in Marine Sediments. In: SCHULZ, H.D. AND ZABEL, M. (eds.): Marine Geochemistry. P. 209-231: Springer, Heidelberg, New York.

HOEHLER, T.M., ALPERIN M.J., ALBERT D.B., MARTENS, C.S. (1994): Field and laboratory studies of methane oxidation in an anoxic marine sediment: Evidence for a methanogen-sulfate reducer consortium.- Global Biogeochem. Cycles, 8, pp. 451-463.

ISENBECK-SCHRÖTER, M. AND K. HAMER (1994): Methoden zur Parameterermittlung für die Simulation geochemischer Prozesse beim Schadstofftransport im Grundwasser. In: Geowissenschaften und Umwelt. Editors: J. Matschullat, G. Müller. P.121-127: Springer-Verlag, Berlin Heidelberg

ISENBECK-SCHRÖTER, M., K. HAMER, F. REITZ, J. SCHUBERT, H.D. SCHULZ (1994): Simulation of arsenic transport in column experiments: Estimation of sorption kinetics of As(III) and As(V) species in simple aquifer systems. In: Transport and Reactive Processes in Aquifers. Editors: T.H. Dracos, F. Stauffer. P.45-51: A.A. Balkema, Rotterdam Brookfield

IVERSEN, N. AND BLACKBURN T.H. (1981): Seasonal rates of methane oxidation in anoxic marine sediments.- Appl. Environ. Microbiol., 41, pp. 1295-1300.

JAHNKE R.A., CRAVEN, D.B. AND GAILLARD, J-F (1994): The influence of organic matter diagenesis on $CaCO_3$ dissolution at the deep-sea floor.- Geochim. Cosmochim. Acta, 58, pp.2799-2809.

JAHNKE R. A., CRAVEN D.B., MCCORKLE D. C., AND REIMERS C. E. (1997): $CaCO_3$ dissolution in California continental margin sediments: The influence of organic matter remineralization.- Geochimica et Cosmochimica Acta, 61(17), 3587-3604.

KASTEN, S., FREUDENTHAL, T., GINGELE, F.X., SCHULZ, H.D. (1998): Simultaneous formation of iron-rich layers at different redox boundaries in sediments of the Amazon deep-sea fan.- Geochim. Cosmochim. Acta, 62, No. 13, pp. 2253-2264.

KEIR R. S. (1980): The dissolution kinetics of biogenic calcium carbonates in seawater.- Geochimica et Cosmochimica Acta, **44**, 241-252.

KEIR R. S. (1983): Variation in the carbonate reactivity of deep-sea sediments: determination from flux experiments.- Deep-Sea Res., 30, 279-296.

KHARAKA Y.K., GUNTER W.D., AGGARWAL P.K., PERKINS E.H. AND DEBRAAL J.D. (1989): SOLMINEQ88: a computer program for geochemical Modeling of water-rock-interactions.- US Geol. Surv., Water-Resources Investigations Report 88-4227, 207 pp.

KINZELBACH, W. (1986): Groundwater modeling. An introduction with sample programs in BASIC.- Elsevier, Amsterdam, 333p.

KINZELBACH, W. (1987): Numerische Methoden zur Modellierung des Transports von Schadstoffen im Grundwasser.- Oldenbourg Verlag, München, Wien, 317 p.

LANDENBERGER, H. (1998): CoTReM, ein Multi-Komponenten Transport- und Reaktions-Modell. 142 p., Diss., Ber. FB5, **110**, Univ. Bremen.

LANDENBERGER, H., C. HENSEN, M. ZABEL, H.D. SCHULZ (1997): Softwareentwicklung zur computerunterstützten Simulation frühdiagenetischer Prozesse in marinen Sedimenten. In: Z. dt. geol. Ges. **148**. P.447-455.

VON LÜHRTE, R., K. HAMER, M. ISENBECK-SCHRÖTER (1994): Das Transportverhalten von Cadmium und Kupfer in Grundwasserleitersanden unter Berücksichtigung von Karbonatgleichgewichten. In: Geowissenschaften und Umwelt. Editors: J. Matschullat, G. Müller. P.129-134: Springer-Verlag, Berlin Heidelberg

MACKENZIE, F.T., BISCHOFF, W.D., BISHOP, F.C., LOIJENS, M., SCHONMAKER, J. AND WOLLAST, R. (1983): Magnesian Calcites: Low-Temperature occurence, solubility and solid-solution behaviour.- In: Reeder, R.J. (ed.): Carbonates: Mineralogy and Chemistry.- P. 97-144: Reviews in Mineralogy, 11, BookCrafters, Inc., Chelsea, Michigan.

MARTIN, W.R. AND SAYLES, F.L. (1996): $CaCO_3$ dissolution in sediments of the Ceara Rise, western equatorial Atlantic.- Geochim. Cosmochim. Acta, **60** (2), pp 243 - 263.

MILLERO, F.J. (1982): The effect of pressure on the solubility of minerals in water and seawater.- Geochim. Cosmochim. Acta, **46**, pp 11-22.

MILLERO, F.J. (1983): Influence of Pressure on Chemical Processes in the Sea.- In: RILEY, J.P. AND CHESTER, R.(eds.): Chemical Oceanography.- Volume **8**, p.1-88. Academic Press, London, New York.

MORSE J. W. (1978): Dissolution Kinetics of Calcium Carbonate in Sea Water: VI. The Near-Equilibrium Dissolution Kinetics of Calcium Carbonate-Rich Deep Sea Sediments.- American Journal of Science, 278, 344-353.

NIEWÖHNER, C., HENSEN, C., KASTEN, S., ZABEL, M., SCHULZ, H.D. (1998): Deep sulfate reduction completly mediated by anaerobic methane oxidation in sediments of the upwelling area off Namibia.- Geochim. Cosmochim. Acta, 62, No. 3, pp. 455-464.

NIEWÖHNER, C., GROBE, H., SIEGER, R., SCHULZ, H.D. (1999): Geochemical Data from the South Atlantic in the information system PANGAEA.- Geol. Rundsch., this volume.

PARKHURST, D.L., THORSTENSEN, D.C., PLUMMER, L.N. (1980): PHREEQE – a computer program for geochemical calculations.- 210 pp., U.S. Geol. Survey Water Resource Invest. Rept. 80-96, Washington D.C.

PARKHURST, D.L. (1995): PHREEQC – User's guide to PHREEQC -A computer program for speciation, reaction-path, advective-transport, and inverse geochemical calculations.- 143 pp., U.S. Geol. Survey Water Resource Invest. Rept. 95-4227, Lakewood, Col.

PFEIFER, K., HENSEN, C., ADLER, M., WENZHÖFER, F. AND SCHULZ, H.D. (in prep.): Modeling of subsurface calcite dissolution regarding oxic respiration and reoxidation processes in the equatorial upwelling off Gabon.

PLUMMER, L.N., JONES, B.F. AND TRUESDELL, A.H. (1976): WATEQF - A FORTRAN IV version of WATEQ, a computer program for calculating chemical equilibrium of natural waters.- U.S. Geological Survey Water Resources Investigation 76-13, 61 p.

PRESS, W.H., FLANNERY, B.P., TEUCHOLSKY, S.A., VETTERLING, W.T. (1992): Numerical recipes in Fortran: The art of scientific computing.- Cambridge University Press, Cambridge, 759 p.

PRESS, W.H., TEUKOLSKY, S.A., VETTERLING, W.T., FLANNERY, B.P. (1992): Numerical Recipes (in FORTRAN). 2nd Edition. Cambridge University Press, Cambridge.

PYZIK, A.J. AND SOMMER, S.E. (1981): Sedimentary iron monosulfides: kinetics and mechanism of formation.- Geochim. Cosmochim. Acta, 45, pp. 687-698.

RABOUILLE, C. AND GAILLARD, J.-F. (1991): Towards the EDGE: Early diagenetic global explanation. A model depicting the early diagenesis of organic matter, O_2, NO_3, Mn, and PO_4.-Geochim. Cosmochim. Acta, 55: 2511-2525.

RAISWELL, R. (1982): Pyrite texture, isotopic composition and the availability of iron.- Am. J. Sci. 282: 1244-1263.

REEBURGH, W.S. (1980): Anaerobic methane oxidation: Rate depth distibutions in Skan Bay sediments.- Earth Planet. Sci. Lett. 47, pp. 345-352.

REEBURGH, W.S. AND ALPERIN, M.J. (1988): Studies on anaerobic methane oxidation.- SCOPE/UNEP, 66, pp. 367-375.

RICKARD, D.T. (1969): The chemistry of iron sulfide formation at low temperatures.- Stockholm. Contr. Geology, 20, pp. 67-95.

RICKARD, D.T. (1974): Kinetics and mechanism of the sulfidation of goethite.- Am. J. Sci. 274: 941-952.

RICKARD, D.T. (1975): Kinetics and mechanism of pyrite formation at low temperatures.- Am. J. Sci. 275: 636-652.

RUTGERS VAN DER LOEFF, M.M. AND VAN BENNEKOM, A.J. (1989): Weddell Sea contributes little to silicate enrichment in Antarctic Bottom Water.- Deep-Sea Res. **42**, pp 31-52.

SCHULZ, H.D. AND REARDON, E.J. (1983): A combined mixing cell - analytical model to describe two-dimensional reactive solute transport for unidirectional ground water flow.- Water Resources Res., **19**, pp. 493-502.

SCHULZ, H.D., DAHMKE, A., SCHINZEL, U., WALLMANN, K., ZABEL, M. (1994): Early diagenetic processes, fluxes, and reaction rates in sediments of the South Atlantic.- Geochim. Cosmochim. Acta, 58: 2041-2060.

SCHULZ, H.D. ET AL. (1998): Report and preliminary results of METEOR cruise M41/1 Malaga - Libreville, 13.02.-15.03.1998. 124 p., Ber. FB5, 114, Univ. Bremen.

SIEGER, R. (1993): Modellierung des Stofftransports in porösen Medien unter Ankopplung kinetisch gesteuerter Sorptions- und Redoxprozesse sowie thermodynamischer Gleichgewichte. 158 p., Diss., Ber. FB5, **40**, Univ. Bremen.

SOETAERT, K., HERMAN, P.M.J., MIDDELBURG, J.J. (1996): A model of early diagenetic processes from the shelf to abyssal depths.- Geochim. Cosmochim. Acta, 60: 1019-1040.

STEEFEL, C.I. AND MACQUARRIE, K.T.B. (1996): Approaches to modeling of reactive transport in porous media.- In: Lichtner, P.C., Steefel, C.I. and Oelkers, E.H. (eds.): Reactive Transport in porous media.- Reviews in Mineralogy, **34**, pp. 83-129.

SWEENEY, R.E. AND KAPLAN, I.R. (1973): Pyrite framboid formation: laboratory synthesis and marine sediments.- Econ. Geology, 68, pp. 618-634.

TRUESDELL, A.H. AND JONES, B.F. (1974): WATEQ - A computer program for calculating chemical equilibria of natural waters.- Journal of Research, U.S. Geological Survey, v. 2, p. 233-274.

ULLMAN, W.J. AND ALLER, R.C. (1982): Diffusion coefficients in nearshore marine sediments.- Limnol. Oceanogr., 27: 552-556.

UNESCO (1987): Thermodynamics of the Carbon Dioxide System in Seawater.- UNESCO Tech. Papers 51.

VAN CAPPELLEN, P. AND WANG, Y. (1996): Cycling of iron and manganese in surface sediments: A general theory for the coupled transport and reaction of carbon, oxygen, nitrogen, sulfur, iron and manganese.- Am. J. Sci., 296: 197-243.

WANG, Y. AND VAN CAPPELLEN, P. (1996): A multicomponent reactive transport model of early diagenesis: Application to redox cycling in coastal marine waters.- Geochim. Cosmochim. Acta, 60: 2993-3014.

WENZHÖFER, F., ADLER, M., KOHLS, O., HENSEN, C., STROTMANN, B., BOEHME, S., SCHULZ, H.D. (submitted): Calcite dissolution driven by benthic mineralization: In situ measurements of Ca^{2+}, pH, pCO_2, O_2, and modeling.

WOLERY, T.J. (1979): Calculation of Chemical Equilibrium Between Aqueous Solution and Minerals: The EQ3/6 Software Package.- Livermore, CA: Lawrence Livermore National Laboratory, Report UCRL-52658.

WOLERY, T.J. (1993): EQ3/6 - A Software Package for Geochemical Modeling of Aqueous Systems.- Lawrence Livermore National Laboratory, California, 247 p.

YANENKO, N.N. (1971): The method of fractional steps.- Springer, Berlin Heidelberg New York.

Danksagung

Herrn Prof. Dr. H. D. Schulz möchte ich sehr herzlich danken für die Vergabe und Betreuung dieser Dissertation. Insbesondere seine Übersicht und umfassenden Kenntnisse zu den Hauptaspekten der vorliegenden Arbeit - Geochemie und numerische Modellierung - und seine Geduld waren mir eine besondere Hilfe und haben mir die Beendigung der Arbeit ermöglicht.

Ebenfalls möchte ich Herrn Dr. habil. T. von Dobeneck für die Übernahme des Zweitgutachtens danken. Finanziert wurde meine Tätigkeit dankenswerterweise über die Deutsche Forschungsgemeinschaft, durch die ich ein Stipendium im Rahmen des Graduiertenkollegs "Stoff-Flüsse in marinen Geosystemen" der Uni Bremen erhielt.

Allen Mitgliedern der Arbeitsgruppe Geochemie und Hydrogeologie möchte ich meinen Dank ausdrücken für ihren - mehr oder minder großen - Einfluß auf diesen prägenden Lebensabschnitt meiner Doktorandenzeit, denn keines der geführten Gespräche und keine der gemachten Erfahrungen, seien sie fachlichen oder sozialen Ursprungs, möchte ich im nachhinein missen.

Mein direkter Vorgänger als Entwickler von CoTReM, Dr. Holger Landenberger, war mir in der Einarbeitungsphase der hilfreiche Mentor in den Details der Modellprogrammierung. Ihm möchte ich dafür danken, daß das Wasser nicht so kalt war, wie es ohne ihn gewesen wäre.

Dr. Frank Wenzhöfer gebührt ein gesonderter Dank dafür, daß er bereit war, seine einzigartigen Messdaten in unsere Zusammenarbeit und damit die Modellierung einzubringen. Kerstin Pfeifer - wie auch allen anderen Anwendern - danke ich für den Elan, die Möglichkeiten des Programms zu erkunden und neue Fragen zu stellen. Die sich daraus ergebenden Problemstellungen führten stets nach Lösung zu lohnenswertem Fortschritt in der Modellentwicklung und Freude über die gewonnenen Erkenntnisse.

Kerstin Pfeifer und Verena Heuer sei Dank für den guten persönlichen Draht, der sich zwischen uns entwickelt hat und den ich als verläßliche Freundschaft sehe. Sven Jensen möchte ich dafür danken, daß er in seiner besonderen, hilfreichen Art manches Lächeln auf mein Gesicht gezaubert hat.

Mein besonderer Dank gilt Dr. Sabine Kasten und Dr. Christian Hensen für die zahllosen fachlichen Anregungen und konkreten Hilfestellungen organisatorischer, überarbeitender oder einfach durchdenkender Art, sowie der Vermittelung manch grundlegender geologischer Sachverhalte.

Sabine sei hier insbesondere ein lieber Dank dafür ausgedrückt, daß sie wohl am entschiedensten bewirkt hat, mich in der Arbeitsgruppe und Bremen zu integrieren. Christian möchte ich speziell danken für das - so wie er es ausdrückte - "stete Geben und Nehmen", wobei er aus meiner Sicht sein "Geben" stets bescheiden untertrieb. Dies gilt sowohl für die fachliche Zusammenarbeit als auch für die prima Freundschaft, die sich daraus entwickelt hat.

Und mein ganz besonderer Dank geht an meine Eltern.

Süß
ist die Erinnerung an
vergangene Mühen

Cicero